DISASTER MANAGEMENT CYCLE-BASED INTEGRATED HUMANITARIAN SUPPLY NETWORK MANAGEMENT

A Dissertation
Presented to
the Graduate School of
Clemson University

In Partial Fulfillment
of the Requirements for the Degree
Doctor of Philosophy
Industrial Engineering

---

by
Kasin Ransikarbum
August 2015

Accepted by:
Dr. Scott J. Mason, Committee Chair
Dr. William G. Ferrell
Dr. Kevin M. Taaffe
Dr. Maria E. Mayorga

ABSTRACT

While logistics research recently has placed increased focus on disruption management, few studies have examined the response and recovery phases in post-disaster operations. We present a multiple-objective, integrated network optimization model for making strategic decisions in the supply distribution and network restoration phases of humanitarian logistics operations. Our model provides an equity- or fairness-based solution for constrained capacity, budget, and resource problems in post-disaster logistics management. We then generate efficient Pareto frontiers to understand the trade-off between the objectives of interest.

Next, we present a goal programming-based multiple-objective integrated response and recovery model. The model prescribes fairness-based compromise solutions for user-desired goals, given limited capacity, budget, and available resources. An experimental study demonstrates how different decision making strategies can be formulated to understand important dimensions of decision making.

Considering multiple, conflicting objectives of the model, generating Pareto-optimal front with ample, diverse solutions quickly is important for a decision maker to make a final decision. Thus, we adapt the well-known Non-dominated Sorting Genetic Algorithm II (NSGA-II) by integrating an evolutionary heuristic with optimization-based techniques called the Hybrid NSGA-II for this NP-hard problem. A Hypervolume-based technique is used to assess the algorithm's effectiveness. The Hazards U.S. Multi-Hazard (Hazus)-generated regional case studies based on earthquake scenarios are used to demonstrate the applicability of our proposed models in post-disaster operations.

DEDICATION

To my mother and father

ACKNOWLEDGMENTS

I would like to express my sincerest gratitude to my advisor, Dr. Scott J. Mason. He has been a great and an inspiring role model of excellent work and research. The guidance, support, time, encouragement, and effort that he has given me are invaluable and enable me to complete my work successfully. Thank you Dr. Mason!

I have also been so fortunate and thankful to my committee members: Dr. William G. Ferrell, Dr. Kevin M. Taaffe, and Dr. Maria E. Mayorga to support me through this process. I am grateful for their valuable suggestions and helpful feedback. My advisor and committee members each have contributed to my education, research, and future.

I also have to thank all of the other faculty members and staffs in the Department of Industrial Engineering. They have supported me through several stages of conducting the research and opened my perspectives by encouraging strong academic knowledge.

I am also highly thankful to all of my friends who have helped me directly and indirectly along the way and have endured this process with me. Moral support, friendship, and time that we have spent together play a significant part for me to complete my work.

Last but not least, I am as ever, indebted to my parents and family for their care and understanding. They have inspired me to be a good person and a good engineer. They have also supported, encouraged, and stood beside me during my work. Without their endless love and tremendous support throughout my life, none of this work would be possible.

TABLE OF CONTENTS

Table of Contents (Continued)

Page

LIST OF TABLES

LIST OF FIGURES

List of Figures (Continued)

CHAPTER ONE

INTRODUCTION AND MOTIVATION

1.1 Introduction

The large global impact of an increasing number of natural and man-made disasters in recent years has resulted in an increased interest and focus by academic, government, and commercial sectors in post-disaster management. According to the World Disaster Report 2014 from the International Federation of Red Cross and Red Crescent Societies (IFRC), approximately 6,500 disasters took place between 2004 and 2013 inclusive of natural and technological disasters. These memorable events include the Ocean Tsunami in 2004, Hurricane Katrina in 2005, the Haiti Earthquake in 2010, and the Earthquake-Tsunami-Nuclear Emergency Japan in 2011. During these years, the IFRC (2014) reported more than 1.1 million casualties, over 1.9 billion affected people, and an estimated $1.67 trillion in economic damage. These significant losses further motivate the need for focused supply chain management (SCM) research on disruption management and humanitarian relief logistics operations.

The humanitarian logistics literature can be categorized into the four phases of the disaster management cycle related to pre- and post-disaster operations (McLoughlin 1985, Celik *et al.* 2012). While pre-disaster phases include 1) mitigation and 2) preparedness, post-disaster phases include both 3) response and 4) recovery. The purpose of mitigation is to prevent disasters from happening, while the focus of preparedness is to get ready for response before a disaster occurs. Further, the response phase, such as supply distribution and evacuation, has the goal of managing available resources efficiently and effectively, as it is important for emergency services and responders to save lives as well as to preserve the financial and physical resources in the response stage (Celik *et al.* 2012). At last, the recovery phase's purpose is to bring both the environment and distribution/supply networks back to a "normal" state (e.g., debris management and network restoration). Several researchers point to the need for post-disaster-related humanitarian logistics research and report that integration among the phases currently is quite limited, but important (Altay and Green 2006, Caunhye *et al.* 2012, Celik *et al.* 2012, and Galindo and Batta 2013).

As the performance of humanitarian operations depends largely on the extent of the efficiency and effectiveness of logistics operations, several strategies to improve performance and manage SCM with disruption are needed and studied (Celik *et al.* 2012 and Ivanov *et al.* 2014). Further, the ripple effect in the supply chain has been recently highlighted to understand how changes to some variables ripple through the rest of the supply chain and influences its performance (Ivanov *et al.* 2013 and Ivanov *et al.* 2014). The same authors discuss an interconnection among efficiency (e.g., cost and service level), flexibility (e.g., structural redundancy), and resilience (e.g., preparedness, mitigation, stabilization, and recovery) framework, and examine the trade-offs among them.

To combat the data acquisition challenges common in post-disaster settings, the Federal Emergency Management Agency (FEMA) developed the Hazards U.S. Multi-Hazard ("Hazus") tool. Based on a geographic information system (GIS), Hazus is a natural hazard loss estimation software package that can estimate potential building and infrastructure losses resulting from catastrophic events from earthquake, hurricane, and floods. FEMA (2014) reports that Hazus currently is used for both mitigation and preparedness, as well as for response and recovery planning by government planners, GIS specialists, and emergency managers to determine losses and plan long-term strategies for communities to reduce their losses.

As few OR specialists currently are studying methods for improving humanitarian operations, there is a need to transfer techniques from commercial SCM to humanitarian logistics research. This is especially true for post-disaster operations, as much of the previous research has focused on pre-disaster operations. Considering that integrated models for analyzing the various phases of disaster relief management are also scarce in the literature, this dissertation will support humanitarian logisticians, fill voids in research communities, and contribute to the open literature. Figure 1.1 depicts the relationship between the problem domain in this dissertation and the disaster management cycle. Specifically, we are interested in equity or fairness of supplying relief items to beneficiaries through a disrupted network after a disaster occurs while trying to provide decision makers with a list of strategic restoration plans for disrupted nodes and arcs in humanitarian operations. We capture both the supply distribution problem during response and the network restoration problem during recovery with an integrated approach. It is important to emphasize that our problem is motivated from the lack of decision support models currently available in the post-disaster area. In addition, an integrated approach is considered since it is well observed that decisions to supply units and to restore a network are dependent. Practitioners can use the developed model to support decisions for organizations in charge of the distribution of supplies and those groups in charge of restoration planning during post-disaster.

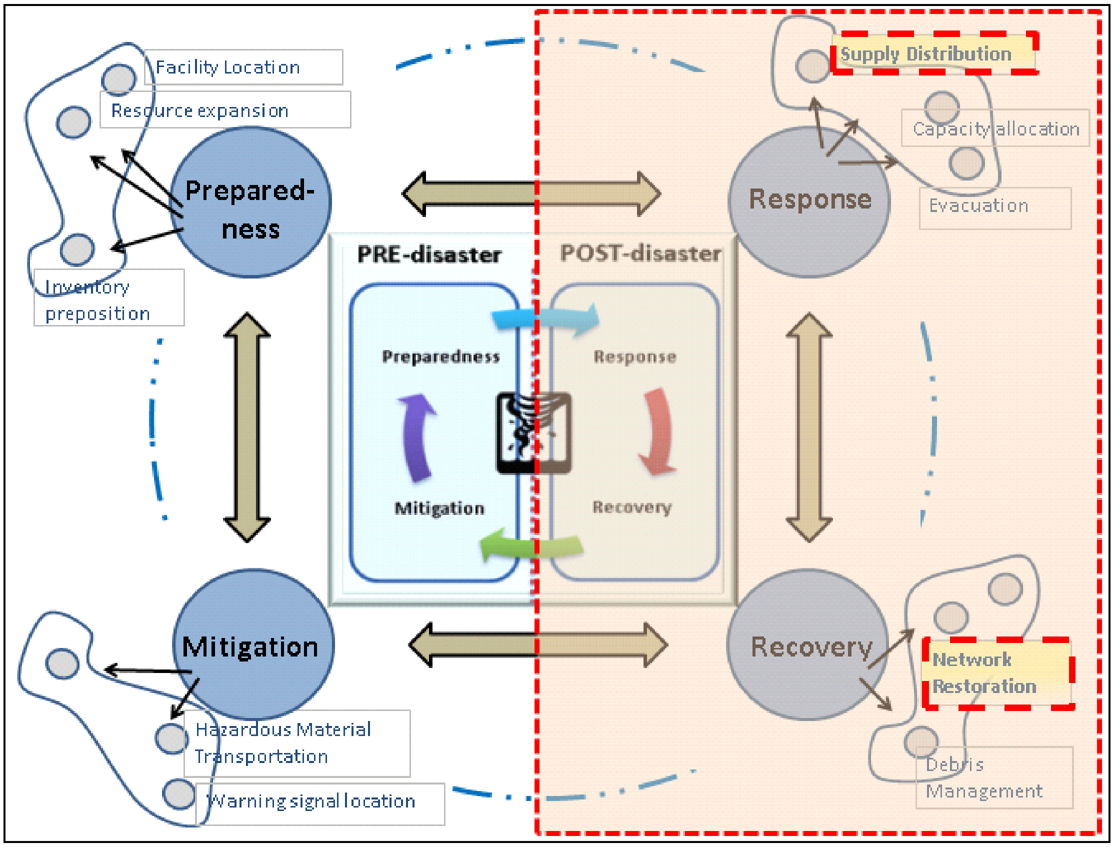

Figure 1.1: Research domain problem in the disaster management cycle

This dissertation is composed of three journal papers focusing on post-disaster humanitarian operations. Some redundancies between chapters are removed to make it easier to comprehend. Furthermore, the dissertation chapters contain more content than is included in the journal submissions. An overview of each chapter/ journal paper is presented as follows.

Multiple-Objective Analysis of Integrated Relief Supply and Network Restoration in Humanitarian Logistics Operations (See publication related to this research in Ransikarbum and Mason, 2014)

This research provides a multiple-objective, integrated network optimization model for making strategic decisions in the supply distribution and network restoration phases of humanitarian logistics operations. The model provides an equity-based solution for constrained capacity, budget, and resource problems in post-disaster logistics management. Designed experiments are conducted for this NP-hard problem to analyze important aspects of the integrated problem for both small- and large-sized networks: full vs. partial restoration and pooled vs. separate budgeting approach. The integrated model is then applied to a Hazus-generated South Carolina (SC) regional case study based on an earthquake scenario. Finally, efficient or Pareto frontiers are generated to understand the trade-off between the objectives of interest.

Goal programming-based post-disaster decision making for integrated relief supply distribution and network restoration (See publication related to this research in Ransikarbum and Mason, 2015a)

This research extends from the previous research by presenting a goal programming-based multiple-objective integrated response and recovery model to investigate important supply distribution and network restoration decisions. The model prescribes fairness-based compromise solutions for user-specified desired goals, given limited capacity, budget, and available resources. An experimental study demonstrates how different decision-making strategies can be formulated to understand important dimensions of decision making. Hazus-generated regional case studies for two regions

(South Carolina and California) demonstrate the applicability of our proposed model in post-disaster operations.

A Bi-Criteria Metaheuristic for Integrated Post-Disaster Relief Supply and Network Restoration Decisions (See publication related to this research in Ransikarbum and Mason, 2015b)

In the previous research, a multiple-objective integrated response and recovery (MOIRR) model is developed for making strategic decisions in both the supply distribution and network restoration phases in post-disaster operations. Considering multiple, conflicting objectives of the model, generating Pareto-optimal front with ample, diverse solutions quickly is important for a decision maker to make an informative, final decision. Thus, the well-known Non-dominated Sorting Genetic Algorithm II (NSGA-II) is adapted in this research by integrating an evolutionary heuristic with optimization-based techniques called the Hybrid NSGA-II for this NP-hard problem. A Hypervolume-based technique is used to assess the algorithm's effectiveness for a Hazus-generated loss scenario in South Carolina (SC) based on an earthquake scenario.

1.2 Motivation

1.2.1 Humanitarian Logistics and the Need for Research

The increase in natural and man-made disasters has recently motivated the increased number of humanitarian logistics and relief operations studies. Based on recent papers calling for more research in humanitarian logistics and a number of literature reviews, several authors (Chandraprakaikul 2010, Tatham and Pettit 2010, Celik *et al.* 2012, Caunhye *et al.* 2012, and Galindo and Batta 2013) point to the need for humanitarian logistics and relief operations research. Chandraprakaikul (2010) and Tatham and Pettit (2010) suggest that there are few OR specialists contributing in the field of humanitarian logistics and call for researchers in commercial supply chain management (SCM) to transfer more techniques into humanitarian logistics research. Chandraprakaikul (2010) reviews the literature from 1990-2010 using keywords "humanitarian supply chains," "humanitarian logistics," "relief chain," "relief operations," and "humanitarian aid". She observes that these terms are used interchangeably in the literature. The author suggests that further research is needed in the following areas:

- Distribution Planning.
- Information and Communication System.
- Sourcing and Supplier Management.
- Supply Chain Coordination and Integration.
- Performance Measurement.
- Transportation, Mode Choice, and Routing.

Tatham and Pettit (2010) discuss the concept of supply network management (SNM), using it interchangeably with SCM, and argue that the fundamental principles of SNM—the five rights: right product, right time, right place, right price, and right quality—as well as additionally the right information, are equally applicable to the humanitarian logistics field. The authors suggest two categories for researchers to follow:

- The application of academic models that target the organizational issues inherent in the management of humanitarian supply networks.
- The application of OR techniques drawn from the commercial SNM environment to humanitarian logistics.

Celik *et al.* (2012) and Caunhye *et al.* (2012) conduct literature reviews based on pre- and post-disaster events and provide similar directions for future research. Celik *et* *al.* (2012) base their review on four phases of the disaster management cycle and categorize groups in each phase. In addition, the authors also present long-term humanitarian development topics addressed in the literature, and suggest that future research is needed in the area of disaster recovery, long-term development, integrated phases of disaster management cycle, and models considering the effects of multiple disasters (e.g., cascading disasters in Japan in 2011 with earthquake and tsunami, followed by the nuclear emergency). Caunhye *et al.* (2012) also segment the literature similarly based on pre- and post-disaster events. Specifically, pre-disaster events relate to facility location (e.g., location-evacuation, location with relief distribution and stock pre-positioning), while post-disaster events include relief distribution and casualty transportation (e.g., resource allocation and commodity flow). The authors provide several research directions:

- While current research focuses on facility location for the pre-disaster phase, research on facility location for post-disaster events is lacking.
- Research in the recovery phase or casualty transportation is limited.
- Research is lacking on objectives other than cost efficiency and responsiveness.
- Research on manpower management during large-scale emergencies is lacking.

1.2.2 Commercial SCM and Humanitarian SCM

Several researchers (Chan 2003, Wassenhove 2005, Beamon and Balcik 2008, Balcik *et al.* 2009, and Haddow *et al.* 2011) highlight the similarities and differences between commercial SCM and humanitarian SCM. Figure 1.2 is adapted from Beamon and Balcik (2008) who illustrate the commercial and humanitarian supply chains. The authors discuss the different characteristics between non-profit and for-profit organizations based on revenue sources, goals, stakeholders, and performance measurement. The different characteristics between for-profit supply chains and humanitarian relief chains are based on strategy goals, demand characteristics and order fulfillment (e.g., lead times, reliability of transportation system, pricing). In addition, customer characteristics are also discussed in their study.

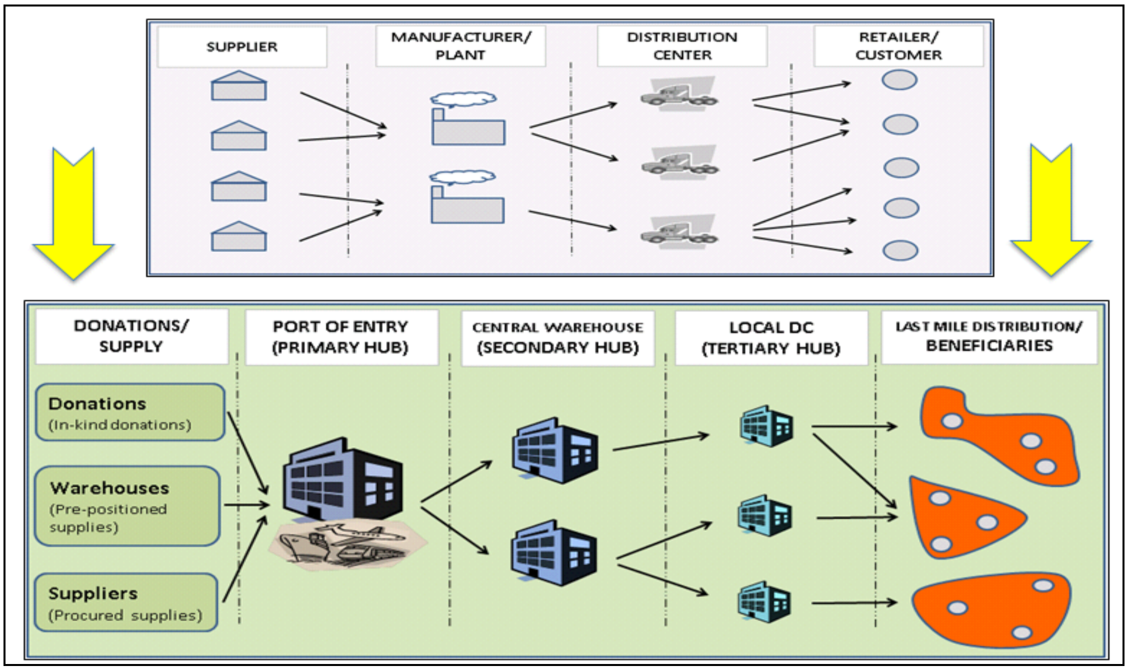

Figure 1.2: Commercial and humanitarian supply chains (adapted from Beamon and Balcik (2008))

With regard to performance measurement, Beamon and Balcik (2008) compare performance measurement in commercial supply chains and with humanitarian relief chain measurement. The authors develop new performance metrics for the humanitarian relief chain and suggest a performance measurement framework for the relief chain using a Sudan relief center as an illustration. Based on the three characteristics used for supply chain performance measurement studied earlier, the authors map the humanitarian relief chain and provide the following performance metrics:

- Resource performance metrics: cost of suppliers, distribution costs, inventory holding costs.
- Output performance metrics: response time, number of items supplied, supply availability.
- Flexibility performance metrics: volume flexibility (e.g., ability to respond to different magnitudes of disasters), delivery flexibility (e.g., time to respond to disasters), mix flexibility (e.g., ability to provide different types of items).

With regard to coordination roles described as the relationships and interactions among different actors operating within the relief environment, Balcik *et al.* (2009) compare and contrast the coordination roles of several actors in commercial supply chains and relief chains. Several classification schemas are suggested. First they discuss *vertical coordination* (e.g., an organization coordinates with upstream or downstream activities, such as when a non-governmental organization (NGO) coordinates with a transportation company). In contrast, *horizontal coordination* occurs when an organization coordinates with other organizations at the same level (e.g., coordination among NGOs). In addition, coordination in the relief chain can also be classified as either *among international relief actors* or as *between international relief actors and local relief actors*. Additionally, coordination involving private sector companies is classified as either *commercial relationships* (e.g., vertical relationship with suppliers) or *philanthropic relationships* (e.g., vertical or horizontal relationship with a private-sector company providing donations).

The authors also suggest that strategic partnerships between logistics firms and relief organizations are important in humanitarian operations (e.g., between FedEx and the American Red Cross or DHL and the International Federation of Red Cross and Red Crescent Societies (IFRC)). In addition, the authors describe six factors affecting coordination in humanitarian operations: number and diversity of actors, donor expectations and funding structure, competition for funding and the effects of the media, unpredictability, resource scarcity and oversupply, and cost of coordination.

1.2.3 Four Phases of the Disaster Management Cycle

The humanitarian logistics literature can be categorized into four phases of the disaster management cycle (McLoughlin 1985). It is important to note that few research studies have been conducted in the response and recovery phase (Celik *et al.* 2012 and Galindo and Batta 2013). Further, as integration among the phases is still limited—these two facts motivate my dissertation research interests.

1.2.3.1 Mitigation Phase

The activities in this phase either prevent disasters from happening or reduce potential effects. The literature can be grouped as follows:

- Hazardous material transportation (e.g., network design, location of DCs).
- Location of early warning systems (e.g., location of nuclear threat detectors).
- Reliable facility location (e.g., facility location with failure considerations).
- Installation of protection systems (e.g., allocation of police patrol areas).

1.2.3.2 Preparedness Phase

The activities in this phase involve getting ready for response before the disaster occurs. The literature is grouped as follows:

- Facility location and supply prepositioning (e.g., quantities of prepositioned supplies, warehouse location).
- Infrastructure preparation (e.g., expansion of medical facilities).

1.2.3.3 Response Phase

The activities in this phase involve responding while the disaster is occurring with the goal of managing available resources efficiently. The literature can be grouped as follows:

- Supply distribution (e.g., supply flow, vehicle routing).
- Inventory management (e.g., order quantities).
- Evacuation (e.g., people transportation, shelter locations).
- Healthcare (e.g., hospital assignments).
- Arcs recovery (e.g., recovery of roads and bridges).

1.2.3.4 Recovery Phase

The activities in this phase involve actions taken after the disaster occurs to bring the environment and network back to a normal state. The literature is grouped as follows:

- Post-disaster debris and waste management (e.g., debris and casualty transportation).
- Infrastructure network restoration (e.g., road and traffic restoration).
- Relief commodity distribution (e.g., vehicle routing).

1.2.4 Recent Disasters and Logistics Lessons Learned

1.2.4.1 Thailand Tsunami (2004)

The tsunami highlighted many issues related to large-scale humanitarian disasters, such as the level of preparedness for such events and how best to manage logistics and supply chain activities in volatile conditions. As pointed out by Pettit *et al.* (2011), many organizations, especially in Thailand, now give more attention to issues related to large-scale emergencies including preparedness and implementation of appropriate plans during emergency relief operations. My research hypothesis is that it is not only before and during disasters, but also post-disaster in the recovery phase that focused efforts are required. As pointed out by the authors, the Asian tsunami disaster affects at least 14 countries, including Thailand. Total casualties are almost 200,000 and the financial costs associated with the tsunami for Thailand alone are estimated at over US$ 500 million. The authors also point that it is obvious that the coordination for humanitarian logistics to embrace commerce, academia and the military is needed.

Economist Intelligence Unit (EIU) (2005) also discusses lessons learned from the tsunami based on a series of interviews with disaster response experts, government officials, relief agencies, and companies involved in aid work in Thailand and Indonesia. Their recommendations are categorized into four main areas:

- *Gaining access*: seek to cooperate with the government of the affected country, look to the UN for leadership, local participation and ownership is critical, keep airport open, recovery work is necessary.
- *Getting the right types of donations*: insist on cash or appropriate donations, source locally, if possible.
- *Distributing supplies and collecting people*: be aware of the threat of intimidation from local officials, recognize the pitfalls of oversupply, keep lines of authority clear, be alert to racial sensitivities and the need for good communication).
- *Private-sector involvement/what logistics provider can do*: establish early on that all assistance is given freely, get in early with the right papers, think long-term, determine resources required for delivery operations, maintain updated database for suppliers, ensure cooperative commitment to disaster response, identify volunteers for airport emergency team, and forge partnership with aid agencies.

1.2.4.2 Hurricane Katrina (2005)

Hildreth (2009) describes emergency financial responses and their consequences during and after hurricane Katrina. Fiscal equilibrium analysis is used in the study as a framework to address fiscal policy issues in the aftermath of a catastrophic disaster. The author chooses to conduct the study during the disaster recovery phase—often the most overlooked phase of disaster management. In addition, Banipal (2006) examines the performance of communication networks and information systems during hurricane Katrina, lists causes of failure, and presents designs for reliable and scalable networks. Integrated disaster management strategies for coordinated response to disasters are described. The author asserts that it is important that organizations involved in the disaster recovery phase have quick and accurate access to as much of the necessary information as possible, since quick response to disasters has the potential to significantly reduce total losses. The author points out that although the resources utilized are enormous (e.g., police officers, national guards, Red Cross, and Federal Emergency Management Agency (FEMA) workers), the majority of workers participating in search and rescue operations are out-of-state residents with little information about the geography of the city, street names, landmarks, etc., which often contributes to longer times for rescue operation to be completed.

1.2.4.3 Haiti Earthquake (2010)

Coles *et al*. (2010) analyze humanitarian operations during the response and recovery phases after the Haitian earthquake via a case study based on interviews with relief agencies. According to the authors, agencies responding to an earthquake can maximize operational efficiency by working together to reduce duplicated services and maximize utilization of available resources. Four areas in the context of optimal resource allocation are addressed in the paper: key dynamics affecting partnership efficiency and logistics, trends in partnership development and utilization, changes in agencies' level of involvement before and after the earthquake, and common metrics that can be used for agency efficiency assessment. In addition, the authors use a commodity flow network to describe the flow of resources and major factors affecting partnership development and sustainability.

1.2.4.4 Japan Earthquake, Tsunami, and Nuclear Emergency (2011)

Mimura *et al*. (2011) discuss the earthquake and tsunami that occurred off the coast of Tohoku, Japan. Although the Tohoku coast developed the most advanced anti-earthquake/tsunami system in the world, it was heavily damaged by the March 2011 event that measured 9.0 on the Richter scale (Mimura *et al.* 2011 and Fuse and Yokota 2012). Infrastructure damages reported include roads, bridges, and railway systems, which in turn have strong effects on recovery and economic activities. After the earthquake and tsunami occurred, significantly widespread damages to roads, railways, and lifelines resulted in insufficient supplies of food and gasoline being available to impacted areas. The authors suggest several directions for future research:

- The earthquake and tsunami generated 25 million tons of wreckage—current disaster management plans focus on refugees, but seldom consider treatment of the wreckage—there is a need to incorporate this issue in disaster recovery planning.
- Disaster prevention should be based not only on improved scientific understanding, but also on the possibility of maximum potential hazards.

Fuse and Yokota (2012) illustrate the "*chain of survival for disasters*" with four chains covering each response activity that should be undertaken from a medical viewpoint. These chains include rapid search and rescue; early care in the field, evacuation centers, and primary clinics; definitive evacuation at disaster-based hospitals; and proper evacuation to unaffected areas. The authors suggest that their concept could be used to guide headquarters operations in dealing with the relief commodities associated with a disaster.

CHAPTER TWO

MULTIPLE-OBJECTIVE ANALYSIS OF INTEGRATED RELIEF SUPPLY AND NETWORK RESTORATION IN HUMANITARIAN LOGISTICS OPERATIONS

2.1 Introduction

In this chapter, we present a multiple-objective, integrated network optimization model for strategic decision-making regarding supply distribution and network restoration decisions during post-disaster operations. Our model seeks to obtain fairness-or-equity-based solutions under constrained capacity, budget, and resource limitations. We employ a designed experiment to investigate several important aspects of the proposed model, such as partial vs. full restoration and pooled vs. separate budgeting, with both small- and large-sized networks to gain managerial insights from the model. Finally, the model is applied to a regional case study using loss data generated from Hazus based on an earthquake scenario to provide decision makers with candidate restoration and distribution plans. This work provides an integrated aspect of distribution and restoration of distribution systems. However, as pointed out by several researchers (e.g., Yan *et al.* 2011, Celik *et al.* 2012, and Ivanov *et al.* 2013), it is also important to consider an integrated approach between production and distribution systems (e.g., setting an inventory level and scheduling a distribution plan) as it provides decision makers with globally, simultaneously optimized decisions.

The remaining sections of this chapter are organized as follows. We overview the pertinent literature in Section 2.2. Then, our multiple-objective integrated response and recovery (MOIRR) model and an experimental design are presented in Section 2.3. Next, an illustrative, Hazus-case study is discussed in Section 2.4. Finally, Section 2.5 presents our research conclusions and outlines directions for future research. This chapter is submitted to the journal with the following citation:

Ransikarbum, K. and Mason, S. J. 2014. Multiple-Objective Analysis of Integrated Relief Supply and Network Restoration in Humanitarian Logistics Operations. *International Journal of Production Research, In Press.*

2.2 Literature Review

With a focus on disaster-related issues, humanitarian logistics research is becoming a key factor in devising improved ways of managing multi-stakeholder relief operations. There are interchangeable terms commonly used for humanitarian logistics in the literature (e.g., humanitarian SCM, relief chain, disrupted SCM, and emergency management). Based on recent papers calling for more research in humanitarian logistics and a number of literature reviews, several authors (e.g., Wassenhove 2005, Chandraprakaikul 2010, Tatham and Pettit 2010, Caunhye *et al.* 2012, Celik *et al.* 2012, Galindo and Batta 2013, and Day 2014) suggest that there is a need for operations research and management science (OR/MS) specialists to transfer more techniques from commercial SCM into humanitarian logistics research. Beamon and Balcik (2008) compare commercial and humanitarian SCM and suggest that the ultimate goal to deliver the right supplies in the right quantities to the right locations at the right time is similar. They also discuss the differences based on revenue sources, goals, stakeholders, and performance measurement between the two. Additionally, while high market incentive and low risk are associated with commercial SCM, low market incentive and high risk can be observed in humanitarian logistics (Christopher and Tatham 2011).

Performance measurement in humanitarian logistics is not necessarily similar to commercial logistics (Chan 2003, Beamon and Balcik 2008, Christopher and Tatham 2011, Celik *et al.* 2012, and Day 2014). Celik *et al.* 2012 point that not only effectiveness, but also efficiency of post-disaster logistics activities are needed to capture performance. Christopher and Tatham (2011) also discuss the need for developing appropriate performance metrics for humanitarian operations that capture the aid recipient's viewpoint. The concept of equity and its measurement receives attention from several researchers in the literature (Marsh and Schilling 1994, Luss 1999, Ogryczak 2000, Kostreva *et al.* 2003, Singh 2007, Viroriano *et al*. 2011, and Zhu *et al.* 2010). Marsh and Schilling (1994) present a conceptual overview and notation for equity measures pertaining to facility location problems. The authors defined equity as each group receiving its fair share of the effect of the facility locating decision. Ogryczak (2000) introduces the concept of equitable efficiency, which links problems to the theories of inequitably measurement using the location problem. Later, Kostreva *et al.* (2003) discuss the concept of equitably efficient solutions to multiple-criteria optimization problems and show that this concept is a specific refinement of Pareto-optimality via a capital budgeting problem illustration. Singh (2007) further develops techniques to find equitably efficient solutions using equitable aggregations. Vitoriano *et al*. (2011) consider a problem in the response phase of humanitarian operations and develop a multiple-objective model that incorporates equity as a criterion in support of the aid distribution. The proportion of satisfied demand at each node is used as an equity measure in their study.

Minimax, maximin, and maxisum techniques are frequently used in equity- or fairness-related research. Luss (1999) studies a resource allocation problem in which it is desirable to allocate limited resources equitably among competing activities using a lexicographic minimax approach. The author points out that it is called *equitable* if no performance function value can be improved without either violating a constraint or degrading an already equal or worse-off performance function value that is associated with a different activity. Further, maximin and lexicographic maximin objectives analogous to minimax and lexicographic minimax approaches are discussed. That is, while the lexicographic minimax objective determines equitable solutions for problems where a smaller performance function value is considered better, the lexicographic maximin applies to the case when a larger performance function value is considered better. Zhu *et al.* (2010) also use a minimax approach to solve an equitable resource allocation problem with multiple depots. The objective is set such that the maximum rate of unsatisfied demand among all nodes is minimized.

Further, the maximin approach has also been applied in several problems (e.g., Kaplan 1973, Tang 1987, Zhang and Melachrinoudis 1999, Salles and Barria 2008, and Sayin 2013). Kaplan (1973) initially discusses the concept of a maximin objective function and shows that it can be transformed and solved by linear programming. Tang (1987) presents manufacturing problems formulated as special cases of the maximin allocation problem. Salles and Barria (2008) formulate the bandwidth allocation problem and employ the lexicographic maximin criterion to return a solution that satisfies both fairness and efficiency properties. The authors find that while this approach guarantees desirable features for the allocation of network resources such as fairness and efficiency, it requires complex optimization procedures and significant computational time to find a solution. Maximin and maxisum approaches also are discussed in the undesirable facility location problem (e.g., Zhang and Melachrinoudis 1999 and Sayin 2013). Sayin (2013) presents a mixed-integer programming formulation for an undesirable facility location problem wherein a facility of undesirable nature is to be located (e.g., nuclear power plant) and suggests that maximizing the minimum distance to existing sites (maximin) or maximizing the sum of distances (maxisum) may be appropriate.

In the emergency management literature, the problems are categorized according to pre- and post-disaster events in the disaster management cycle (McLoughlin 1985). Several researchers have recently published OR-based literature review papers and segmented the literature based on this cycle (e.g., Caunhye *et al.* 2012, Celik *et al.* 2012, and Galindo and Batta 2013). They suggest similarly that future research is needed in the area of post-disaster operations with specific focus on disaster recovery, long-term development, integrated phases of the disaster management cycle, and models considering the effects of multiple disasters. The National Hazards Center (2006) and FEMA (2011) suggest that disaster recovery planning should start before a disaster since pre-disaster activities have been shown to have a dramatic impact upon a community's ability to respond. For example, in disaster-prone regions, communities can pre-plan debris removal and utility restoration enabling speed and a successful recovery plan by having the necessary processes and protocols in place prior to a disaster. This suggestion highlights the importance of post-disaster model integration.

Literature involving mathematical models to alleviate the issues in post-disaster relief operations typically considers problems in each phase individually (e.g., Matisziw *et al*. 2009 and Viroriano *et al*. 2011). However, some recent attempts consider phase-integrating models (e.g. Balcik *et al.* 2008 and Celik *et al*. 2012). Matisziw *et al.* (2009) focus on the recovery phase via a telecommunication network restoration problem. Decision variables to restore disrupted nodes and arcs in a multi-period problem are included in their work. Viroriano *et al.* (2011) develop a goal programming model for the response phase based on loads and vehicles to support the aid distribution problem. Balcik *et al.* (2008) develop an integrated preparedness and response model for a last mile distribution system in which a local DC stores inventories and distributes emergency relief supplies to a number of demand locations. Finally, Celik *et al*. (2012) discuss an integrated approach to combine two models: a medical response model (response) and a debris clearance model (recovery). Considering that integrated models for analyzing disaster relief management are scarce and that an integrated model that captures both the supply distribution problem during response and the network restoration problem during recovery does not exist, we present such a model in this chapter.

2.3 A Multiple-Objective Integrated Response and Recovery (MOIRR) Model

Multiple-criteria mathematical programming models (MCMP) can be solved by either preemptive or non-preemptive methods (Ignizio and Cavalier 1993, Ravindran 2007). In a preemptive approach, if the decision maker provides the objectives in priority order (e.g., the first objective has the highest priority p_1, the second objective has the second highest priority p_2, etc.), the model can be solved by sequential optimization. On the other hand, under a non-preemptive approach, the model is formulated with importance factors or criteria weights for each objective (e.g., the first objective has associated weight w_1, the second objective has associated weight w_2, etc.). It follows that the model can be solved as a single, linear (weighted) objective model.

Common techniques to formulate and solve MCMP models include criteria normalization and criteria weight computations (Ravindran 2007). When criteria have different units of measure, the relative rating of alternatives may change merely because of their units of measures' scales. Therefore, criteria normalization methods (e.g., linear normalization, vector normalization, the use of 10 raised to an appropriate power, etc.) can be used to allow inter-criterion comparison. Further, several methods (e.g., weights from ranks, rating method, ratio weighting method, etc.) can be used to compute weights proportional to the relative values of unit changes in criteria value functions.

2.3.1 MOIRR Model Formulation

Both response-phase supply distribution options and recovery-phase network restoration decisions to reestablish services in a damaged network to pre-disruption performance levels so that relief supplies can be transported to affected areas are considered in our problem. We present our model formulation and demonstrate how it is solved as a weighted objective model with linear normalization. The model is intended to provide decision makers with a set of strategic restoration plans for disrupted nodes and arcs in a network such that relief items can be equitably supplied to those in need.

2.3.1.1 Notation

<u>Sets</u>

$G(N, A)$	Graph consisting of nodes N and arcs A
N	Set of nodes
A	Set of arcs
S	Set of supply port nodes $\in N$
T	Set of transhipment (relief warehouse) nodes $\in N$
D	Set of demand/beneficiary nodes $\in N$
S^F	Set of functional supply port nodes $\in S$
S^D	Set of disrupted supply port nodes $\in S$
T^F	Set of functional transhipment (relief warehouse) nodes $\in T$
T^D	Set of disrupted transhipment (relief warehouse) nodes $\in T$
Λ	Set of arcs between supply port and relief warehouse nodes $\in A$
Π	Set of arcs between relief warehouse and demand/beneficiary nodes $\in A$
Λ^F	Set of functional arcs between supply port and warehouse nodes $\in \Lambda$
Λ^D	Set of disrupted arcs between supply port and warehouse nodes $\in \Lambda$
Π^F	Set of functional arcs between relief warehouse and demand nodes $\in \Pi$
Π^D	Set of disrupted arcs between relief warehouse and demand nodes $\in \Pi$
Γ^N	Set of disrupted nodes, where $\Gamma^N = S^D \cup T^D$
Γ^A	Set of disrupted arcs, where $\Gamma^A = \Lambda^D \cup \Pi^D$

<u>Parameters</u>

s_i	Supply units available at each supply port node $i \in S$
d_i	Demand units required at each demand/beneficiary node $i \in D$
α_i	Relief warehouse capacity for each relief warehouse node $i \in T$
$\delta_{i,j}^{ST}$	Road capacity for each arc between port and warehouse node $(i, j) \in \Lambda$
$\delta_{i,j}^{TD}$	Road capacity for each arc between warehouse and demand $(i, j) \in \Pi$
φ_i	Capacity needed for each unit flow to use relief warehouse node $i \in T$

$\psi_{i,j}^{ST}$ Capacity needed for each unit flow to use road (arc) between supply port and relief warehouse node *(i, j)* ∈ Λ

$\psi_{i,j}^{TD}$ Capacity needed for each unit flow to use road (arc) between relief warehouse and demand/beneficiary node *(i, j)* ∈ Π

$c_{i,j}$ Cost for transporting each unit flow per mile through each arc *(i, j)* ∈ *A*

η_i^S Cost for restoring each disrupted supply port node $i \in S^D$

η_i^T Cost for restoring each disrupted relief warehouse node $i \in T^D$

$\lambda_{i,j}^{ST}$ Cost for restoring each disrupted arc between supply port and relief warehouse node *(i, j)* ∈ Λ^D

$\lambda_{i,j}^{TD}$ Cost for restoring each disrupted arc between relief warehouse and demand/beneficiary node *(i, j)* ∈ Π^D

b^N Budget for total disrupted node restoration

b^A Budget for total disrupted arc restoration

b^F Budget for total network flow transportation

ν^S Fixed charge for restoring disrupted supply port node

ν^T Fixed charge for restoring disrupted relief warehouse node

ω^{ST} Fixed charge for restoring disrupted arc between supply port and relief warehouse node

ω^{TD} Fixed charge for restoring disrupted arc between relief warehouse and demand/beneficiary node

θ^N Maximum allowable number for disrupted node restoration

θ^A Maximum allowable number for disrupted arc restoration

$d_{i,j}^{OD}$ Distance in miles between each origin and destination pair *(i, j)* ∈ *A*

w_i Important weight setting associated with objective *i*

<u>*Decision Variables*</u>

$X_{i,j}$ Commodity flow integer variable for supplies through arc *(i, j)* ∈ *A*

K_i Binary variable to restore disrupted supply port node $i \in S^D$

L_i Binary variable to restore disrupted relief warehouse node $i \in T^D$

$M_{i,j}$ Binary variable to restore disrupted arc between port and warehouse *(i, j)* $\in \Lambda^D$

$N_{i,j}$ Binary variable to restore disrupted arc between relief warehouse and demand/beneficiary *(i, j)* $\in \Pi^D$

R_i Units of unsatisfied unit variable for each demand node $i \in D$

V Minimum percentage of satisfied demand

Y_i^S Binary variable for setup cost to restore disrupted supply port $i \in S^D$

Y_i^T Binary variable for setup cost to restore disrupted warehouse $i \in T^D$

$Y_{i,j}^{ST}$ Binary variable for setup cost to restore disrupted arc between supply port and warehouse *(i, j)* $\in \Lambda^D$

$Y_{i,j}^{TD}$ Binary variable for setup cost to restore disrupted arc between relief warehouse and demand *(i, j)* $\in \Pi^D$

2.3.1.2 Formulation

The first objective function in the model is to maximize equity or fairness modelled using maximin approach. This can be modelled as a linear program to compute the minimum percentage of satisfied demand.

$$\text{Maximize } V \tag{2.1}$$

$$\text{Subject to } \quad V \leq \left(\sum_{i \in T} \frac{X_{i,j}}{d_j} \right) 100 \qquad ; \forall \ j \in D \tag{2.2}$$

The second objective is to minimize total unsatisfied demand. It can be defined as the sum of unsatisfied units across all demand/beneficiary nodes.

$$\text{Minimize} \left(\sum_{i \in D} R_i \right) \tag{2.3}$$

The third objective is to minimize the total network cost calculated as the funds spent to restore disrupted nodes, restore disrupted arcs, and transport supply units based on origin-destination (O-D) pair information.

$$\text{Minimize} \quad \begin{array}{l} \left(\sum_{i\in S^D} \eta_i^S K_i\right)+\left(\sum_{i\in T^D} \eta_i^T L_i\right)+\left(\sum_{i\in S^D} \nu^S Y_i^S\right)+\left(\sum_{i\in T^D} \nu^T Y_i^T\right)+\cdots \\ \left(\sum_{(i,j)\in \Lambda^D} \lambda_{i,j}^{ST} M_{i,j}\right)+\left(\sum_{(i,j)\in \Pi^D} \lambda_{i,j}^{TD} N_{i,j}\right)+\left(\sum_{(i,j)\in \Lambda^D} \omega^{ST} Y_{i,j}^{ST}\right)+\left(\sum_{(i,j)\in \Pi^D} \omega^{TD} Y_{i,j}^{TD}\right)+\cdots \\ \left(\sum_{(i,j)\in A} c_{i,j} d_{i,j}^{OD} X_{i,j}\right) \end{array} \qquad (2.4)$$

Objective functions (2.1), (2.3), and (2.4) can be normalized using a linear normalization technique to allow inter-criterion comparison. This technique converts objectives to a range between 0 and 1 based on ideal and anti-ideal solutions. Then, the weighted objective method can be applied. The objective functions can be formulated as a single linear maximization objective function as

$$\text{Maximize} \quad w_1\left(\frac{(1)-L_1^*}{H_1^*-L_1^*}\right)+w_2\left(\frac{L_2^*-(3)}{L_2^*-H_2^*}\right)+w_3\left(\frac{L_3^*-(4)}{L_3^*-H_3^*}\right) \qquad (2.5)$$

In (2.5), we note the following definitions:

H_j^* is an ideal solution (i.e., Max $C_j(x)$ for benefit and Min $C_j(x)$ for cost criteria)

L_j^* is an anti-ideal solution (i.e., Min $C_j(x)$ for benefit and Max $C_j(x)$ for cost criteria)

$\frac{C_j(x)-L_j^*}{H_j^*-L_j^*}$ is a normalized term for benefit criterion and $\frac{L_j^*-C_j(x)}{L_j^*-H_j^*}$ is a normalized term for cost criterion

$\sum_{1}^{3} w_i = 1$.

Now that the model's objection function has been established, we turn our focus to developing the model's constraints.

$$\left(\sum_{(i,j)\in A} c_{i,j} d_{i,j}^{OD} X_{i,j} \right) \leq b^F \tag{2.6}$$

$$\left(\sum_{i\in S^D} \eta_i^S K_i \right) + \left(\sum_{i\in T^D} \eta_i^T L_i \right) + \left(\sum_{i\in S^D} \nu^S Y_i^S \right) + \left(\sum_{i\in T^D} \nu^T Y_i^T \right) \leq b^N \tag{2.7}$$

$$\left(\sum_{(i,j)\in \Lambda^D} \lambda_{i,j}^{ST} M_{i,j} \right) + \left(\sum_{(i,j)\in \Pi^D} \lambda_{i,j}^{TD} N_{i,j} \right) + \left(\sum_{(i,j)\in \Lambda^D} \omega^{ST} Y_{i,j}^{ST} \right) + \left(\sum_{(i,j)\in \Pi^D} \omega^{TD} Y_{i,j}^{TD} \right) \leq b^A \tag{2.8}$$

Constraint set (2.6) ensures that the transportation cost computed based on the O-D pair for all commodities through the network does not exceed the available transportation budget. Constraint sets (2.7) and (2.8) also ensure that restoration costs inclusive of setup cost for disrupted nodes and arcs will not exceed the restoration budgets.

$$\sum_{i\in T} X_{i,j} + R_j = d_j \qquad ;\forall\ j \in D \tag{2.9}$$

Further, demand may not necessarily be satisfied. Constraint set (2.9) is modeled such that demand uncertainty can be accommodated (e.g., demand is higher or lower than supply units).

$$\sum_{j\in T} X_{i,j} \leq s_i \qquad ;\forall\ i \in S^F \tag{2.10}$$

$$\sum_{j \in T} X_{i,j} \leq s_i K_i \qquad ; \forall\, i \in S^D \tag{2.11}$$

Constraint sets (2.10) and (2.11) ensure that the units flowing out of supply nodes do not exceed available supply. While supply items are available for functional supply nodes, supply items for disrupted supply nodes will be available if and only if they are restored by the model.

$$\sum_{i \in S} X_{i,j} - \sum_{k \in D} X_{j,k} = 0 \qquad ; \forall\, j \in T \tag{2.12}$$

Constraint set (2.12) is a flow conservation constraint ensuring that unit flows out of and in to each relief warehouse are equal.

$$\sum_{i \in S} \varphi_j X_{i,j} \leq \alpha_j \qquad ; \forall\, j \in T^F \tag{2.13}$$

$$\sum_{i \in S} \varphi_j X_{i,j} \leq \alpha_j L_j \qquad ; \forall\, j \in T^D \tag{2.14}$$

Relief warehouse capacities are restricted by constraint sets (2.13) and (2.14), as capacities at a relief warehouse node are available only when the node is functional.

$$\psi_{i,j}^{ST} X_{i,j} \leq \delta_{i,j}^{ST} \qquad ; \forall\, (i,j) \in \Lambda^F \tag{2.15}$$

$$\psi_{i,j}^{ST} X_{i,j} \leq \delta_{i,j}^{ST} M_{i,j} \qquad ; \forall\, (i,j) \in \Lambda^D \tag{2.16}$$

$$\psi_{i,j}^{TD} X_{i,j} \leq \delta_{i,j}^{TD} \qquad ; \forall\, (i,j) \in \Pi^F \tag{2.17}$$

$$\psi_{i,j}^{TD} X_{i,j} \leq \delta_{i,j}^{TD} N_{i,j} \qquad ; \forall\, (i,j) \in \Pi^D \tag{2.18}$$

Constraint sets (2.15) and (2.16) restrict road capacities between a supply node and relief warehouse nodes and ensure that road capacities are available only if these roads are functional. Constraint sets (2.17) and (2.18) similarly restrict road capacities between a relief warehouse and demand nodes.

$$K_j \leq Y_j^S \qquad ;\forall\ j \in S^D \tag{2.19}$$

$$L_j \leq Y_j^T \qquad ;\forall\ j \in T^D \tag{2.20}$$

$$M_{i,j} \leq Y_{i,j}^{ST} \qquad ;\forall\ (i,j) \in \Lambda^D \tag{2.21}$$

$$N_{i,j} \leq Y_{i,j}^{TD} \qquad ;\forall\ (i,j) \in \Pi^D \tag{2.22}$$

Constraint sets (2.19) through (2.22) ensure that setup costs are incurred when restoration decisions for a disrupted supply point (2.19), a disrupted warehouse (2.20), a disrupted arc between a supply point and a warehouse (2.21), and a disrupted arc between a warehouse and demand nodes are made by the model (2.22).

$$\sum_{j \in S^D} K_j + \sum_{j \in T^D} L_j \leq \theta^N \tag{2.23}$$

$$\sum_{(i,j) \in \Lambda^D} M_{i,j} + \sum_{(i,j) \in \Pi^D} N_{i,j} \leq \theta^A \tag{2.24}$$

Constraint sets (2.23) and (2.24) limit the maximum allowable number of disrupted nodes and disrupted arcs that can be restored based on available resources. Finally, constraint sets (2.25) through (2.35) are variable-type constraints.

$X_{i,j} = \{0,1,2,\ldots,n\} \qquad ;\forall\ (i,j) \in A$ (2.25), $\quad K_i = \{0,1\} \qquad ;\forall\, i \in S^D$ (2.26)

$L_i = \{0,1\} \qquad ; \forall\, i \in T^D \qquad (2.27), \qquad M_{i,j} = \{0,1\} \qquad ; \forall\, (i,j) \in \Lambda^D \qquad (2.28)$

$N_{i,j} = \{0,1\} \qquad ; \forall\, (i,j) \in \Pi^D \qquad (2.29), \qquad R_i \geq 0 \qquad ; \forall\, i \in D \qquad (2.30)$

$V \geq 0 \qquad (2.31), \qquad Y_i^S = \{0,1\} \qquad ; \forall\, i \in S^D \qquad (2.32)$

$Y_i^T = \{0,1\} \qquad ; \forall\, i \in T^D \qquad (2.33), \qquad Y_{i,j}^{ST} = \{0,1\} \qquad ; \forall\, (i,j) \in \Lambda^D \qquad (2.34)$

$$Y_{i,j}^{TD} = \{0,1\} \qquad ; \forall\, (i,j) \in \Pi^D \qquad (2.35)$$

2.3.2 Model Experimentation

Initial toy problems were created and solved both manually and by the proposed model to verify and validate the model's functionality. Once model validity was determined, we shifted our focus to various scenario-based experiments based on discussions with emergency relief decisions makers and our review of the open literature.

2.3.2.1 Experiment 1: Pooled vs. Separate Budgets

Our first set of experiments investigates the cases of 1) when budgets for restoration and transportation are pooled together (e.g., one decision maker authorizes all the budgets) vs. 2) individually specified restoration and transportation budgets. Mathematically, this can be accomplished by combining constraint sets (2.6), (2.7), and (2.8) as follows:

$$\left[\begin{array}{l}\left(\sum_{(i,j)\in A} c_{i,j} d_{i,j}^{OD} X_{i,j}\right)+\cdots \\ \left(\sum_{i\in S^D} \eta_i^S K_i\right)+\left(\sum_{i\in T^D} \eta_i^T L_i\right)+\left(\sum_{i\in S^D} \nu^S Y_i^S\right)+\left(\sum_{i\in T^D} \nu^T Y_i^T\right)+\cdots \\ \left(\sum_{(i,j)\in \Lambda^D} \lambda_{i,j}^{ST} M_{i,j}\right)+\left(\sum_{(i,j)\in \Pi^D} \lambda_{i,j}^{TD} N_{i,j}\right)+\left(\sum_{(i,j)\in \Lambda^D} \omega^{ST} Y_{i,j}^{ST}\right)+\left(\sum_{(i,j)\in \Pi^D} \omega^{TD} Y_{i,j}^{TD}\right)\end{array}\right] \le \left(b^F+b^N+b^A\right) \tag{2.36}$$

While the separate budgeting approach typically reflects the reality of how budgets are approved and distributed for individual organization, the pooled budgeting approach can provide decision makers which additional flexibility.

2.3.2.2 Experiment 2: Partial vs. Full Restoration

Our second experiment illustrates the scenario that occurs when a decision maker is allowed to restore a disrupted node partially (i.e., in some fractional amount) or in full (i.e., an all-or-nothing approach). In this analysis, we restrict disrupted supply points to be fully restored if at all. For a relief warehouse node, we allow the model to choose to restore either half or a whole disrupted node. For all disrupted arcs, which assumed to represent four-lane highways, we allow the model to restore one, two, three, or all four lanes. To accomplish this, we add the following parameters, decision variables, and constraint sets to the model:

<u>*Parameters*</u>

f_i^{T1} 50% fractional restoration for disrupted warehouse node $i \in T^D$

f_i^{T2} 100% fractional restoration for disrupted warehouse node $i \in T^D$

$f_{i,j}^{ST1}$ 25% fractional restoration for damaged arc between supply port and relief warehouse node (i, j) $\in \Lambda^D$

$f_{i,j}^{ST2}$ 50% fractional restoration for damaged arc between supply port and relief warehouse node (i, j) ∈ Λ^{D}

$f_{i,j}^{ST3}$ 100% fractional restoration for damaged arc between supply port and relief warehouse node (i, j) ∈ Λ^{D}

$f_{i,j}^{TD1}$ 25% fractional restoration for damaged arc between relief warehouse and demand node (i, j) ∈ Π^{D}

$f_{i,j}^{TD2}$ 50% fractional restoration for damaged arc between relief warehouse and demand node (i, j) ∈ Π^{D}

$f_{i,j}^{TD3}$ 100% fractional restoration for damaged arc between relief warehouse and demand node (i, j) ∈ Π^{D}

Decision Variables

L_{i} Continuous variable to partially restore disrupted warehouse node $i \in T^{D}$

$M_{i,j}$ Continuous variable to partially restore disrupted arc between supply port and relief warehouse node (i, j) ∈ Λ^{D}

$N_{i,j}$ Continuous variable to partially restore disrupted arc between relief warehouse and demand node (i, j) ∈ Λ^{D}

Q_{i}^{T1} Binary variable to restrict 50% restoration for disrupted warehouse node $i \in T^{D}$

Q_{i}^{T2} Binary variable to restrict 100% restoration for disrupted warehouse node $i \in T^{D}$

$Q_{i,j}^{ST1}$ Binary variable to restrict 25% restoration for disrupted arc between supply port and relief warehouse node (i, j) ∈ Λ^{D}

$Q_{i,j}^{ST2}$ Binary variable to restrict 50% restoration for disrupted arc between supply port and relief warehouse node (i, j) ∈ Λ^{D}

$Q_{i,j}^{ST3}$ Binary variable to restrict 100% restoration for disrupted arc between supply port and relief warehouse node (i, j) ∈ Λ^{D}

$Q_{i,j}^{TD1}$ Binary variable to restrict 25% restoration for disrupted arc between relief warehouse and demand node (i, j) ∈ Π^{D}

$Q_{i,j}^{TD2}$ Binary variable to restrict 50% restoration for disrupted arc between relief warehouse and demand node (i, j) ∈ Π^{D}

$Q_{i,j}^{TD3}$ Binary variable to restrict 100% restoration for disrupted arc between relief warehouse and demand node (i, j) ∈ Π^{D}

Constraint Sets

$$L_i = f_i^{T1} Q_i^{T1} + f_i^{T2} Q_i^{T2} \qquad ; \forall\ i \in T^{D} \tag{2.37}$$

$$L_i \le f_i^{T2} \qquad ; \forall\ i \in T^{D} \tag{2.38}$$

Constraint sets (2.37) and (2.38) combine to restrict the new decision variables to partially restore a disrupted relief warehouse node at two levels: 50% or 100%.

$$M_{i,j} = f_{i,j}^{ST1} Q_{i,j}^{ST1} + f_{i,j}^{ST2} Q_{i,j}^{ST2} + f_{i,j}^{ST3} Q_{i,j}^{ST3} \qquad ; \forall\ (i, j) \in \Lambda^{D} \tag{2.39}$$

$$M_{i,j} \le f_{i,j}^{ST3} \qquad ; \forall\ (i, j) \in \Lambda^{D} \tag{2.40}$$

$$N_{i,j} = f_{i,j}^{TD1} Q_{i,j}^{TD1} + f_{i,j}^{TD2} Q_{i,j}^{TD2} + f_{i,j}^{TD3} Q_{i,j}^{TD3} \qquad ; \forall\ (i, j) \in \Pi^{D} \tag{2.41}$$

$$N_{i,j} \le f_{i,j}^{TD3} \qquad ; \forall\ (i, j) \in \Pi^{D} \tag{2.42}$$

Constraint sets (2.39) and (2.40) allow partially disrupted arcs between a supply point and a relief warehouse to be restored at four levels: 25%, 50%, 75%, or 100%. Similarly, constraint sets (2.41) and (2.42) restrict the new decision variables to partially restore disrupted arcs between relief warehouses and demand nodes.

$$L_i \ge 0 \qquad ; \forall\ i \in T^{D} \tag{2.43}$$

$$M_{i,j} \ge 0 \qquad ; \forall\ (i, j) \in \Lambda^{D} \tag{2.44}$$

$$N_{i,j} \ge 0 \qquad ; \forall\ (i, j) \in \Pi^{D} \tag{2.45}$$

Original constraint sets (2.27), (2.28), and (2.29) are modified to become (2.43), (2.44), and (2.45), respectively, so that the model can restore a disrupted relief warehouse, a disrupted arc between a supply point and a relief warehouse, and a disrupted arc between a relief warehouse and a demand node. Finally, constraint sets (2.46) through (2.53) restrict the new decision variables to be binary.

$$Q_i^{T1} = \{0,1\} \quad ;\forall\, i \in T^D \quad (2.46), \qquad Q_i^{T2} = \{0,1\} \quad ;\forall\, i \in T^D \quad (2.47)$$

$$Q_{i,j}^{ST1} = \{0,1\} \quad ;\forall\, (i,j) \in \Lambda^D \quad (2.48), \qquad Q_{i,j}^{ST2} = \{0,1\} \quad ;\forall\, (i,j) \in \Lambda^D \quad (2.49)$$

$$Q_{i,j}^{ST3} = \{0,1\} \quad ;\forall\, (i,j) \in \Lambda^D \quad (2.50), \qquad Q_{i,j}^{TD1} = \{0,1\} \quad ;\forall\, (i,j) \in \Pi^D \quad (2.51)$$

$$Q_{i,j}^{TD2} = \{0,1\} \quad ;\forall\, (i,j) \in \Pi^D \quad (2.52), \qquad Q_{i,j}^{TD3} = \{0,1\} \quad ;\forall\, (i,j) \in \Pi^D \quad (2.53)$$

2.3.3 MOIRR Complexity

The complexity of the proposed MOIRR model is assessed through a reduction technique (Karp 1972). Initially, the set of disrupted nodes and disrupted arcs can be set to null, which results in a fully operational network (i.e., S^D, T^D, Λ^D, and $\Pi^D = \varnothing$). It follows that Γ^N and $\Gamma^A = \varnothing$, which make all sets represent only functional network elements ($S^F = S$, $T^F = T$, $\Lambda^F = \Lambda$, and $\Pi^F = \Pi$). Then, several parameters (η_i^S, η_i^T, $\lambda_{i,j}^{ST}$, $\lambda_{i,j}^{TD}$, b^N, b^A, ν^S, ν^T, ω^{ST}, ω^{TD}, θ^N, and θ^A) and decision variables (K_i, L_i, $M_{i,j}$, $N_{i,j}$, Y_i^S, Y_i^T, $Y_{i,j}^{ST}$, and $Y_{i,j}^{TD}$) associated with disruption and restoration are discarded from the model: constraint sets (11), (14), (16), and (18) associated with node and arc disruption; constraint sets (19)-(22) associated with restoration setup cost; constraint sets (23)-(24) associated with maximum allowable restoration number; and constraint sets (26)-(29) and (32)-(35) associated with restoration binary variables. Finally, the third objective function (4) is revised such that only the transportation cost term is included.

The revised model is therefore reduced to a maximum concurrent flow problem (MCFP). We note that while the simplest multi-commodity flow problem (MFP) is the maximum multi-commodity flow problem (MMFP), a more complex variation is the MCFP (Karakostas 2008). As the parameters (s_i, d_i, α_i, $\delta_{i,j}^{ST}$, $\delta_{i,j}^{TD}$, φ_i, $\psi_{i,j}^{ST}$, $\psi_{i,j}^{TD}$, $c_{i,j}$, b^F, and $d_{i,j}^{OD}$) and variables ($X_{i,j}$ and R_i) for unit flows, capacity, cost, budget, and distance in the model are integral values, the problem further reduces to the multi-commodity integral flow problem (MIFP), which is known to be NP-complete (Even *et al.* 1976, Karp 1975). Therefore, through this reduction argument, the complexity of MOIRR is NP-hard: $MOIRR \propto MCFP \propto MIFP$.

2.3.4 Model Validation

In order to gain initial insights into significant model factors, we conduct a full factorial experimental design on three factors at two levels each: restoration type (full and partial), budget spending approach (pooled and separate), and network size (small and large). Full restoration uses an all-or-nothing approach allowing either only full restoration for any disrupted node or arc, while partial restoration allows for fractional restoration. The pooled budget factor level pools all budgeted funds for transportation, node restoration, and arc restoration together, while the separate budget level considers each category separately. Finally, the small network contains at most 45 nodes, while the large network contains at most 450 nodes. In total, there are eight experimental scenarios of interest:

- Base Scenario: full restoration, separate budget, small network
- Scenario 1: full restoration, separate budget, large network
- Scenario 2: full restoration, pooled budget, small network
- Scenario 3: full restoration, pooled budget, large network
- Scenario 4: partial restoration, separate budget, small network
- Scenario 5: partial restoration, separate budget, large network
- Scenario 6: partial restoration, pooled budget, small network
- Scenario 7: partial restoration, pooled budget, large network

The MOIRR is modeled in AMPL (Fourer *et al.* 2002) and analyzed using CPLEX solver. We use the parameters in Table 2.1 to randomly generate 50 test data sets with different levels of disruption to test and verify model functionality. All data sets are analyzed on a PC with an Intel (R) Core (TM) i7- 2600 CPU @3.40 GHz and 16.0 GB of RAM. The maximum computational time limit allowed for the small and large network is 1200 and 3600 seconds for each data set, respectively.

2.3.4.1 Small-Sized Network Results

The percent demand satisfied (a surrogate measure for fairness) and required computational time are analyzed for small-size networks in four scenarios: base, 2, 4, and 6. The average percent demand satisfied and computational time across the data sets for these cases are shown in Table 2.2. Graphical comparisons for percent of demand satisfied and required computational time for the small network scenarios are shown in Figure 2.1(a) and Figure 2.1(b), respectively, for all 50 test data sets. The percent of satisfied demand (fairness) fluctuates across these data sets primarily due to the randomness of network disruption. In terms of computation time, although lesser restoration costs result from partial restoration, partial restoration-based models (scenarios 4 and 6) require higher computational time. Intuitively, this trade-off exists as more variables are required in the partial restoration scenarios.

2.3.4.2 Large-Sized Network Results

A similar comparison for large-sized networks is conducted using scenarios 1 3, 5, and 7. The average percent of demand satisfied and computational time across data sets for these models are also shown in Table 2.2. Figure 2.2(a) and Figure 2.2(b) graphically illustrate the percent demand satisfied and required computation time across the 50 test data sets for all large network scenarios. It is clear that scenarios 3 and 7 that use pooled budgeting provide a much higher percent demand satisfaction than do scenarios 1 and 5 that employ separate budgeting. The pooled budget approach provides flexibility across organizations, given that budget parameters are limited in the larger network that contains comparably higher levels of disruption. Further, computation time, while fluctuating across the large network test data sets, increases with problem size as expected due to the NP-hard complexity of the MOIRR model.

Table 2.1: Parameters for an experimental design.

Activities	Symbol	Parameters
Supply relief port node		
Number of supply port nodes	S	Uniform (1,5)[a]
Number of disrupted supply port nodes	S^D	Random
Supply units available at each supply port node	s_i	Uniform (30000, 50000)
Cost for restoring each disrupted supply port node	η_i^s	Uniform (400000, 600000)
Relief warehouse node		
Number of transhipment (relief warehouse) nodes	T	Uniform (3,10)[a]
Number of disrupted transhipment (relief warehouse) nodes	T^D	Random
Capacity for each transhipment (relief warehouse) node	α_i	Uniform (50000, 100000)
Capacity needed for each unit flow to use relief warehouse node	φ_i	Uniform (1,2)
Cost for restoring each disrupted relief warehouse node	η_i^T	Uniform (400000, 600000)
Demand node		
Number of demand/ beneficiary nodes	D	Uniform (10,30)[a]
Demand units required at each demand/ beneficiary node	d_i	Uniform (5000, 10000)
Arc between supply port and relief warehouse nodes		
Number of disrupted arcs between supply port and relief warehouse nodes	Λ^D	Random
Road capacity for each arc between port and relief warehouse node	$\delta_{i,j}^{ST}$	Uniform (20000, 30000)
Capacity needed to use road (arc) between supply port and relief warehouse node	$\psi_{i,j}^{ST}$	Uniform (1,2)
Cost for transporting each unit flow per mile through each arc	$c_{i,j}$	Uniform (5,10)
Cost for restoring each disrupted arc between supply port and relief warehouse node	$\lambda_{i,j}^{ST}$	Uniform (100000, 200000)
Arc between relief warehouse and demand nodes		
Number of disrupted arcs between relief warehouse and demand nodes	Π^D	Random
Road capacity for each arc between warehouse and demand node	$\delta_{i,j}^{TD}$	Uniform (10000, 20000)
Capacity needed to use road (arc) between warehouse and demand node	$\psi_{i,j}^{TD}$	Uniform (1,2)
Cost for transporting each unit flow per mile through each arc	$c_{i,j}$	Uniform (5,10)
Cost for restoring each disrupted arc between warehouse and demand node	$\lambda_{i,j}^{TD}$	Uniform (100000, 200000)
Others		
Budget for total disrupted node restoration	b^N	Uniform (1000000, 3000000)
Budget for total disrupted arc restoration	b^A	Uniform (1000000, 3000000)
Budget for total network flow transportation	b^F	Uniform (1000000, 3000000)

[a]Uniform (10, 50), Uniform (30, 100), and Uniform (100, 300) are replaced for supply, warehouse, and demand, respectively in large network size analysis.

Table 2.2: Average satisfied demand and computational time across data sets.

Scenario number	Restoration		Budgeting		Network size		Average satisfied demand (%)	Average computational time (s)
	Full	Partial	Separate	Pooled	Small	Large		
Base scenario	✓		✓		✓		59.54	24.7
Scenario 1	✓		✓			✓	13.86	2679.7
Scenario 2	✓			✓	✓		66.38	37.0
Scenario 3	✓			✓		✓	69.03	885.5
Scenario 4		✓	✓		✓		60.10	380.3
Scenario 5		✓	✓			✓	14.03	2930.0
Scenario 6		✓		✓	✓		66.38	378.8
Scenario 7		✓		✓		✓	69.03	1126.8

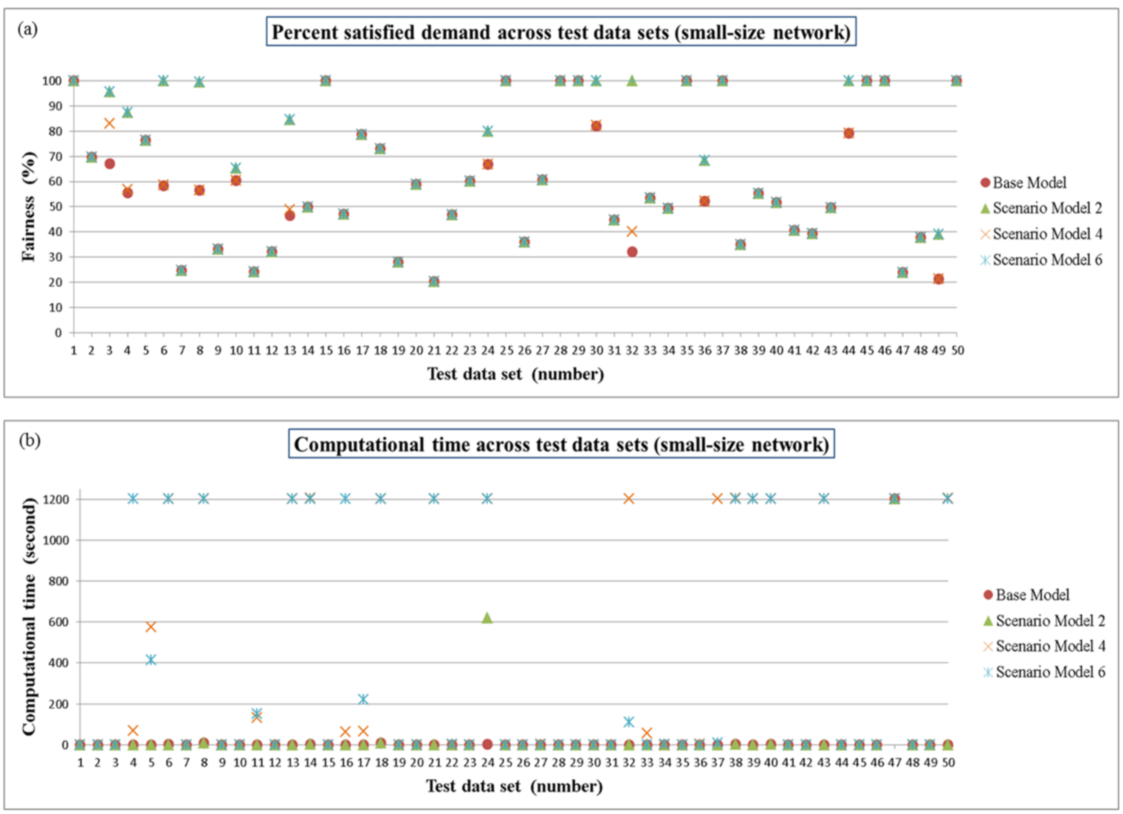

Figure 2.1: Results across data sets on small network: (a) fairness, (b) computational time.

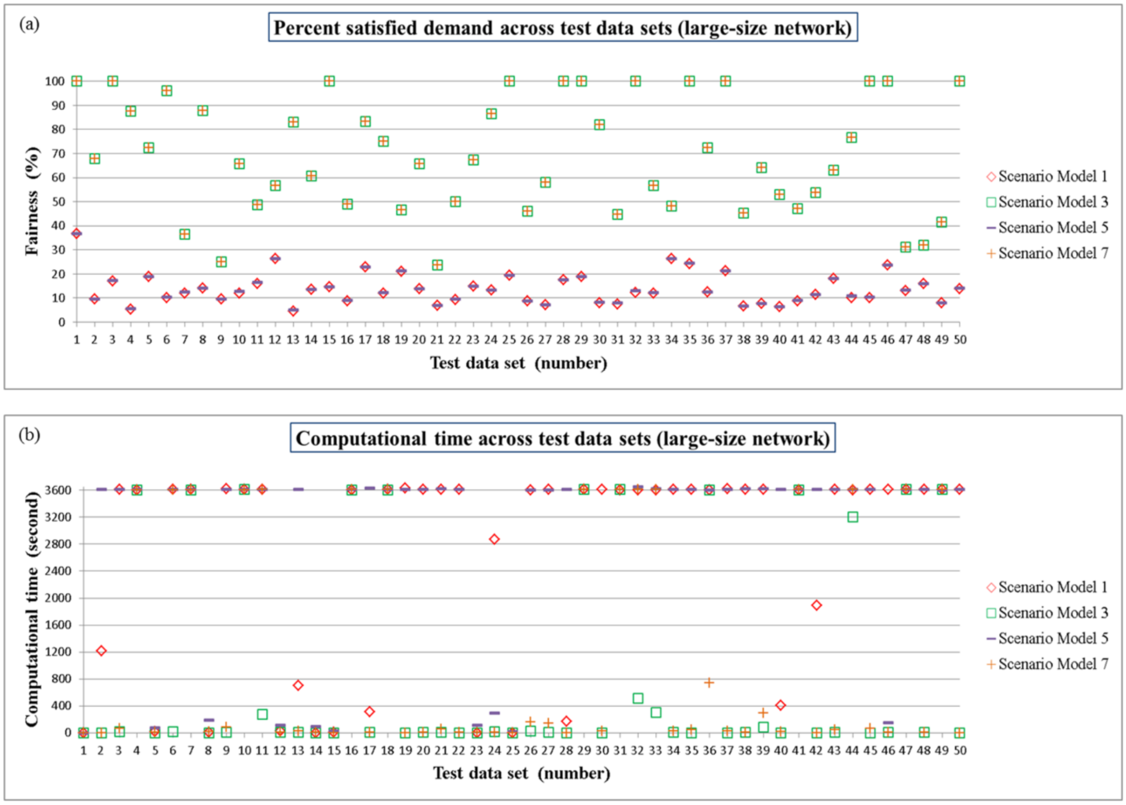

Figure 2.2 Results across data sets on large network: (a) fairness, (b) computational time.

2.4 HAZUS Case Study

2.4.1 Methodology, Assumptions, and Analysis

While researchers typically have issues with data acquisition for post-disaster operations, data is usually available in pre-disaster studies (e.g., inventory position, warehouse location) (Galindo and Batta 2013). We use FEMA's GIS-based natural hazard loss estimation software Hazus as a case study to illustrate the applicability of the MOIRR model. We generate a disaster instance with Hazus to obtain predicted loss data in a study region of interest in the United States: our university's home state of South

Carolina. Hazus requires both an inventory collection module and a hazard identification module as input to the natural hazard impact assessment module. Hazus then calculates its output in a risk evaluation module and the resulting Hazus loss data is then used as input to the MOIRR model.

The parameter data and necessary assumptions associated with our Hazus case study are given in Table 2.3. While most loss data can be obtained directly from Hazus, some parameters are extrapolated from available data. Six major South Carolina airports are chosen as relief supply points: Charleston, Columbia, Florence, Greenville, Hilton Head, and Myrtle Beach. Hazus's inventory collection module reports that there are 47 emergency operations centers (EOCs) in the state; we model them as relief warehouses.

To simulate a major disruption event, a 9.0 magnitude earthquake with 50 kilometer depth is modeled to occur in the Columbia, South Carolina metropolitan area (Latitude 33.89, Longitude 81.06). The Hazus loss data-related criteria are as follows: 5:00 pm is considered as the peak commute time; the affected population is based on single families and commuters, and Level 1 injuries occur requiring basic medical aid without hospitalization. Capacity-related data are extrapolated based on the size and infrastructure of selected supply points and warehouses. Census track-based demand data is obtained from Hazus's natural impact assessment module.

We illustrate how our MOIRR model works with Hazus loss data by setting the model with partial restoration and separate budgeting. Although pooled budget allows flexible operations with budgeted funds, current practice on how budgets are distributed depends on different organization's functions (Day, 2014). Further, equal objective weights are used implying that fairness, total unsatisfied demand, and total network cost have equal importance. CPLEX solver solves the case study optimally in 21.5 seconds. The main experimental results for detailed restoration and distributed supply information from the relief points are shown in Table 2.4. Further, Hazus-based “before and after” disaster instance maps are presented in Figure 2.3. Figure 2.3(a) presents the position of the earthquake, as well as the existing infrastructure in South Carolina inclusive of the six relief supply points and 47 relief warehouses. Then, Figure 2.3(b) shows loss data output from Hazus based on a chosen complete damage probability level of 70% or higher: one disrupted relief supply point, 16 disrupted relief warehouses, and 143 demand census tracks affected by the earthquake.

Table 2.3: Hazus-related assumption list.

Activities	Symbol	Category	Descriptive detail
Supply relief port node			
Number of supply port nodes	S	Hazus	
Number of disrupted supply port nodes	S^D	Hazus	
Cost for restoring each disrupted supply port node	η_i^S	Hazus	
Supply units available at each supply port node	s_i	Extrapolation	From port size and demand units
Fixed charge for restoring disrupted supply port node	ν^S	Extrapolation	From port node's restoration cost
Relief warehouse node			
Number of transhipment (relief warehouse) nodes	T	Hazus	
Number of disrupted transhipment (relief warehouse) nodes	T^D	Hazus	
Cost for restoring each disrupted relief warehouse node	η_i^T	Hazus	
Fixed charge for restoring disrupted relief warehouse node	ν^T	Extrapolation	From warehouse node's restoration cost
Capacity for each transhipment (relief warehouse) node	α_i	Extrapolation	From warehouse size (Hazus's inventory)
Capacity needed for each unit flow to use relief warehouse node	φ_i	Not available	1 unit assumption
Demand node			
Number of demand/ beneficiary nodes	D	Hazus	
Demand units required at each demand/ beneficiary node	d_i	Hazus	
Arc between supply port and relief warehouse nodes			
Cost for restoring each disrupted arc between supply port and warehouse node	$\lambda_{i,j}^{ST}$	Hazus	
Distance in miles between each origin and destination pair based on latitude/longitude	$d_{i,j}^{OD}$	Hazus	
Fixed charge for restoring disrupted arc between supply port and warehouse node	ω^{ST}	Extrapolation	From arc's restoration cost
Number of disrupted arcs between supply port and relief warehouse nodes	Λ^D	Not available	Randomly distributed; 30% disruption
Road capacity for each arc between port and relief warehouse node	$\delta_{i,j}^{ST}$	Not available	5000 unit assumption
Capacity needed to use road (arc) between supply port and relief warehouse node	$\psi_{i,j}^{ST}$	Not available	1 unit assumption
Cost for transporting each unit flow per mile through each arc	$c_{i,j}$	Not abailable	$15 per unit per mile assumption
Arc between relief warehouse and demand nodes			
Cost for restoring each disrupted arc between warehouse and demand node	$\lambda_{i,j}^{TD}$	Hazus	
Distance in miles between each origin and destination pair based on latitude/longitude	$d_{i,j}^{OD}$	Hazus	
Fixed charge for restoring disrupted arc between warehouse and demand node	ω^{TD}	Extrapolation	From arc's restoration cost
Number of disrupted arcs between relief warehouse and demand nodes	Π^D	Not available	Randomly distributed; 30% disruption
Road capacity for each arc between warehouse and demand node	$\delta_{i,j}^{TD}$	Not available	2500 unit assumption
Capacity needed to use road (arc) between warehouse and demand node	$\psi_{i,j}^{TD}$	Not available	1 unit assumption
Cost for transporting each unit flow per mile through each arc	$c_{i,j}$	Not available	$8 per unit per mile assumption
Others			
Budget for total disrupted node restoration	b^N	Extrapolation	Based on total node restoration cost
Budget for total disrupted arc restoration	b^A	Extrapolation	Based on total arc restoration cost
Budget for total network flow transportation	b^F	Extrapolation	Based on total transportation cost
Maximum allowable number for disrupted node restoration	θ^N	Not available	At most 8 node assumption
Maximum allowable number for disrupted arc restoration	θ^A	Not available	At most 300 arc assumption

Table 2.4: Key results from Hazus-based case study.

Objective function	Ideal solution[a]	Percent achieved from an ideal solution[b]
Percent fairness	75.01	95%
Total unsatisfied demand units	201496	95%
Total spent cost ($ million)	0	41%
Restoration decision	**Disrupted number**	**Percent restored from disrupted number**
Disrupted supply port node	1	100%
Disrupted relief warehouse node	16	44%
Disrupted arc between port and warehouse nodes	85	11%
Disrupted arc between warehouse and demand nodes	2017	0%

Supply unit decision from port (S) to warehouse (T)

	T1[c]	*T2*	*T3*	*T4*	*T5*[d]	*T6*	*T7*	*T8*[c]	*T9*[c]	*T10*	*T11*[c]	*T12*	*T13*	*T14*	*T15*[c]	*T16*
S1	5000	5000	0	5000	0	5000	5000	5000	5000	5000	5000	5000	5000	5000	0	5000
S2	0	0	2500	0	0	0	0	2500	0	5000	0	5000	5000	0	5000	5000
S3[c]	0	0	5000	5000	0	0	0	0	2500	0	0	5000	0	5000	0	0
S4	0	0	0	0	0	0	5000	5000	0	0	5000	5000	0	0	5000	0
S5	5000	5000	0	0	0	5000	5000	0	0	0	0	0	0	0	0	0
S6	5000	0	0	5000	0	5000	0	2500	0	5000	5000	0	5000	5000	5000	0

	T17[d]	*T18*	*T19*	*T20*[d]	*T21*	*T22*	*T23*	*T24*[c]	*T25*	*T26*	*T27*[c]	*T28*[c]	*T29*[d]	*T30*[d]	*T31*	*T32*
S1	0	5000	5000	0	5000	5000	5000	5000	5000	5000	0	5000	0	0	0	4957
S2	0	0	0	0	0	0	0	5000	0	0	5000	5000	0	0	5000	5000
S3[c]	0	0	0	0	0	0	0	5000	5000	0	0	0	0	0	5000	0
S4	0	5000	5000	0	5000	5000	5000	0	0	0	2500	5000	0	0	5000	2500
S5	0	0	0	0	5000	0	0	0	0	0	0	5000	0	0	0	0
S6	0	5000	5000	0	0	5000	5000	0	5000	5000	0	5000	0	0	0	0

	T33	*T34*	*T35*	*T36*[d]	*T37*[c]	*T38*	*T39*	*T40*[d]	*T41*	*T42*	*T43*	*T44*	*T45*	*T46*	*T47*
S1	5000	5000	5000	0	5000	5000	5000	0	5000	5000	5000	5000	0	5000	5000
S2	5000	5000	5000	0	5000	5000	0	0	5000	0	5000	0	5000	5000	0
S3[c]	0	0	0	0	5000	5000	0	0	0	0	0	0	2500	0	0
S4	5000	5000	5000	0	0	0	5000	0	0	5000	0	0	5000	0	5000
S5	0	0	0	0	0	0	0	0	0	5000	5000	5000	0	0	5000
S6	0	0	0	0	0	0	5000	0	5000	0	0	5000	2500	5000	0

[a] An ideal solution is obtained from solving one objective alone

[b] Based on equal weight for all objectvies

[c] Disrupted and is restored

[d] Disrupted and is not restored

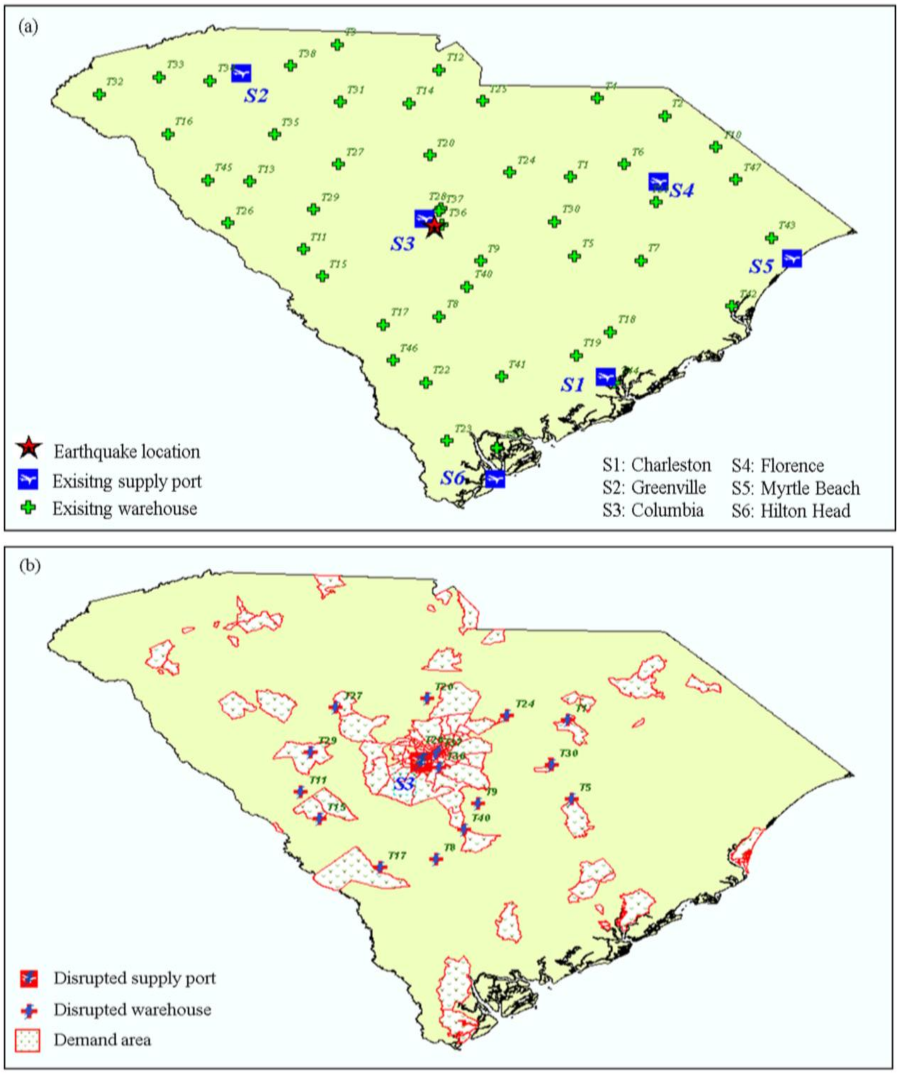

Figure 2.3: Hazus-based South Carolina map illustration: (a) infrastructure before a disaster, (b) loss data after a disaster.

Figure 2.4 shows MOIRR model output for restoration and supply flow decisions. Figure 2.4(a) illustrates the model's resulting restoration decisions comprising five existing and one restored relief point, as well as 31 existing, five fully-restored, and four partially-restored relief warehouses. Further, Figure 2.4(b) and Figure 2.4(c) show examples of flow decisions from the restored Columbia supply point to its relief warehouses and from these warehouses to their associated demand points, respectively.

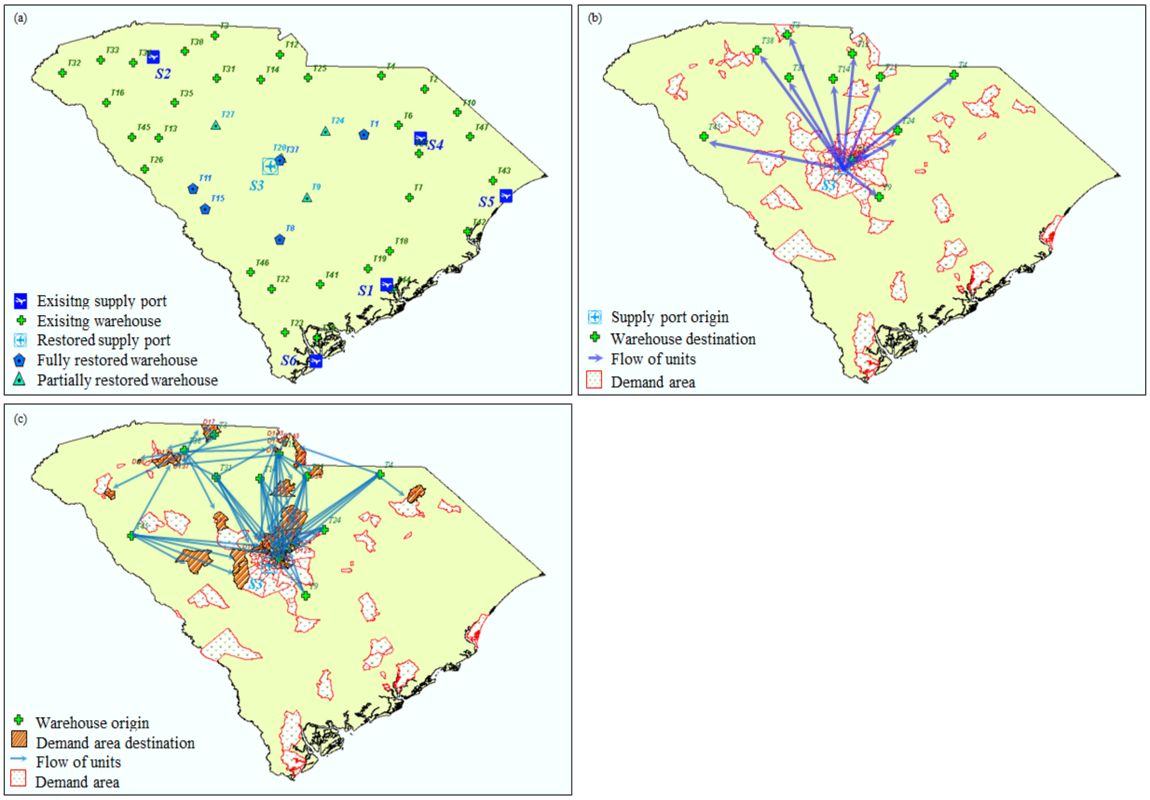

Figure 2.4: MOIRR-based South Carolina map illustration: (a) restoration decisions, (b) flow supply decisions from ports, (c) flow supply decisions from warehouses.

2.4.2 Developing an Approximate Efficient Frontier

In a minimization example, a solution $x^0 \in S$ is said to be efficient, non-dominated, or Pareto optimal if $f_k(x) > f_k(x^0)$ for some $x \in S$ implies that $f_j(x) < f_j(x^0)$ for at least one other index j. An efficient solution is therefore a feasible solution that is not dominated by any other feasible solution and has the property that an improvement in any one objective is possible only at the expense of a poorer solution in at least one other objective (Ravindran, 2007). The set of all efficient solutions, the efficient frontier, is commonly used to evaluate trade-offs among decision criteria as it is useful for visually evaluating a multi-criteria solution space.

We now develop an approximate efficient frontier based on a selected set of efficient solutions to study solution trade-offs for two different pairs of objectives: Pair 1 (fairness vs. cost) and Pair2 (unsatisfied demand vs. cost). For two chosen objectives, we first calculate a weight pair for each efficient solution on an approximate efficient frontier based on the rating method (Ravindran, 2007). To illustrate nine efficient points on a frontier, we use a scale from one to nine, where nine is the highest importance, so that a summation of all ratings is restricted to ten making it convenient to normalize each rating, r_i, to be between 0 and 1 (2.54). For example, the first efficient point is based on a rating of one for the first objective and nine for the second objective, and is converted to a weight pair of 0.1 and 0.9, respectively. Then, the second efficient point is based on a rating of two and eight, and is converted to a weight pair of 0.2 and 0.8. We do this until the ninth efficient point is obtained using a rating of nine for the first objective and one for the second objective, which is converted to a weight pair of 0.9 and 0.1, respectively. That is, weight w_i for objective i is discretely varied from 0.1 to 0.9 at 0.1 increments. Then, given these efficient solution points, we use a polynomial trendline plot to generate the predictive objectives in Figure 2.5.

$$w_i = \frac{r_i}{\sum_{j=1}^{k} r_j} \quad \text{, where } k \text{ is the number of objectives} \tag{2.54}$$

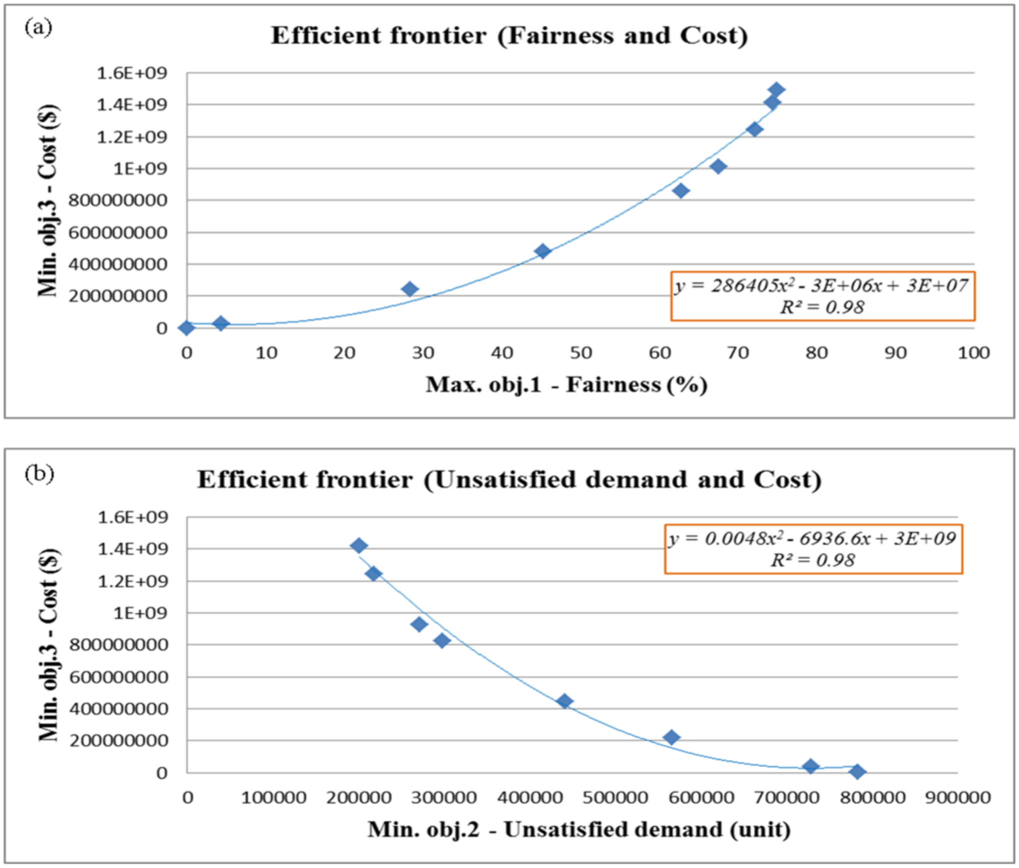

Figure 2.5: Efficient frontier: (a) objective pair (fairness and cost) (b) objective pair (unsatisfied demand and cost).

The fairness and cost objective functions in (2.1) and (2.4) are first normalized using a linear normalization technique to allow inter-criterion comparison for the Pair 1 study (2.55). This technique converts a measure of criteria to a proportion between 0 and 1 along the allowed range of measure based on ideal (H_j^*) and anti-ideal (L_j^*) solutions, where we can obtain from solving one objective alone (Ravindran, 2007). We note that $\frac{C_j(x) - L_j^*}{H_j^* - L_j^*}$ is a normalized term for benefit criterion and $\frac{L_j^* - C_j(x)}{L_j^* - H_j^*}$ is a normalized term for cost criterion, where $C_j(x)$ is a criterion value before normalization. As all criteria after normalization are transformed to a maximization problem, we can then use the weighted objective method as follows:

$$\text{Maximize} \quad w_1\left(\frac{(1)-L_1^*}{H_1^*-L_1^*}\right)+w_3\left(\frac{L_3^*-(4)}{L_3^*-H_3^*}\right) \tag{2.55}$$

By varying the weights from 0.1 to 0.9, the model can be solved to obtain non-dominated solutions and the approximate efficient frontier (Figure 2.5(a)), thereby allowing decision makers to evaluate trade-offs between these two objectives.

Similarly, the objective functions in (2.3) and (2.4) are normalized and combined using the weighted objective method in constraint (2.56) for Pair 2. The approximate efficient frontier generated from the Pair 2 study is presented in Figure 2.5(b).

$$\text{Maximize} \quad w_2\left(\frac{L_2^*-(3)}{H_2^*-L_2^*}\right)+w_3\left(\frac{L_3^*-(4)}{L_3^*-H_3^*}\right) \tag{2.56}$$

2.4.3 Results

While Figure 2.5(a) illustrates an approximate efficient frontier for a pair of maximized and minimized objectives, Figure 2.5(b) shows the frontier for two minimized objectives. In Figure 2.5(a), when more weight is given to the fairness objective (e.g., w_1=0.7, implying that w_3=0.3), the corresponding objective values for fairness and total cost are 72.2% demand satisfaction and $1,245,152,004, respectively. However, when more weight is given to the cost objective (e.g., w_1=0.3 and w_3=0.7), the corresponding objective values are 28.4% percent demand satisfaction and $239,515,108 for total cost, respectively.

Consider the Pair 2 study, when more weight is given to the unsatisfied demand objective in Figure 2.5(b) (e.g., w_2=0.7, implying that w_3=0.3), the corresponding objective values for unsatisfied demand units and cost are 218,996 units and $1,245,079,768, respectively. However, when more weight is given to the cost objective (e.g., w_2=0.3 and w_3=0.7), the corresponding objective values are 567,132 units of unsatisfied demand and $220,371,277 in total cost.

In both the Pair 1 and Pair 2 studies for two objectives, we illustrate the 0.3 and 0.7 weight setting for the first and second objectives of interest, and vice versa, to show how the objectives values react. A decision maker can, however, choose several combinations of objective weights for the MOIRR model. For example, a decision maker can select any weight pair from 0 to 1 along the frontier, where $\sum_{i=1}^{n} w_i = 1$ (e.g., 0.1 and 0.9, 0.2 and 0.8, and so on). Further, using a polynomial trend line analysis, a decision maker can quickly examine how different objective weights affect important trade-offs. It is clear that these two approximated Pareto fronts (trade-off curves) can provide benefits to a decision maker in visualizing the solution space. The preferred point on a particular Pareto front can be identified and optimal decisions can be obtained as illustrated earlier. Further, the fronts also provide an objective trade-off in that they inform a decision maker on how improving one objective can deteriorate the second one's performance along the curve.

2.5 Conclusions and Future Research

Existing models in post-disaster disruption management are scarce and often lack an integrated perspective. We develop a multiple-objective model that integrates the supply distribution problem encountered during disaster response with the restoration problem that arises during recovery operations, the MOIRR model. As performance measures of interest in relief operations are not only cost-based, we also consider an equity- or fairness-based solution approach in our multi-criteria analysis.

It is evident that partial restoration decisions under pooled budgeting approach provides flexibility for organizations when budgets are limited in a highly disrupted network. Given a hypothetical earthquake scenario, the MOIRR model was applied to a South Carolina-based case study using loss data estimated from FEMA's geographic information system-based loss estimation software, Hazus. Our model recommended network restoration and supply distribution plans in multi-criteria space, providing decision makers with approximately efficient frontiers with which to understand trade-offs between the different objectives of interest.

This chapter provides a practical case study for our multiple-objective model with capacity, budget, and resource constraints. Hazus is a valuable tool that can and should be employed by other researchers interested in post-disaster studies. If a decision maker can express his or her desired levels or thresholds of objective function values, a Goal Programming (GP) approach that yields a compromise solution could be further developed. As it is also important to solve large-scale network problems to obtain effective, near-optimal solutions quickly in a real-world disaster scenario, multiple-objective metaheuristic approaches can be further investigated and applied to this problem in an effort to provide practical, effective solutions to this NP-hard problem in a timely manner.

Further, although our research is motivated from a disruption in humanitarian logistics domain, it is analogous to a production system. Consider a complex production plant, for example, it is similar to when analyzing how raw materials are supplied to different machines (i.e., supply distribution problem) given that these machines are subject to a simultaneous failure from a power outage (i.e., recovery problem). Another direction is also to investigate an integrated aspect between production and distribution systems.

CHAPTER THREE

GOAL PROGRAMMING-BASED POST-DISASTER DECISION MAKING FOR INTEGRATED RELIEF SUPPLY DISTRIBUTION AND NETWORK RESTORATION

3.1 Introduction

In this chapter, we extend our previous multiple-objective integrated response and recovery (MOIRR) model in the previous chapter (Ransikarbum and Mason 2014) by proposing a goal programming (GP)-based methodology for decision makers, given completely pre-specified preferences of the decision maker. In the regular multi-criteria programming model, these preferences are treated as requirements with hard constraints. However, these hard constraints are not sufficient to describe user requirements in a real scenario and may be no way to satisfy all the preferences at all. Thus, a decision maker has to make a compromise to select a feasible solution. On the other hand, GP treats these preferences as targets or goals to aspire for. The model then attempts to find an optimal solution that comes as close as possible to the goals using soft constraints. These soft constraints make GP find a compromise solution when the regular multi-criteria programming model does not have a solution thanks to the negotiation feature (Ravindran 2007 and Cui *et al.* 2011).

We develop key managerial insights by analyzing our GP-based methodology in a designed experiment to investigate several important factors: solution method (preemptive vs. non-preemptive); objective function formulation (objective-driven, goal-driven, vs. mixed objective- and goal-driven); and degree of compromise (compromise vs. non-compromise). Our methodology is applied in two Hazus regional case studies with differing population densities: South Carolina (SC) and California (CA). Hazus-generated earthquake scenario loss data is used in the study to provide decision makers with appropriate candidate restoration and distribution plans.

The remaining sections of this paper are organized as follows. First, we discuss related previous research efforts in Section 3.2 and problem statement in Section 3.3. Then, we present our GP-based MOIRR model and its experimental design in Section 3.4. Hazus-based case studies and managerial insights are discussed in Sections 3.5 and 3.6, respectively. Finally, Section 3.7 presents our research conclusions and overviews potential directions for future research studies. This chapter is submitted to the journal with the following citation:

Ransikarbum, K. and Mason, S. J. 2015a. Goal Programming Model for an Integrated Relief Supply and Network Restoration during Post-Disaster Decisions – Hazus based Case Studies. *Working Paper.*

3.2 Literature Review

Sheu (2007) suggests that humanitarian logistics is "a process of planning, managing and controlling the efficient flows of relief, information, and services from the points of origin to the points of destination to meet the urgent needs of the affected people under emergency conditions." Over the course of the last decade, operations research and management science specialists have focused on adapting commercial supply chain management techniques to the humanitarian logistics domain (Wassenhove 2005, Altay and Green 2006, Sheu 2007, Tatham and Pettit 2010, Caunhye *et al.* 2012, Celik *et al.* 2012, Galindo and Batta 2013, Day 2014).

The performance of a humanitarian logistics system is not measured in the same way as that of a commercial logistics system (Chan 2003, Beamon and Balcik 2008, Christopher and Tatham 2011, Celik *et al.* 2012, Day 2014). Celik *et al.* (2012) assert that not only the effectiveness, but also the efficiency of post-disaster logistics activities must be analyzed appropriately to measure performance. Previous researchers suggested a number of strategies to improve emergency relief systems' performance (Celik *et al.* 2012 and Ivanov *et al.* 2014). Although the vast majority of the metrics used to monitor supply network operations are financially based to capture the effectiveness of Non-Governmental Organization's (NGO) response, there is a need to include metrics that capture the recipient's viewpoint in order to improve the delivery of goods and services to aid recipients, such as fairness or equity (Christopher and Tatham 2011).

The concept of equity and how it is measured has been widely studied in the literature (Ogryczak 2000, Kostreva *et al.* 2003, Singh 2007, Zhu *et al.* 2010, Vitoriano *et al*. 2011, Ransikarbum and Mason 2014). Minimax, maximin, and maxisum techniques are frequently used in equity- or fairness-related research efforts. Lexicographic minimax (maximin) techniques seek equitable solutions for problems wherein a smaller (larger) performance or objective function value is desirable (Kaplan 1973, Luss 1999, Zhang and Melachrinoudis 1999, Salles and Barria 2008, Sayin 2013, Ransikarbum and Mason 2014). Kaplan (1973) initially discusses the concept of a maximin objective function and shows that it can be transformed and solved by linear programming. Salles and Barria (2008) formulate the bandwidth allocation problem and employ the lexicographic maximin criterion to return a solution that satisfies both fairness and efficiency properties. While this approach guarantees desirable features for the allocation of network resources, such as fairness and efficiency, it requires complex optimization procedures and significant computation time to find a solution. Ransikarbum and Mason (2014) develop an integrated response and recovery model under supply disruption with multiple objectives and use a maximin technique to obtain “fair” solutions in a distributed system.

The humanitarian logistics literature can be categorized according the four phases of the disaster management cycle and how it relates to pre- and post-disaster operations (McLoughlin 1985). While most efforts are related to pre-disaster issues (Jia *et al.* 2007, Balcik and Beamon 2008, Doerner *et al.* 2009, Liberatore *et al.* 2012, Akgun *et al.* 2014), recent research points to the need for analyzing post-disaster-related operations with models that consider the integrated aspects and/or the effects of multiple disasters (Altay and Green 2006, Caunhye *et al.* 2012, Celik *et al.* 2012, Galindo and Batta 2013). Recent studies examine the resilience and reliability domains related to infrastructure networks both pre- and post-disaster. Liberatore *et al.* (2012) propose a facility protection model that considers the possibility of interdependencies among disruptions for large area disruptions to improve the reliability of an existing network using an attacker-defender paradigm. Using the same paradigm, Alderson *et al.* (2014) illustrate how to build and solve a sequence of models to assess and improve the resilience of an infrastructure system after disruptive events. Akgun *et al*. (2014) develop a pre-disaster phase model to locate prepositioned supplies close to disaster-prone areas such that a reliable facility network results that minimizes response time to demand points.

Studies focusing on post-disaster relief operations typically consider the problems in each phase individually (Matisziw *et al*. 2009, Vitoriano *et al*. 2011). Matisziw *et al.* (2009) recovery phase-focused study examines a telecommunication network restoration problem using decision variables related to restoring disrupted nodes and arcs in a multi-period environment. Vitoriano *et al.* (2011) develop a GP response phase model focused on the loads and vehicles that support aid distribution in order to maximize goal attributes related to relief operations: equity, reliability, and security. The Humanitarian Aid Distribution System is a web-based decision support platform designed to aid non-experienced users to make more effective decisions during the response phase (Vitoriano *et al.* 2010, Ortuño *et al.* 2011).

Recently, research efforts have trended towards phase-integrating models (Balcik *et al.* 2008, Celik *et al*. 2012, Liberatore *et al.* 2014, Ransikarbum and Mason 2014). Balcik *et al.* (2008) develop an integrated preparedness and response model for last mile distribution systems in which a local DC stores inventories and distributes emergency relief supplies to a number of demand locations. Celik *et al*. (2012) provide an integrated approach for two post-disaster questions: medical response (response) and debris clearance (recovery). The hierarchical compromise model "RecHADS" was developed by Liberatore *et al.* (2014) to consider both relief distribution and disrupted arcs recovery in order to improve reliability and security. The authors compare sequential and coordinated optimization to highlight the importance of cooperation among agents. Ransikarbum and Mason's MOIRR model (2014) integrates supply distribution (response) and network restoration decisions (recovery) for post-disaster operations under a fairness-based objective.

Finally, while “hard” (real) constraints are typically formulated in multi-objective mathematical programs, GP models often contain “soft” (goal) constraints. The primary difference is that real constraints are absolute restrictions whereas goal constraints are desirable but not mandatory restrictions to achieve goals (Ravindran 2007). Cui *et al.* (2011) develop a GP model for a web service problem and suggest that including only real constraints is not sufficient for describing user requirements; further, there may be no way to satisfy all of the real constraints simultaneously. In practice, the user will be forced to compromise and select a feasible solution—this is 1) the purpose of the goal constraints in GP models and 2) the primary motivation for the proposed GP model in this paper. We adapt our previously-developed MOIRR model (Ransikarbum and Mason 2014) to a GP-based framework and analyze it using an experimental design extended from Cui *et al.* (2011). Next, motivated by Galindo and Batta (2013) who note the lack of application-based analyses of mathematical models for post-disaster operations, we assess the proposed GP model’s capabilities using two Hazus-generated case studies of varying population density.

3.3 Problem Statement

The MOIRR model of Ransikarbum and Mason (2014) integrates both response-phase supply distribution options and recovery-phase network restoration decisions to reestablish services in a damaged network to pre-disruption performance levels so that relief supplies can be transported to affected areas. The model also directs decision makers to restore disrupted node(s) and/or disrupted arc(s) when necessary such that fairness, unsatisfied demand, and cost-based criteria are optimized. In this paper, our focus shifts to the decision space containing multiple, conflicting objective functions. Given the set of any decision maker's pre-specified preferences or desired goals, we seek to provide a set of restoration plans for the disrupted nodes and arcs in a humanitarian relief logistics network that allow for relief items to be quickly and equitably supplied to those in need. Figure 3.1 illustrates an instance of a disrupted network. Clearly, the network can become disconnected. Unless disrupted nodes (N2 and N3) and/or arcs (A2, A4, A6, A7, A8, and A9) are restored, no relief items can reach victims.

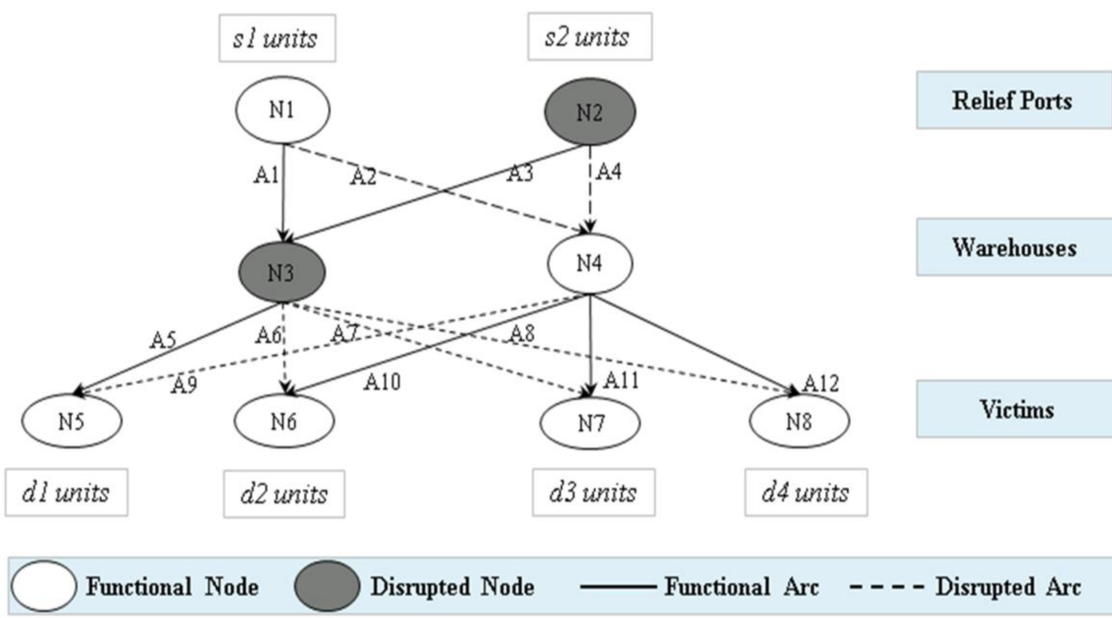

Figure 3.1: Disrupted network problem instance

3.4 A Goal Programming-based Multiple-Objective Integrated Response and Recovery Model

In goal (aka compromise) programming, a decision maker specifies his/her goals as desired levels or threshold values for problem attributes (objective functions) of interest. GP treats these goals as aspirations to pursue, not as absolute constraints or requirements. In other words, GP models seek feasible solutions that most closely approach or meet the goals. In stating one or more goals, the decision maker is suggesting that although a true optimal solution is desired, he/she would be satisfied by any model solution that achieves or is “close” to the stated goal(s). Given desired goal(s) or target value(s), GP models prescribe decisions that minimize the deviation(s) from these targets. As a branch of multiple-objective programming (MOP), GP models are typically solved by either preemptive or non-preemptive methods (Ignizio and Cavalier 1993, Ravindran 2007). Under a preemptive approach, once the decision maker states the objectives in priority order (e.g., the first objective has highest priority p_1, the second objective has second highest priority p_2, and so on), the model can be solved by sequential optimization (Arthur and Ravindran 1980). In contrast, non-preemptive approaches typically are characterized by models containing importance factors/criteria weights for each objective that are solved as a single, linear (weighted) objective model (e.g., the i^{th} objective is given weight w_i).

We formulate the GP analogue of the MOIRR model with a partial restoration developed by Ransikarbum and Mason (2014). In this analysis, we do not allow disrupted supply points to be partially restored (i.e., all or nothing restoration is required at supply points). However, relief warehouse nodes can be either not restored, have one-half of their capabilities restored, or be fully restored. Finally, each disrupted arc in the relief network can be restored in increments of 25% of the arc's capacity (i.e., 0%, 25%, 50%, 75%, or 100% restoration).

3.4.1 Model Notation

<u>*Sets*</u>

$G(N,A)$	Graph consisting of nodes N and arcs A
N (A)	Set of nodes (arcs)
S (D)	Set of supply port (demand) nodes $\in N$
T	Set of transhipment (relief warehouse) nodes $\in N$
S^F (S^D)	Set of functional (disrupted) supply port nodes $\in S$
T^F (T^D)	Set of functional (disrupted) transhipment (relief warehouse) nodes $\in T$
Λ	Set of arcs between supply port and relief warehouse nodes $\in A$
Π	Set of arcs between relief warehouse and demand nodes $\in A$
Λ^F (Λ^D)	Set of functional (disrupted) arcs between supply port and warehouse nodes $\in \Lambda$
Π^F (Π^D)	Set of functional (disrupted) arcs between relief warehouse and demand nodes $\in \Pi$
Γ^N	Set of disrupted nodes, where $\Gamma^N = S^D \cup T^D$
Γ^A	Set of disrupted arcs, where $\Gamma^A = \Lambda^D \cup \Pi^D$

<u>*Parameters*</u>

s_i	Supply units available at each supply port node $i \in S$
d_i	Demand units required at each demand node $i \in D$

α_i	Relief warehouse capacity for each relief warehouse node $i \in T$
$\delta_{i,j}^{ST}$	Road capacity for each arc between port and warehouse node $(i, j) \in \Lambda$
$\delta_{i,j}^{TD}$	Road capacity for each arc between warehouse and demand $(i, j) \in \Pi$
φ_i	Capacity needed for each unit flow to use relief warehouse node $i \in T$
$\psi_{i,j}^{ST}$	Capacity needed for each unit flow to use road (arc) between supply port and relief warehouse node $(i, j) \in \Lambda$
$\psi_{i,j}^{TD}$	Capacity needed for each unit flow to use road (arc) between relief warehouse and demand node $(i, j) \in \Pi$
$c_{i,j}$	Cost for transporting each unit flow per mile through each arc $(i, j) \in A$
η_i^S (η_i^T)	Cost for restoring each disrupted supply port node $i \in S^D$ (relief warehouse node $i \in T^D$)
$\lambda_{i,j}^{ST}$	Cost for restoring each disrupted arc between port and relief warehouse node $(i, j) \in \Lambda^D$
$\lambda_{i,j}^{TD}$	Cost for restoring each disrupted arc between warehouse and demand node $(i, j) \in \Pi^D$
b^N (b^A)	Budget for total disrupted node (arc) restoration
b^F	Budget for total network flow transportation
ν^S (ν^T)	Fixed charge for restoring disrupted supply port (relief warehouse) node
ω^{ST}	Fixed charge for restoring disrupted arc between supply port and relief warehouse node
ω^{TD}	Fixed charge for restoring disrupted arc between relief warehouse and demand node
θ^N (θ^A)	Maximum allowable number for disrupted node (arc) restoration
$d_{i,j}^{OD}$	Distance in miles between each origin and destination pair $(i, j) \in A$
w_i (p_i)	Importance weight setting (priority) associated with objective i

Partial Restoration Parameters

f_i^{T1}, (f_i^{T2})	50%, (100%) restoration for disrupted warehouse node $i \in T^D$
$f_{i,j}^{ST1}$, ($f_{i,j}^{ST2}$), ($f_{i,j}^{ST3}$)	25%, (50%), (100%) restoration for damaged arc between supply port and relief warehouse node $(i, j) \in \Lambda^D$
$f_{i,j}^{TD1}$, ($f_{i,j}^{TD2}$), ($f_{i,j}^{TD3}$)	25%, (50%), (100%) restoration for damaged arc between relief warehouse and demand node $(i, j) \in \Pi^D$

Goal Parameters

g_F	Minimal fairness decision maker would accept for percent of satisfied demand at each node
g_U	Maximum total units of unsatisfied demands decision maker will tolerate
g_C	Maximum total cost decision maker will pay for network restoration and aid transportation

Decision Variables

$X_{i,j}$	Commodity flow variable for supplies through arc $(i, j) \in A$; integer
K_i	Restore disrupted supply port node $i \in S^D$; binary
L_i	Partially restore disrupted warehouse node $i \in T^D$
$M_{i,j}$	Partially restore disrupted arc between supply port and relief warehouse node $(i, j) \in \Lambda^D$
$N_{i,j}$	Partially restore disrupted arc between relief warehouse and demand node $(i, j) \in \Lambda^D$
R_i	Units of unsatisfied demand for each demand node $i \in D$; integer
V	Minimum percentage of satisfied demand
Y_i^S	Setup cost to restore disrupted supply port $i \in S^D$; binary
Y_i^T	Setup cost to restore disrupted warehouse $i \in T^D$; binary
$Y_{i,j}^{ST}$	Setup cost to restore disrupted arc between supply port and warehouse $(i, j) \in \Lambda^D$; binary

$Y_{i,j}^{TD}$ Setup cost to restore disrupted arc between relief warehouse and demand *(i, j)*$\in \Pi^{D}$; binary

Partial Restoration Decision Variables

Q_{i}^{T1}, (Q_{i}^{T2}) Restrict 50%, (100%) restoration for disrupted warehouse node $i \in T^{D}$; binary

$Q_{i,j}^{ST1}$, $(Q_{i,j}^{ST2})$, $(Q_{i,j}^{ST3})$ Restrict 25%, (50%), (100%) restoration for disrupted arc between supply port and relief warehouse node $(i, j) \in \Lambda^{D}$; binary

$Q_{i,j}^{TD1}$, $(Q_{i,j}^{TD2})$, $(Q_{i,j}^{TD3})$ Restrict 25%, (50%), (100%) restoration for disrupted arc between relief warehouse and demand node $(i, j) \in \Pi^{D}$; binary

Goal Decision Variables

D^{+F} (D^{-F}) Positive (negative) deviation of fairness goal

D^{+U} (D^{-U}) Positive (negative) deviation of unsatisfied demand goal

D^{+C} (D^{-C}) Positive (negative) deviation of cost goal

3.4.2 Model

The GP analogue of the MOIRR model is guided by three different objective functions: maximizing equity (fairness), minimizing unsatisfied relief demand, and minimizing total network costs. Further, it minimizes three undesired deviational variables associated with each goal.

Maximize $Z_1 = V$ (3.1)

Minimize $Z_2 = \left(\sum_{i \in D} R_i \right)$ (3.2)

$$\text{Minimize } Z_3 = \begin{bmatrix} \left(\sum_{i \in S^D} \eta_i^S K_i\right) + \left(\sum_{i \in T^D} \eta_i^T L_i\right) + \left(\sum_{i \in S^D} \nu^S Y_i^S\right) + \left(\sum_{i \in T^D} \nu^T Y_i^T\right) + \cdots \\ \left(\sum_{(i,j) \in \Lambda^D} \lambda_{i,j}^{ST} M_{i,j}\right) + \left(\sum_{(i,j) \in \Pi^D} \lambda_{i,j}^{TD} N_{i,j}\right) + \left(\sum_{(i,j) \in \Lambda^D} \omega^{ST} Y_{i,j}^{ST}\right) + \ldots \\ \left(\sum_{(i,j) \in \Pi^D} \omega^{TD} Y_{i,j}^{TD}\right) + \left(\sum_{(i,j) \in A} c_{i,j} d_{i,j}^{OD} X_{i,j}\right) \end{bmatrix} \tag{3.3}$$

$$\text{Minimize } Z_4 = D^{-F} \tag{3.4}$$

$$\text{Minimize } Z_5 = D^{+U} \tag{3.5}$$

$$\text{Minimize } Z_6 = D^{+C} \tag{3.6}$$

Objective function (3.1), when coupled with constraint set (3.7), maximizes equity (fairness) via a maximin approach.

$$V \leq \left(\sum_{i \in T} \frac{X_{i,j}}{d_j}\right) 100 \qquad ; \forall \; j \in D \tag{3.7}$$

Objective function (3.2) minimizes the total sum of unsatisfied relief units across all demand nodes while objective (3.3) minimizes total network costs which are calculated as the total funds spent to restore disrupted nodes, restore disrupted arcs, and transport supply units between origin-destination pairs. Finally, objective functions (3.4)-(3.6) minimize deviational variables based on the fairness, unsatisfied demand, and cost goals, respectively.

The model's constraint sets ensure that any required restrictions or limits are followed by any of the GP model's recommended solutions. Constraint set (3.8) ensures that total transportation costs do not exceed the available transportation budget. Similarly, constraint sets (3.9)-(3.10) ensure that total restoration costs do not exceed available restoration funds.

$$\sum_{(i,j)\in A} c_{i,j} d_{i,j}^{OD} X_{i,j} \leq b^F \tag{3.8}$$

$$\left(\sum_{i\in S^D} \eta_i^S K_i\right) + \left(\sum_{i\in T^D} \eta_i^T L_i\right) + \left(\sum_{i\in S^D} \nu^S Y_i^S\right) + \left(\sum_{i\in T^D} \nu^T Y_i^T\right) \leq b^N \tag{3.9}$$

$$\left(\sum_{(i,j)\in \Lambda^D} \lambda_{i,j}^{ST} M_{i,j}\right) + \left(\sum_{(i,j)\in \Pi^D} \lambda_{i,j}^{TD} N_{i,j}\right) + \left(\sum_{(i,j)\in \Lambda^D} \omega^{ST} Y_{i,j}^{ST}\right) + \left(\sum_{(i,j)\in \Pi^D} \omega^{TD} Y_{i,j}^{TD}\right) \leq b^A \tag{3.10}$$

As it is possible that all demands may not be satisfied, constraint set (3.11) accounts for demand uncertainty (i.e., demand is higher or lower than available supply units).

$$\sum_{i\in T} X_{i,j} + R_j = d_j \qquad ;\forall\ j\in D \tag{3.11}$$

Constraint sets (3.12)-(3.13) ensure that total flow out of the supply nodes does not exceed the available supply. While supply items are available from functional supply nodes, supply items for disrupted supply nodes are available if and only if the disrupted node is restored.

$$\sum_{j\in T} X_{i,j} \leq s_i \qquad ;\forall\ i\in S^F \tag{3.12}$$

$$\sum_{j\in T} X_{i,j} \leq s_i K_i \qquad ;\forall\ i\in S^D \tag{3.13}$$

Constraint set (3.14) ensures flow conservation such that unit flows out of and into each relief warehouse are equal.

$$\sum_{i\in S} X_{i,j} - \sum_{k\in D} X_{j,k} = 0 \qquad ;\forall\ j\in T \tag{3.14}$$

Relief warehouse capacities are restricted by constraint sets (3.15)-(3.16), as relief warehouse nodes only provide capacity when the node is functional.

$$\sum_{i \in S} \varphi_j X_{i,j} \leq \alpha_j \qquad ; \forall \quad j \in T^F \tag{3.15}$$

$$\sum_{i \in S} \varphi_j X_{i,j} \leq \alpha_j L_j \qquad ; \forall \quad j \in T^D \tag{3.16}$$

Constraint sets (3.17)-(3.18) restrict road capacities between supply nodes and relief warehouse nodes by ensuring that road capacities are available only if the corresponding roads are functional. Similarly, constraint sets (3.19)-(3.20) restrict road capacity utilization between relief warehouses and demand nodes.

$$\psi_{i,j}^{ST} X_{i,j} \leq \delta_{i,j}^{ST} \qquad ; \forall \ (i, j) \in \Lambda^F \tag{3.17}$$

$$\psi_{i,j}^{ST} X_{i,j} \leq \delta_{i,j}^{ST} M_{i,j} \qquad ; \forall \ (i, j) \in \Lambda^D \tag{3.18}$$

$$\psi_{i,j}^{TD} X_{i,j} \leq \delta_{i,j}^{TD} \qquad ; \forall \ (i, j) \in \Pi^F \tag{3.19}$$

$$\psi_{i,j}^{TD} X_{i,j} \leq \delta_{i,j}^{TD} N_{i,j} \qquad ; \forall \ (i, j) \in \Pi^D \tag{3.20}$$

Constraint sets (3.21) through (3.24) enforce setup cost realization when restoration decisions for disrupted supply points (3.21), disrupted warehouses (3.22), disrupted arcs between a supply point and a warehouse (3.23), and disrupted arcs between a warehouse and demand nodes (3.24) are prescribed by the model.

$$K_j \leq Y_j^S \qquad ; \forall \ j \in S^D \tag{3.21}$$

$$L_j \leq Y_j^T \qquad ; \forall \ j \in T^D \tag{3.22}$$

$$M_{i,j} \leq Y_{i,j}^{ST} \qquad ; \forall \ (i, j) \in \Lambda^D \tag{3.23}$$

$$N_{i,j} \leq Y_{i,j}^{TD} \qquad ; \forall \ (i, j) \in \Pi^D \tag{3.24}$$

Next, constraint sets (3.25)-(3.26) restrict the number of disrupted nodes and disrupted arcs that can be restored based on available resources.

$$\sum_{j \in S^D} K_j + \sum_{j \in T^D} L_j \le \theta^N \tag{3.25}$$

$$\sum_{(i,j) \in \Lambda^D} M_{i,j} + \sum_{(i,j) \in \Pi^D} N_{i,j} \le \theta^A \tag{3.26}$$

In terms of the GP model's partial restoration decisions, constraint sets (3.27)-(3.28) combine to restrict the model's decision variables to partially restore disrupted relief warehouse nodes at only two levels: 50% or 100%.

$$L_i = f_i^{T1} Q_i^{T1} + f_i^{T2} Q_i^{T2} \qquad ; \forall\ i \in T^D \tag{3.27}$$

$$L_i \le f_i^{T2} \qquad ; \forall\ i \in T^D \tag{3.28}$$

Similarly, constraint sets (3.29)-(3.30) allow partially disrupted arcs between supply points and relief warehouses to be restored at four levels: 25%, 50%, 75%, or 100%, while constraint sets (3.31)-(3.32) restrict the partial restoration of disrupted arcs between relief warehouses and demand nodes.

$$M_{i,j} = f_{i,j}^{ST1} Q_{i,j}^{ST1} + f_{i,j}^{ST2} Q_{i,j}^{ST2} + f_{i,j}^{ST3} Q_{i,j}^{ST3} \qquad ; \forall\ (i,j) \in \Lambda^D \tag{3.29}$$

$$M_{i,j} \le f_{i,j}^{ST3} \qquad ; \forall\ (i,j) \in \Lambda^D \tag{3.30}$$

$$N_{i,j} = f_{i,j}^{TD1} Q_{i,j}^{TD1} + f_{i,j}^{TD2} Q_{i,j}^{TD2} + f_{i,j}^{TD3} Q_{i,j}^{TD3} \qquad ; \forall\ (i,j) \in \Pi^D \tag{3.31}$$

$$N_{i,j} \le f_{i,j}^{TD3} \qquad ; \forall\ (i,j) \in \Pi^D \tag{3.32}$$

We now turn our focus to the constraint necessary for goal formulation. Given three threshold parameters for goals, real constraint sets for the fairness goal (3.33), the total unsatisfied demand goal (3.34), and the total network cost goal (3.35) can be formulated as follows:

$$V \geq g_F \tag{3.33}$$

$$\sum_{i\in D} R_i \leq g_U \tag{3.34}$$

$$\left[\begin{array}{l} \left(\sum_{i\in S^D} \eta_i^S K_i\right) + \left(\sum_{i\in T^D} \eta_i^T L_i\right) + \left(\sum_{i\in S^D} \nu^S Y_i^S\right) + \left(\sum_{i\in T^D} \nu^T Y_i^T\right) + \cdots \\ \left(\sum_{(i,j)\in \Lambda^D} \lambda_{i,j}^{ST} M_{i,j}\right) + \left(\sum_{(i,j)\in \Pi^D} \lambda_{i,j}^{TD} N_{i,j}\right) + \left(\sum_{(i,j)\in \Lambda^D} \omega^{ST} Y_{i,j}^{ST}\right) + \ldots \\ \left(\sum_{(i,j)\in \Pi^D} \omega^{TD} Y_{i,j}^{TD}\right) + \left(\sum_{(i,j)\in A} c_{i,j} d_{i,j}^{OD} X_{i,j}\right) \end{array}\right] \leq g_C \tag{3.35}$$

In the case when no feasible solution exists that satisfies all goal requirements, one can provide the decision maker with a compromise solution by converting the real constraints on goals into goal constraints (3.36-3.38) via the introduction of both positive and negative deviation variables:

$$V + D^{-F} - D^{+F} = g_F \tag{3.36}$$

$$\sum_{i\in D} R_i + D^{-U} - D^{+U} = g_U \tag{3.37}$$

$$\begin{array}{l} \left(\sum_{i\in S^D} \eta_i^S K_i\right) + \left(\sum_{i\in T^D} \eta_i^T L_i\right) + \left(\sum_{i\in S^D} \nu^S Y_i^S\right) + \left(\sum_{i\in T^D} \nu^T Y_i^T\right) + \left(\sum_{(i,j)\in \Lambda^D} \lambda_{i,j}^{ST} M_{i,j}\right) + \left(\sum_{(i,j)\in \Pi^D} \lambda_{i,j}^{TD} N_{i,j}\right) + \\ \left(\sum_{(i,j)\in \Lambda^D} \omega^{ST} Y_{i,j}^{ST}\right) + \left(\sum_{(i,j)\in \Pi^D} \omega^{TD} Y_{i,j}^{TD}\right) + \left(\sum_{(i,j)\in A} c_{i,j} d_{i,j}^{OD} X_{i,j}\right) + D^{-C} - D^{+C} = g_C \end{array} \tag{3.38}$$

Clearly, as one of the negative or positive deviational variable will be active in the GP model's objective function (depending on the corresponding maximization or minimization directive), it follows that one of the variables in each deviation pair will equal zero.

For example, consider the real fairness constraint (3.33) and its associated goal constraint (3.36). If $D^{-F}>0$ ($D^{+F}>0$), it follows that $V < g_F$ ($V > g_F$). As the goal is to satisfy $V \geq g_F$, only D^{-F} should be minimized in the objective function and D^{+F} is unconstrained. This is in direct contrast to the real constraints on unsatisfied demand (3.34) and total costs (3.35) wherein minimal values are desirable. In the unsatisfied demand goal constraint (3.37), if $D^{-U} > 0$ ($D^{+U} > 0$), it follows that $\sum_{i \in D} R_i < g_U$ ($\sum_{i \in D} R_i > g_U$). Thus, only D^{+U} should be minimized in the objective function while D^{-U} is unconstrained.

Finally, constraint sets (3.39)-(3.49) are variable-type constraints, constraint sets (3.50)-(3.57) are binary variables required for partial restoration decisions, and constraint sets (3.58)-(3.63) denote variable-type constraints for goal-related variables.

$X_{i,j} = \{0,1,2,\ldots,n\} \quad ; \forall \ (i,j) \in A$ (3.39), $K_i = \{0,1\} \quad ; \forall i \in S^D$ (3.40)

$L_i \geq 0 \quad ; \forall i \in T^D$ (3.41), $M_{i,j} \geq 0 \quad ; \forall \ (i,j) \in \Lambda^D$ (3.42)

$N_{i,j} \geq 0 \quad ; \forall \ (i,j) \in \Pi^D$ (3.43), $R_i \geq 0 \quad ; \forall \ i \in D$ (3.44)

$V \geq 0$ (3.45), $Y_i^S = \{0,1\} \quad ; \forall i \in S^D$ (3.46)

$Y_i^T = \{0,1\} \quad ; \forall i \in T^D$ (3.47), $Y_{i,j}^{ST} = \{0,1\} \quad ; \forall \ (i,j) \in \Lambda^D$ (3.48)

$Y_{i,j}^{ST} = \{0,1\} \quad ; \forall \ (i,j) \in \Lambda^D$ (3.49), $Q_i^{T1} = \{0,1\} \quad ; \forall \ i \in T^D$ (3.50)

$Q_i^{T2} = \{0,1\} \quad ; \forall \ i \in T^D$ (3.51), $Q_{i,j}^{ST1} = \{0,1\} \quad ; \forall \ (i,j) \in \Lambda^D$ (3.52)

$Q_{i,j}^{ST2} = \{0,1\} \quad ; \forall \ (i,j) \in \Lambda^D$ (3.53), $Q_{i,j}^{ST3} = \{0,1\} \quad ; \forall \ (i,j) \in \Lambda^D$ (3.54)

$Q_{i,j}^{TD1} = \{0,1\} \quad ; \forall \ (i,j) \in \Pi^D$ (3.55), $Q_{i,j}^{TD2} = \{0,1\} \quad ; \forall \ (i,j) \in \Pi^D$ (3.56)

$Q_{i,j}^{TD3} = \{0,1\} \quad ; \forall \ (i,j) \in \Pi^D$ (3.57), $D^{-F} \geq 0$ (3.58)

$D^{+F} \geq 0$ (3.59), $D^{-U} \geq 0$ (3.60)

$D^{+U} \geq 0$ (3.61), $D^{-C} \geq 0$ (3.62)

$D^{+C} \geq 0$ (3.63)

3.4.3 Complexity

The complexity of the above model can be assessed through a reduction technique (Karp 1972) to show that the GP-based MOIRR model can be reduced to the MOIRR model, which is known to be NP-hard (Ransikarbum and Mason 2014). Set all parameters (g_F, g_U, and g_C) and decision variables ($D^{-F}, D^{+F}, D^{-U}, D^{+U}, D^{-C}$,and D^{+C}) associated with decision maker goals equal to zero (i.e., discard them from the model). It follows that the constraint sets (3.30)-(3.35) and (3.55)-(3.60) that are associated with these parameters and decision variables can be ignored. The revised model reduces to the MOIRR model with partial restoration. Therefore, through such a reduction argument, the complexity of the proposed GP-based MOIRR model is NP-hard as $GP - based\ MOIRR \propto MOIRR$.

3.4.4 Experimentation Plan

A designed experiment is conducted to investigate 1) how multiple objective problems are solved (preemptive vs. non-preemptive); 2) how model objective functions are formulated (objective-driven vs. goal-driven vs. mixed objective- and goal-driven); and 3) how constraint sets are restricted (compromise vs. non-compromise). We seek to understand how these three experimental factors impact a) computation time; b) optimal directive; and c) infeasibility handling through the following model cases (Table 3.1):

Multiple-Objective Programming (MOP)

- Case 0 MOP: non-preemptive, objective-driven, and non-compromise
- Case 1 MOP: preemptive, objective-driven, and non-compromise

Multiple-Objective Goal Programming with Goal-Driven Solutions (MOGPG)

- Case 2 (MOGPGO): non-preemptive, goal-driven, and compromise
- Case 3 (MOGPGO): preemptive, goal-driven, and compromise

Multiple-Objective Goal Programming with Mixed Objective- and Goal-Driven Solutions (MOGPMOG)

- Case 4 (MOGPMOG): non-preemptive, mixed obj.-/goal-driven, and compromise
- Case 5 (MOGPMOG): preemptive, mixed obj.-/goal-driven, and compromise

We note that Case 0 is the MOIRR model of Ransikarbum and Mason (2014) with the weighted objective (i.e., non-preemptive) method for all objective functions (1)-(3), subject to the real constraints set. In this paper, we introduce Cases 1-5. While Case 1 examines the preemptive approach for MOP, Cases 2-5 are GP-based model variations to be investigated.

Table 3.1: Scenario analyses for GP-based MOIRR model

Scenario Model	Category	Multiple-Objective Solution Method		Objective Function Formulation			Constraint Set Compromise	
		Non-preemptive	Preemptive	Objective-driven	Goal-driven	Mixed Obj./Goal	Non-compromise	Compromise
Case 0	MOP	✓		✓			✓	
Case 1	MOP		✓	✓			✓	
Case 2	MOGPG	✓			✓			✓
Case 3	MOGPG		✓		✓			✓
Case 4	MOGPMOG	✓				✓		✓
Case 5	MOGPMOG		✓			✓		✓

MOP denotes Multiple-Obj. Programming
MOGPG denotes Multiple-Obj. Goal programming with Goal-Driven Solutions
MOGPMOG denotes Multiple-Obj. Goal programming with Mixed Objective- and Goal-Driven Solutions

3.4.4.1 Non-Preemptive vs. Preemptive Model Objectives

While non-preemptive approaches typically employ criteria weights (e.g., w_i) for each objective to solve a single, linear (weighted) objective function model, preemptive approaches involve prioritized objectives (e.g., p_i) that are solved by sequential optimization. Some difficulties can occur when calculating appropriate weights in a non-preemptive approach. In terms of computation time, the computation time for a non-preemptive-based model is determined by running a single, weighted objective model one time. Alternately, a preemptive-based model's computation time is computed as the sum of each sequential model run's total run time. Therefore, given a computational time limit l for the non-preemptive case, the corresponding time limit for the preemptive model study will be l * (# of objectives under study). It follows that to investigate the trade-off between computation time and solution quality for the different approaches of interest, three pairwise comparative studies are required: 1) Case 0 vs. Case 1, 2) Case 2 vs. Case 3, and 3) Case 4 vs. Case 5.

As objectives under the preemptive method are solved sequentially based on given priorities, there is no need to use ideal and anti-ideal solutions for inter-criterion comparison. On the other hand, objectives for the non-preemptive method must be normalized using a linear normalization technique to allow inter-criterion comparison. This technique converts each objective function's values to a range between 0 and 1 based on ideal and anti-ideal solutions. Then, the weighted objective method can be applied and the model is solved as a single linear maximization model. The following definitions are used in our non-preemptive methods:

- $c_j(x)$ is a criterion value before normalization
- H_j^* is an ideal solution (i.e., Max $c_j(x)$ for benefit and Min $c_j(x)$ for cost criteria)

- L_j^* is an anti-ideal solution (i.e., Min $C_j(x)$ for benefit and Max $C_j(x)$ for cost criteria)
- $\frac{C_j(x) - L_j^*}{H_j^* - L_j^*}$ is a normalized benefit criterion and $\frac{L_j^* - C_j(x)}{L_j^* - H_j^*}$ is a normalized cost criterion
- $\sum_{i=1}^{n} w_i = 1$, where n is the number of objectives used in an inter-criterion comparison

3.4.4.2 Objective-Driven, Goal-Driven, vs. Mixed Objective/Goal-Driven Case

The objective functions are formulated differently among the MOP, MOGPG, and MOGPMOG: objective functions (1)-(3) are used in MOP; objective functions (4)-(6) are used in MOGPG; and objective functions (1) and (4)-(6) are used in MOGPMOG. While the MOP yields optimal solutions under three objective functions, the MOGPG generates optimal solutions that meet as many goals as possible in a shorter amount of computation time under three goal-driven deviational variables. The MOGPMOG is a hybrid version of the MOP and MOGPG in that it generates an optimal solution for the fairness objective/goal using objective functions (1) and (4) while providing optimal solutions driven from both the unsatisfied demand and cost goals in objective functions (5) and (6). However, depending on the decision maker's perspective, other combinations of objective functions can also be evaluated using the MOGPMOG.

Given that a trade-off exists between computation time and solution optimality, we examine the following two tuples: 1) Case 0 vs. Case 2 vs. Case 4 and 2) Case 1 vs. Case 3 vs. Case 5. In particular, objective functions for each case is as follows:

Case 0: Maximize $w_1\left(\frac{Z_1 - L_1^*}{H_1^* - L_1^*}\right) + w_2\left(\frac{L_2^* - Z_2}{L_2^* - H_2^*}\right) + w_3\left(\frac{L_3^* - Z_3}{L_3^* - H_3^*}\right)$ (3.64)

Case 1: Maximize $p_1 Z_1$, Minimize $p_2 Z_2$, Minimize $p_3 Z_3$ (3.65)

Case 2: Maximize $w_1\left(\frac{L_4^* - Z_4}{L_4^* - H_4^*}\right) + w_2\left(\frac{L_5^* - Z_5}{L_5^* - H_5^*}\right) + w_3\left(\frac{L_6^* - Z_6}{L_6^* - H_6^*}\right)$ (3.66)

Case 3: Minimize $p_1 Z_4$, Minimize $p_2 Z_5$, Minimize $p_3 Z_6$ (3.67)

Case 4: Maximize $w_1\left(\frac{Z_1 - L_1^*}{H_1^* - L_1^*}\right) + w_2\left(\frac{L_4^* - Z_4}{L_4^* - H_4^*}\right) + w_3\left(\frac{L_5^* - Z_5}{L_5^* - H_5^*}\right) + w_4\left(\frac{L_6^* - Z_6}{L_6^* - H_6^*}\right)$ (3.68)

Case 5: Minimize $p_1 Z_1$, Minimize $p_1 Z_4$, Minimize $p_2 Z_5$, Minimize $p_3 Z_6$ (3.69)

3.4.4.3 Non-Compromise vs. Compromise Case

Finally, while real (non-compromise) constraints are typically formulated in multi-objective mathematical programs, GP models contain goal (compromise) constraints. As one might expect, infeasibility can be an issue when no feasible solution exists that satisfies all real constraints on goals in the model. On the other hand, the GP model with goal constraints provides compromise solutions regardless of whether or not a goal(s) is achieved. With this in mind, we again conduct a comparative study on the two tuples: 1) Case 0 vs. Cases 2 and 4 and 2) Case 1 vs. Cases 3 and 5. In particular, the constraint sets can be formulated in two ways, depending on whether real constraints on goals (3.70) or goal constraints (3.71) are used:

Real constraints (7), (8) - (32), *Real constraints on goals* (33) - (35), and *variable-type constraints* (3.70)

Real constraints (7), (8) - (32), *Goal constraints* (36) - (38), and *variable-type constraints* (3.71)

3.5 Hazus-based Regional Case Studies

3.5.1 Methodology and Assumptions

While researchers commonly have available data for pre-disaster studies (e.g., inventory positions, warehouse locations, etc.), data availability for post-disaster studies is limited (Galindo and Batta 2013). In this paper, we use Hazus, FEMA's GIS-based natural hazard loss estimation software, to demonstrate the applicability of our GP-based MOIRR model. Hazus requires both an inventory collection module and a hazard identification module as inputs to calculate its risk evaluation module's outputs. We use the resulting Hazus loss data as input to the GP-based MOIRR model for all cases in our designed experiment. We implement the above mathematical model in AMPL (Fourer *et al.* 2002) and analyze it using CPLEX on a PC with an Intel® Core™ i7- 2600 CPU running @3.40 GHz with 16 GB of RAM. The maximum computation time allowed is limited to one hour as per Ransikarbum and Mason (2014).

We generate two disaster instances using Hazus's earthquake module to obtain predicted loss data in two different study regions of interest: 1) a small-sized, low-density area as exemplified by SC and 2) a larger-sized, high-density area such as CA. Hazus reports that SC has an area of 32,020 square miles with 867 total census tracts, while CA has an area of 163,696 square miles with 8,057 total census tracts.

Two different threshold levels are examined for both the SC and CA case studies to illustrate how goal settings can affect the GP-based MOIRR model: conservative and aggressive. While the conservative case (low-expectation threshold) is meant to represent a decision maker's goal choices for fairness, unsatisfied demand, and total costs that are presumably easy to achieve (based on budget, capacity, etc.), the aggressive case (high-expectation threshold) represents comparably harder to achieve goals.

3.5.1.1 Hazus-generated SC Assumptions

The parameter data and necessary assumptions associated with the SC case study are shown in Table 3.2. While most of the loss data can be obtained directly from Hazus, some parameters must be extrapolated from available data. For example, capacity-related data are extrapolated based on the size and infrastructure of selected supply points and warehouses. Six major SC airports are chosen as relief supply points: Charleston, Columbia, Florence, Greenville, Hilton Head, and Myrtle Beach. Hazus's inventory collection module reports that there are 47 emergency operations centers (EOCs) in the state; we model them as relief warehouses. We simulate a 9.0 magnitude earthquake in the Columbia, SC metropolitan area. Hazus-based "before and after" disaster instance maps for the SC case study are shown in Figure 3.2. Figure 3.2(a) presents the position of the earthquake, as well as the existing infrastructure in SC, while Figure 3.2(b) shows loss data output from Hazus: one disrupted relief supply point, 16 disrupted relief warehouses, and 143 demand census tracks affected by the earthquake.

3.5.1.2 Hazus-generated CA Assumptions

For comparison purposes, similar assumptions to those in Table 3.2 are used in our CA case study. Seven major CA airports are chosen as relief supply points: Sacramento, Oakland, San Diego, Jon Wayne, San Francisco, Los Angeles, and San Jose. A total of 40 EOCs from Hazus's inventory collection module are modeled as relief warehouses. A 9.0 magnitude earthquake is modeled to occur near Los Angeles. Figure 3.2(c) presents the position of the earthquake, as well as the existing infrastructure inclusive of relief supply points and warehouses in CA. Next, Figure 3.2(d) shows loss data output: one disrupted relief supply point, 12 disrupted relief warehouses, and 1,268 demand census tracks affected by the earthquake.

3.5.2 Experimental Study

The loss data obtained from Hazus for both the SC and CA case studies are used as inputs to the GP-based MOIRR model for all Cases 0-5 in the designed experiment in order to obtain outputs related to distribution and system restoration decisions. In any non-preemptive approach, we use equal objective weights, implying that all objectives and/or goal are of equal importance to the decision maker.

3.5.2.1 SC-specific Results

Objective Functions Results

Objective function values for all experimental cases for the SC study are shown in Table 3.3. The results are further differentiated based on goal-seeking levels, and then associated undesired deviational variables and computation time are reported. We note that as the GP-based MOIRR model is a mixed-integer program (MIP) with a limited computation time, solutions with MIP optimality gaps are reported. On average, the achieved fairness, unsatisfied demand, and total costs values across all cases and goal seeking levels are 72.12%, ~224K units, and $1.36 billion, respectively.

Table 3.2: Hazus parameter and data list for SC and CA regional case studies

Activities	Symbol	Category	Descriptive detail
Supply relief port node			
Number of supply port nodes	S	Hazus	
Number of disrupted supply port nodes	S^D	Hazus	
Cost for restoring each disrupted supply port node	η_i^S	Hazus	
Supply units available at each supply port node	s_i	Extrapolation	From port size and demand units
Fixed charge for restoring disrupted supply port node	ν^S	Extrapolation	From port node's restoration cost
Relief warehouse node			
Number of transhipment (relief warehouse) nodes	T	Hazus	
Number of disrupted transhipment (relief warehouse) nodes	T^D	Hazus	
Cost for restoring each disrupted relief warehouse node	η_i^T	Hazus	
Fixed charge for restoring disrupted relief warehouse node	ν^T	Extrapolation	From warehouse node's restoration cost
Capacity for each transhipment (relief warehouse) node	α_i	Extrapolation	From warehouse size (Hazus's inventory)
Capacity needed for each unit flow to use relief warehouse node	φ_i	Not available	1 unit assumption
Demand node			
Number of demand/ beneficiary nodes	D	Hazus	
Demand units required at each demand/ beneficiary node	d_i	Hazus	
Arc between supply port and relief warehouse nodes			
Cost for restoring each disrupted arc between supply port and warehouse node	$\lambda_{i,j}^{ST}$	Hazus	
Distance in miles between each origin and destination pair based on latitude/longitude	$d_{i,j}^{OD}$	Hazus	
Fixed charge for restoring disrupted arc between supply port and warehouse node	ω^{ST}	Extrapolation	From arc's restoration cost
Number of disrupted arcs between supply port and relief warehouse nodes	Λ^D	Not available	Randomly distributed; 30% disruption
Road capacity for each arc between port and relief warehouse node	$\delta_{i,j}^{ST}$	Not available	5000 unit assumption
Capacity needed to use road (arc) between supply port and relief warehouse node	$\psi_{i,j}^{ST}$	Not available	1 unit assumption
Cost for transporting each unit flow per mile through each arc	$c_{i,j}$	Not abailable	$15 per unit per mile assumption
Arc between relief warehouse and demand nodes			
Cost for restoring each disrupted arc between warehouse and demand node	$\lambda_{i,j}^{TD}$	Hazus	
Distance in miles between each origin and destination pair based on latitude/longitude	$d_{i,j}^{OD}$	Hazus	
Fixed charge for restoring disrupted arc between warehouse and demand node	ω^{TD}	Extrapolation	From arc's restoration cost
Number of disrupted arcs between relief warehouse and demand nodes	Π^D	Not available	Randomly distributed; 30% disruption
Road capacity for each arc between warehouse and demand node	$\delta_{i,j}^{TD}$	Not available	2500 unit assumption
Capacity needed to use road (arc) between warehouse and demand node	$\psi_{i,j}^{TD}$	Not available	1 unit assumption
Cost for transporting each unit flow per mile through each arc	$c_{i,j}$	Not available	$8 per unit per mile assumption
Others			
Budget for total disrupted node restoration	b^N	Extrapolation	Based on total node restoration cost
Budget for total disrupted arc restoration	b^A	Extrapolation	Based on total arc restoration cost
Budget for total network flow transportation	b^F	Extrapolation	Based on total transportation cost
Maximum allowable number for disrupted node restoration	θ^N	Not available	At most 8 node assumption
Maximum allowable number for disrupted arc restoration	θ^A	Not available	At most 300 arc assumption

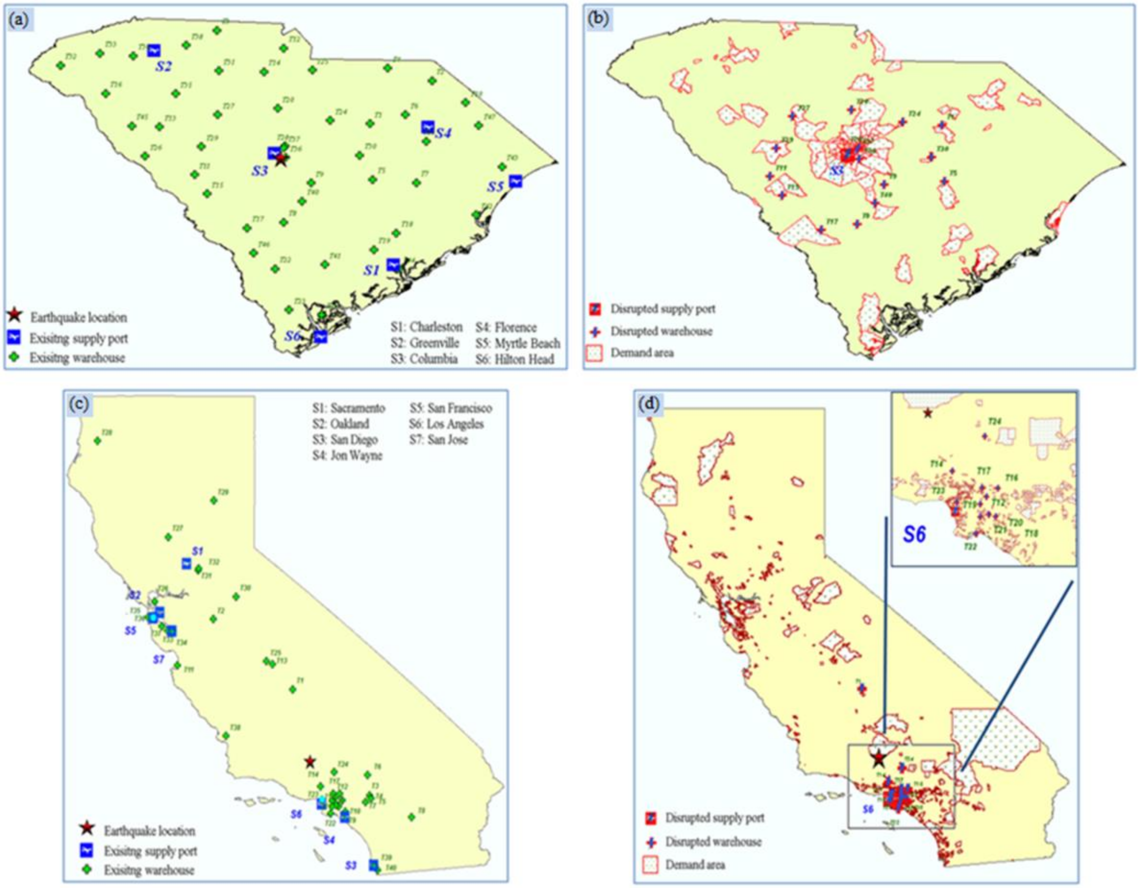

Figure 3.2: Hazus-based infrastructure map illustration given an earthquake: (a) SC before , (b) SC after, (c) CA before, and (d) CA after

Considering the conservative threshold goal, the associated objective values for the MOP (Cases 0 and 1) show optimal values depending on whether different weights are assigned or different priorities are given. Although different objective values are obtained between the cases, similar objective values are expected when w_1 is much larger than w_2 and w_3. On the other hand, optimal objective values for the MOGPG (Cases 2 and 3) are based on goals that are not necessarily similar to the MOP due to different driven objectives. With regard to the MOGPMOG (Cases 4 and 5), an optimal value for the fairness is driven by both fairness objective and deviational variable for fairness goal and is found to be similar to the MOP, while optimal values for the total unsatisfied demand and cost are only driven by goals. There is also a trade-off between computation time and optimal values driven by objectives alone, goals alone, or a combination of objectives and goals.

Table 3.3: GP-based MOIRR experimental results: SC and CA case studies

Case Study Description	**Scenario Model**	**Solution Method**	**Obj.1 (%)**	**Obj.2 (Units)**	**Obj.3 ($)**	D^{-F} **(%)**	D^{+U} **(Units)**	D^{+C} **($)**	**Computation Time (Seconds)**
SC Case Study									
Case 1 (low threshold)	*Case 0*	$w_1 = w_2 = w_3$	71.28	231,496	1.19 billion	N/A	N/A	N/A	24
: ***Goal 1*** *(g_F) = 70 % (Fairness)*	*Case 1*	$p_1 \rightarrow p_2 \rightarrow p_3$	75.01	201,496	1.49 billion	N/A	N/A	N/A	3,725
: ***Goal 2*** *(g_U) = 300,000 units (Unsatisfied Demand)*	*Case 2*	$w_1 = w_2 = w_3$	70.00	239,704	1.49 billion	0	0	0	20
: ***Goal 3*** *(g_C) = $1.50 billion (Total Cost)*	*Case 3*	$p_1 \rightarrow p_2 \rightarrow p_3$	70.00	241,884	1.50 billion	0	0	0	715
	Case 4	$w_1 = w_2 = \dots w_4$	75.01	201,496	1.50 billion	0	0	0	25
	Case 5	$p_1 \rightarrow p_2 \rightarrow \dots p_4$	75.01	201,496	1.49 billion	0	0	0	840
Case 2 (high threshold)	*Case 0*	$w_1 = w_2 = w_3$		Infeasible		N/A	N/A	N/A	N/A
: ***Goal 1*** *(g_F) = 80 % (Fairness)*	*Case 1*	$p_1 \rightarrow p_2 \rightarrow p_3$		Infeasible		N/A	N/A	N/A	N/A
: ***Goal 2*** *(g_U) = 100,000 units (Unsatisfied Demand)*	*Case 2*	$w_1 = w_2 = w_3$	67.26	263,996	0.99 billion	12.74	163,996	0	1,312
: ***Goal 3*** *(g_C) = $1.00 billion (Total Cost)*	*Case 3*	$p_1 \rightarrow p_2 \rightarrow p_3$	75.01	201,496	1.49 billion	4.99	101,496	0.49 billion	2,485
	Case 4	$w_1 = w_2 = \dots w_4$	67.58	261,496	1.01 billion	12.42	161,496	0.01 billion	1,420
	Case 5	$p_1 \rightarrow p_2 \rightarrow \dots p_4$	75.01	201,496	1.49 billion	4.99	161,496	0.49 billion	2,647
	Mean		***72.12***	***224,606***	***1.36 billion***				***1,321***
CA Case Study									
Case 1 (low threshold)	*Case 0*	$w_1 = w_2 = w_3$	22.78	3,937,090	5.00 billion	N/A	N/A	N/A	765
: ***Goal 1*** *(g_F) = 20 % (Fairness)*	*Case 1*	$p_1 \rightarrow p_2 \rightarrow p_3$	22.87	3,932,270	4.90 billion	N/A	N/A	N/A	2,228
: ***Goal 2*** *(g_U) = 4,500,000 units (Unsatisfied Demand)*	*Case 2*	$w_1 = w_2 = w_3$	20.00	4,078,590	5.00 billion	0	0	0	51
: ***Goal 3*** *(g_C) = $5.00 billion (Total Cost)*	*Case 3*	$p_1 \rightarrow p_2 \rightarrow p_3$	20.00	4,077,974	5.00 billion	0	0	0	470
	Case 4	$w_1 = w_2 = \dots w_4$	23.07	3,922,149	5.00 billion	0	0	0	3,600
	Case 5	$p_1 \rightarrow p_2 \rightarrow \dots p_4$	23.50	3,900,151	5.21 billion	0	0	0.21 billion	10,200
Case 2 (high threshold)	*Case 0*	$w_1 = w_2 = w_3$		Infeasible		N/A	N/A	N/A	N/A
: ***Goal 1*** *(g_F) = 50 % (Fairness)*	*Case 1*	$p_1 \rightarrow p_2 \rightarrow p_3$		Infeasible		N/A	N/A	N/A	N/A
: ***Goal 2*** *(g_U) = 2,500,000 units (Unsatisfied Demand)*	*Case 2*	$w_1 = w_2 = w_3$	22.72	3,940,156	4.96 billion	27.28	1,440,156	1.96 billion	139
: ***Goal 3*** *(g_C) = $3.00 billion (Total Cost)*	*Case 3*	$p_1 \rightarrow p_2 \rightarrow p_3$	22.87	3,932,270	4.90 billion	27.13	1,432,270	1.90 billion	5,600
	Case 4	$w_1 = w_2 = \dots w_4$	22.56	3,948,237	5.21 billion	27.44	1,448,237	2.21 billion	194
	Case 5	$p_1 \rightarrow p_2 \rightarrow \dots p_4$	22.65	3,943,237	5.26 billion	27.35	1,443,237	2.26 billion	9,700
	Mean		***22.30***	***3,961,212***	***5.04 billion***				***3,295***

Further, as all deviational variables (D^{-F}, D^{+U}, and D^{+C}) are driven to zero for the low-threshold cases, this confirms that all conservative goals are achieved in the conservative threshold cases. Considering our aggressive threshold goals, the MOP did not find a feasible solution that satisfies the real constraints on goals. However, the approaches using GP (MOGPG and MOGPMOG) obtain compromise solutions that satisfy the goal constraints, regardless of whether or not a goal can be achieved. The deviational variables for the high-threshold case that are greater than zero confirm that some goals cannot be achieved.

Computation Time Results

In terms of computation time, the non-preemptive approach (Cases 0, 2, and 4) requires less computation time than does the preemptive approach (Cases 1, 3, and 5), in general. However, it can be challenging to choose appropriate levels for weights. On average, the computation time for the SC case study is ~1,300 seconds. Table 3.4 depicts the computation time trade-offs resulting from different solution methods, model categories, desired goal settings, and model approaches. Required computation time is monotonically non-decreasing with an increase in the number of objectives under the preemptive method. In terms of each modelling approach's average computation time, MOGPG < MOGPMOG < MOP, in general. While high computation time for MOP is caused by the method reaching the imposed 3600 second time limit while trying to achieve its objective optimality directive, MOGPG requires less computation time to seek goal optimality directive. It is clear that given different expected goal thresholds, the aggressive case consumes more computation time as compared to the conservative case due to its tighter constraints. Finally, while the MOP high-threshold case is infeasible, the required computation time for the high-threshold MOGPG and MOGPMOG cases are significantly higher than for the corresponding low-threshold cases.

Table 3.4: Aggregated computation time by modeling approach for SC and CA case studies

Category			Average Computation Time (Seconds)	
			SC Case Study	CA Case Study
By solution method	Non-preemptive		471	919
	Preemptive		2356	5071
By model category	MOP		1875	1497
	MOGPG		1133	1565
	MOGPMOG		1233	5924
By threshold value	Low-threshold		892	2886
	High-threshold		1966	3908
By model category by threshold value	MOP	Low-threshold	1875	1497
		High-threshold	N/A	N/A
	MOGPG	Low-threshold	368	261
		High-threshold	1898	2870
	MOGPMOG	Low-threshold	433	6900
		High-threshold	2034	4947

Distribution and Restoration Decision Results

The model's recommended flow decisions are illustrated using maps of SC for Case 0 and Case 2 under a low-expectation threshold to portray both MOP and GP results (Figure 3.3). While Figures 3.3(a) and 3.3(b) show examples of the flow decisions resulting from the restored Columbia supply point to its relief warehouses and to their associated demand points, respectively, for Case 0, Figure 3.3(c) and Figure 3.3(d) illustrate the corresponding flows for Case 2. The results confirm that longer travel distances are required in Case 2, along with higher transportation costs, due to the underlying Origin-Destination (O-D) matrix.

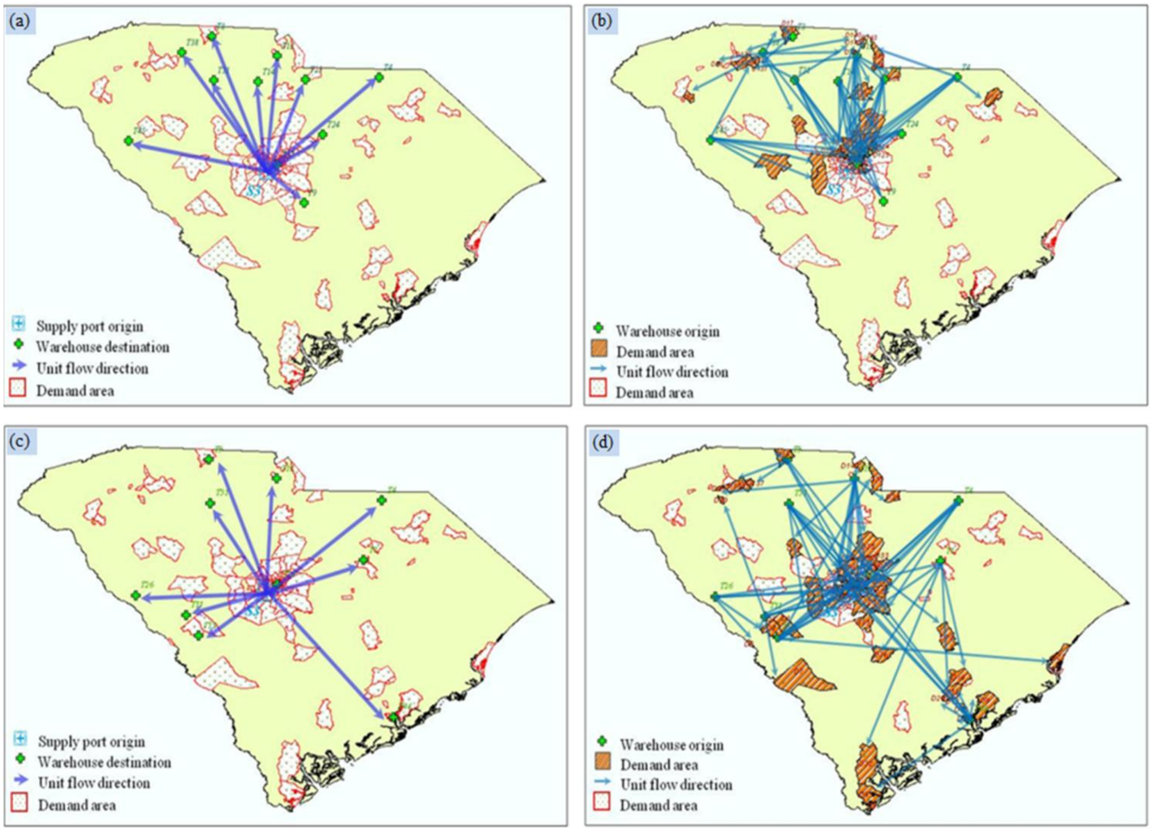

Figure 3.3: SC case study: (a) Flow from port for Case 0, (b) Flow from warehouse for Case 0, (c) Flow from port for Case 2, and (d) Flow from warehouse for Case 2

Table 3.5 reveals the restoration decisions recommended for all experimental cases: the percent restoration inclusive of partial and full restoration based on the number of 1) disrupted port nodes, 2) disrupted warehouse nodes, 3) disrupted arcs between port and warehouse nodes, and 4) disrupted arcs between warehouse and demand nodes. For the conservative case, restoration decisions are similar in most of the cases, except for the MOGPG (Cases 4-5) wherein restoration decisions for disrupted arcs between warehouses and demand nodes are recommended. However, this is not the case for the aggressive scenario. In this environment, restoration decisions are similar for all GP-based cases (Cases 2-7) as the goal constraints are tight with unachievable goals.

Table 3.5: Restoration Decisions for SC and CA case studies

Case Study Description	Loss Data		Percent Restoration from Disrupted Number					
			Case 0	Case 1	Case 2	Case 3	Case 4	Case 5
SC Case Study								
Case 1 (low threshold)	Number of disrupted port node	1	100.00%	100.00%	100.00%	100.00%	100.00%	100.00%
	Number of disrupted warehouse node	16	43.75%	43.75%	43.75%	43.75%	43.75%	43.75%
	Numberof disrupted arc b/w port and warehouse nodes	85	11.18%	30.88%	25.88%	26.76%	31.47%	31.47%
	Number of disrupted arc b/w warehouse and demand nodes	2017	0.00%	0.00%	0.45%	0.42%	0.00%	0.00%
Case 2 (high threshold)	Number of disrupted port node	1	Infeasible	Infeasible	100.00%	100.00%	100.00%	100.00%
	Number of disrupted warehouse node	16			43.75%	43.75%	43.75%	43.75%
	Numberof disrupted arc b/w port and warehouse nodes	85			1.76%	30.88%	2.35%	30.88%
	Number of disrupted arc b/w warehouse and demand nodes	2017			0.00%	0.00%	0.00%	0.00%
CA Case Study								
Case 1 (low threshold)	Number of disrupted port node	1	100.00%	100.00%	0.00%	0.00%	100.00%	100.00%
	Number of disrupted warehouse node	12	29.17%	29.17%	50.00%	50.00%	29.17%	29.17%
	Numberof disrupted arc b/w port and warehouse nodes	84	77.98%	72.62%	50.00%	77.08%	75.00%	78.57%
	Number of disrupted arc b/w warehouse and demand nodes	15216	0.00%	0.00%	0.01%	0.02%	0.00%	0.00%
Case 2 (high threshold)	Number of disrupted port node	1	Infeasible	Infeasible	100.00%	100.00%	100.00%	100.00%
	Number of disrupted warehouse node	12			29.17%	29.17%	29.17%	29.17%
	Numberof disrupted arc b/w port and warehouse nodes	84			78.57%	72.62%	75.00%	72.02%
	Number of disrupted arc b/w warehouse and demand nodes	15216			0.00%	0.00%	0.00%	0.00%

3.5.2.2 CA-specific Results

<u>Objective Functions Results</u>

The CA case study results' objective functions values are also shown in Table 3.3. Although the results are comparable to the SC case study, some observed differences are evident. Clearly, a much lower fairness, higher unsatisfied demand, and higher cost are reported due to the large disruption and dense demand in CA. On average, 22.30% fairness, 3.96M units of unsatisfied demand, and $5.04 billion in total costs resulted from our Hazus model investigations. Further, in contrast to the SC study, the unwanted deviational variable for total cost goal (D^{+C}) in the low threshold environment for Case 5 is positive (i.e., the goals are not achieved), while the associated deviational variables for fairness and unsatisfied demand goals equal zero. This occurs because the most important priority is fairness, while the least important is total cost in the preemptive approach.

Computation Time Results

Although the average computation time for the CA case is much higher than that of the SC instance (~3,300 vs. ~1,300 secs), similar trends as those present in the SC case are evident. The computation time for the CA study is higher due to the size of the problem instance and the NP-hard nature of the problem under study. Computation time is also aggregated based on different factors in Table 3.4. The average computation time for the preemptive approach is much higher than for the non-preemptive cases. In contrast to the SC case study, the average computation time for MOGPMOG is much higher than either MOP or MOGPG. This is noteworthy as four objective functions are used in the MOGPMOG, while three objectives are used in both MOP and MOGPG. When different goal expectations are compared, both the conservative and aggressive cases are shown to require quite similar amounts of computation time. Finally, while the average computation time for MOGPG in the high-threshold case is higher than the low-threshold case as expected, this is not the case for the MOGPMOG.

Distribution and Restoration Decision Results

Table 3.5 shows the models' resulting restoration decisions for experimental cases in the CA case study. A discussion similar to the SC case study can be drawn with respect to the MOGPG wherein some restoration decisions for disrupted arcs between warehouse and demand nodes are suggested. The recommended restoration and flow decisions for a restored relief port and relief warehouses are displayed on CA maps in Figure 3.4. Figure 3.4(a) illustrates the model's restoration decisions which comprise six existing and one restored relief port, as well as 28 existing and seven partially-restored relief warehouses—no full-restoration decisions are recommended. Figure 3.4(b) shows examples of flow decisions from the restored Los Angeles airport to its relief warehouses, while Figures 3.4(c) and 3.4(d) illustrate flow decisions from northern and southern relief warehouses to their demand points, respectively.

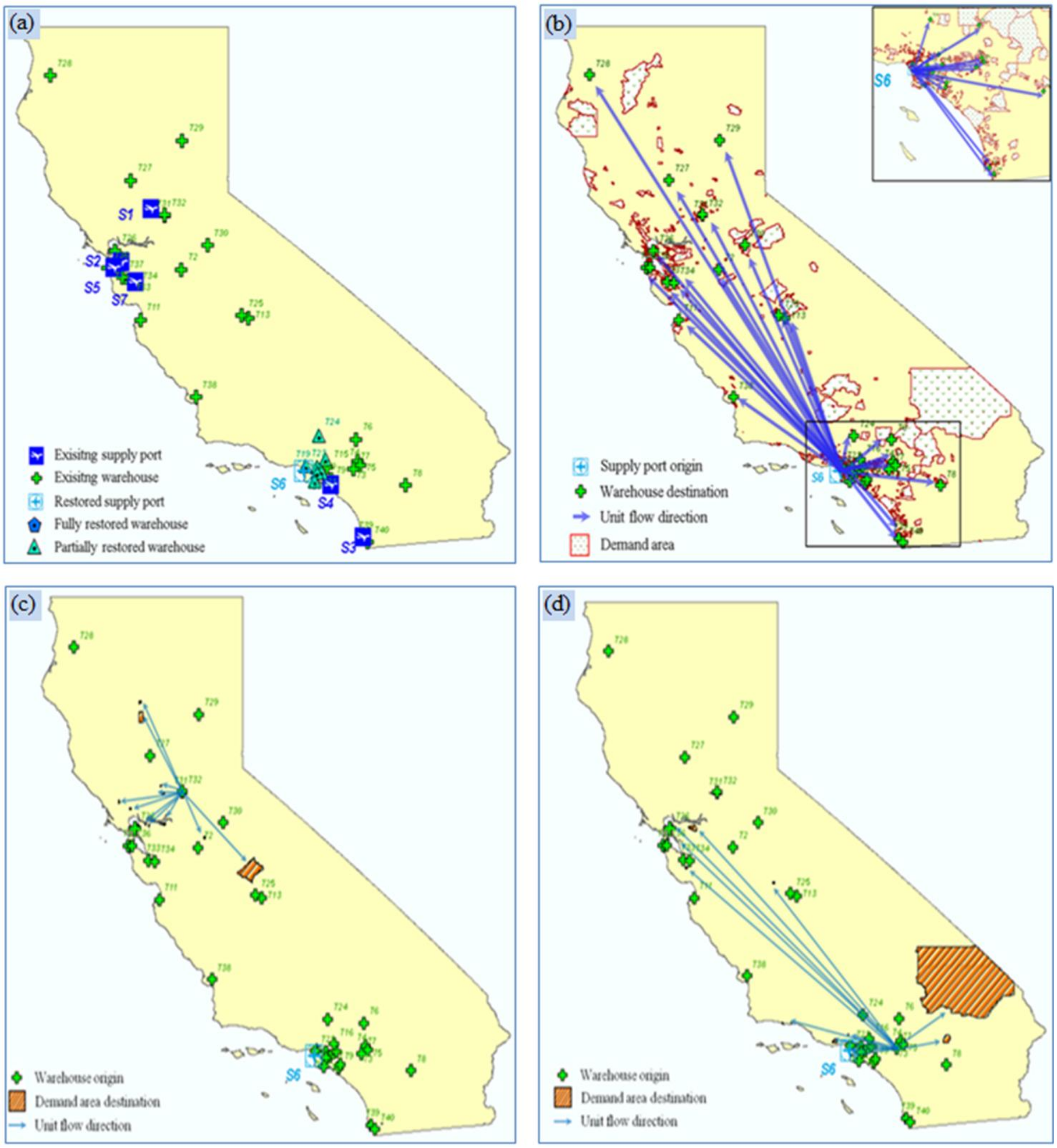

Figure 3.4: CA case study: (a) Restoration decisions, (b) Flow from port, (c) Flow from northern warehouse, and (d) Flow from southern warehouse

3.5.3 Developing the Efficient Frontier (EF)

We now develop the efficient (non-dominated; Pareto optimal) frontier for the CA case study to explore the trade-offs that exist between objectives. By definition, a solution $x^0 \in S$ is said to be efficient if $f_k(x) > f_k(x^0)$ for some $x \in S$ implies that $f_j(x) < f_j(x^0)$ for at least one other index j. It is therefore a feasible solution that is not dominated by any other feasible solution and has the property that an improvement in any one objective is possible only at the expense of a poorer solution in at least one other objective (Ravindran, 2007). The set of all efficient solutions, the efficient frontier, is commonly used to evaluate trade-offs among decision criteria in objective space.

We examine two objective pairs using the non-preemptive approach and the rating method in Ransikarbum and Mason (2014): 1) max z_1 fairness vs. min z_3 cost and 2) min z_2 unsatisfied demand vs. min z_3 cost. A selected set of efficient solutions is generated by varying the weight w_i for objective i discretely from 0.1 to 0.9 at 0.1 increments; this yields at most nine efficient solutions points. Given these points, we generate a polynomial trendline to describe the objectives. By using similar notation as in Section 3.4, Pairs 1 and 2 are normalized using a linear normalization technique to allow inter-criterion comparison in (3.72) and (3.73), respectively:

$$\text{Maximize } w_1\left(\frac{Z_1 - L_1^*}{H_1^* - L_1^*}\right) + w_2\left(\frac{L_3^* - Z_3}{L_3^* - H_3^*}\right) \tag{3.72}$$

$$\text{Maximize } w_1\left(\frac{L_2^* - Z_2}{H_2^* - L_2^*}\right) + w_2\left(\frac{L_3^* - Z_3}{L_3^* - H_3^*}\right) \tag{3.73}$$

3.5.3.1 EF Sensitivity Analysis

The fairness achieved in the CA case study is relatively low when compared to the SC case. Thus, a sensitivity analysis is conducted by varying parameters that restrict the fairness for the CA high demand case. Initial experiments with several parameters identified a key parameter that restricts the increase in fairness achievable: the capacity of an arc between relief supply port and warehouse nodes ($\delta_{i,j}^{ST}$). An implication of varying this parameter is that when a disruption occurs under expected high demand, a post-disaster strategy to increase road capacity could be employed (e.g., reversing a lane's traffic flow). We conduct the following sensitivity analyses:

- EF Base Case: $\delta_{i,j}^{ST}$ is set to 5,000 units (the 'as-is' parameter value in Table 3.2)
- EF Case 1: $\delta_{i,j}^{ST}$ is set to 10,000 units (the 'what-if' parameter value)
- EF Case 2: $\delta_{i,j}^{ST}$ is set to 20,000 units (the 'what-if' parameter value)

3.5.3.2 EF Results

Figure 3.5(a) (3.5(b)) illustrates the approximate EFs for the Case 1 (Case 2) pair of objectives. It is clear that increasing capacity improves fairness and lowers unsatisfied demand, but at the expense of higher costs. Using Figure 3.5(a) with the EF Base case as an example, when more weight is given to the fairness objective (e.g., w_1 =0.6, w_2 =0.4), the corresponding objective values for fairness and total cost are 23.35% and \$5.27 billion, respectively. However, when more weight is given to the cost objective (e.g., w_1 =0.4, w_2 =0.6), the corresponding objective values are 13.59% and \$1.78 billion. A similar interpretation can be drawn from EF Exp. 1 and EF Exp. 2, when arc capacity is increased.

An interpretation for the second pair of objectives study is quite similar (Figure 3.5(b)). Given a (w_1 =0.8, w_2 =0.2) weighting preference, the corresponding objective values for unsatisfied demand units and cost for EF base, EF Exp. 1, and EF Exp. 2 are

(3.89M units, \$5.12 billion), (2.69M units, \$9.36 billion), and (713K units, \$15.75 billion), respectively. If/when a decision maker can cost-justify increasing arc capacities, such as in EF Cases 1 and 2, the benefit will be increasing fairness to an acceptable or desired level.

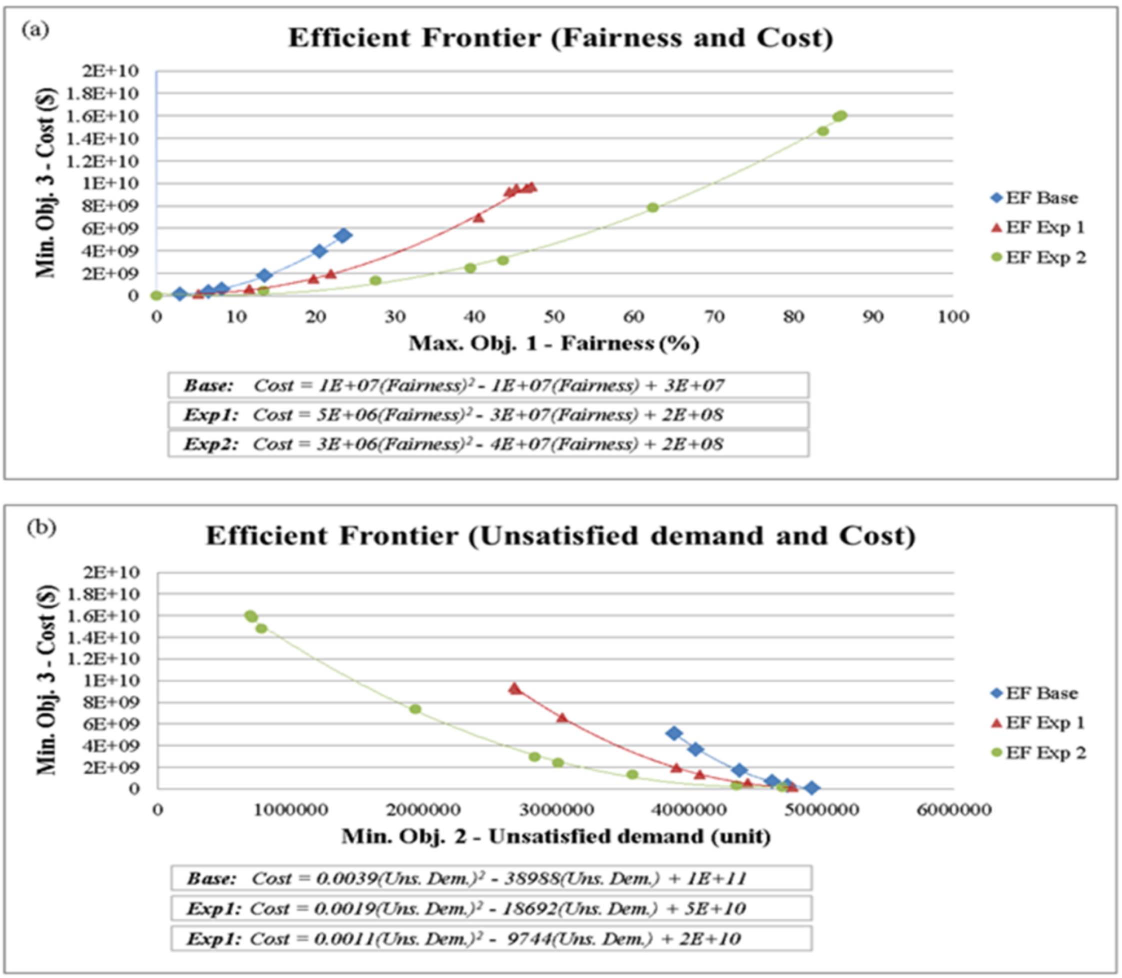

Figure 3.5: Efficient frontier for CA case study with sensitivity analysis: (a) Fairness and Cost, (b) Unsatisfied demand and Cost

This approximate EF can also be used to fit a polynomial trendline so that the general shape of the front can be quickly obtained for any case and objective pair set. Considering objective pair 1 in Figure 3.5(a), if 20% fairness is desired, a decision maker can see that the associated costs for EF base, EF Case 1, and EF Case 2 are ~$4.0B, ~$2.0B, and ~$0.6B, respectively. Similarly, if a decision maker is interested to spend at most $4.0B, it follows from the trendline that the corresponding expected fairness values would be 20%, 31%, and 43%, respectively.

3.6 Managerial Insights

One way to treat multiple criteria is to select one criterion as the primary one used in the objective function and consider the others as secondary objectives that can be assigned "acceptable" values in constraint right hand sides. However, if careful consideration is not given while selecting the acceptable levels by decision makers, a feasible design that satisfies all the constraints may not exist—our GP-based model overcomes this potential issue.

Further, a trade-off clearly exists between solution quality and computation time. A decision maker can choose a combination of model scenarios related to a chosen multiple-objective solution method, optimality directive, and compromise tolerance that satisfy his/her requirements. While the non-preemptive method requires less computation time than the preemptive method, this comes at the expense of difficulty in specifying appropriate weights. If a near- (non-) optimal solution is acceptable, computation time can also be decreased. The use of goal constraints can also benefit decision makers via compromise solutions.

The EF sensitivity analysis we describe suggests that capacity-related strategic planning can be implemented for a high disruption event. An understanding of the trade-offs among objectives via an exploration of the EF is important as these frontiers can help a decision maker to visualize the objective space. The Pareto fronts also provide an objective function trade-off curve that informs a decision maker on how improving one objective can deteriorate the second one's performance, and vice versa.

3.7 Conclusions and Future Research

A review of the post-disaster disruption management research reveals little if any models that produce integrated recommendations across the disaster management cycle. We transform the previously developed multiple-objective response and recovery model for the integrated supply distribution and the restoration problem into a goal programming model. This new, extended model, using goal constraints, provides decision makers with compromise solutions under desired goals for this challenging, practically-motivated research problem.

Analysis of our experimental study confirms that the GP-based model provides a compromise solution when no solution exists that satisfies strict or real constraints. Road capacity-related decisions are investigated to increase fairness given a disruption. Further, by analyzing a combination of design factors, we present the trade-off that exists between solution quality and computation time so that decision makers can choose the most appropriate modelling approach for their use. Two case studies, based on hypothetical earthquake scenario loss data estimated from FEMA's Hazus software, are used to provide efficient frontier and sensitivity analysis results discussion.

This GP-based multiple-objective approach contains capacity, budget, and resource constraints for which a decision maker can express his/her desired levels or goals. As it is important to analyze large-scale disaster relief network problems quickly to obtain a diverse collection of effective, near-optimal solutions in a real-world disaster scenario, multiple-objective metaheuristic approaches could be further investigated—their application to this problem would provide practical, effective solutions to this NP-hard problem in a timely manner to aid in critical disaster relief decisions.

CHAPTER FOUR

A BI-CRITERIA METAHEURISTIC FOR INTEGRATED POST-DISASTER RELIEF SUPPLY AND NETWORK RESTORATION DECISIONS

4.1 Introduction

In this chapter, we investigate a metaheuristic optimization approach using an evolutionary algorithm (EA) for our MOIRR model developed earlier (Ransikarbum and Mason 2014). The MOIRR provides a strategic decision-making tool aiding supply distribution and network restoration decisions with fairness- or-equity-based solutions under constrained capacity, budget, and resource limitations. Considering multiple, conflicting objectives of the model, generating Pareto-optimal front with ample, diverse solutions quickly is important for a decision maker to make an informative, final decision. By decomposing this problem, we adapt the NSGA-II (Deb *et al.* 2002) by integrating an evolutionary heuristic with optimization-based techniques called the Hybrid NSGA-II in this paper to find multiple, non-dominated solutions quickly in real-world scenarios for this NP-hard problem. After applying the algorithm to a Hazus-generated loss scenario in SC from an earthquake, comparisons between the mathematical model and the Hybrid NSGA-II algorithm are done using a Hypervolume-based technique, percentage of solutions in the first front, and computation time.

The remaining sections of this chapter are organized as follows. We overview the pertinent literature in Section 4.2 and discuss the MOIRR model in Section 4.3. The Hybrid NSGA-II algorithm with a designed experiment and experimental results are discussed in Section 4.4 and Section 4.5, respectively. Finally, Section 4.6 presents our managerial insights and Section 4.7 shows research conclusions and outlines directions for future research. This chapter is submitted to the journal with the following citation:

Ransikarbum, K. and Mason, S. J. 2015b. A Metaheuristic for Post-Disaster Integrated Relief Supply and Network Restoration Decisions. *Working Paper.*

4.2 Literature Review

Humanitarian logistics research is becoming a key driver for devising improved ways of managing multi-stakeholder relief operations. Sheu (2007) defines humanitarian logistics as “a process of planning, managing, and controlling the efficient flows of relief, information, and services from the points of origin to the points of destination to meet the urgent needs of the affected people under emergency conditions.” A number of literature reviews suggest that more research in humanitarian logistics is needed (Wassenhove 2005, Altay and Green 2006, Tatham and Pettit 2010, Caunhye *et al.* 2012, Celik *et al.* 2012, Galindo and Batta 2013, and Day 2014). In addition, previous authors commonly cite the need to transfer more techniques from commercial SCM into humanitarian logistics research.

Performance measurement in humanitarian logistics differs from commercial logistics metrics (Chan 2003, Beamon and Balcik 2008, and Christopher and Tatham 2011). Beamon and Balcik (2008) discuss the different characteristics between non-profit and for-profit organizations based on revenue sources, goals, stakeholders, and performance measurement. Haddow *et al.* (2011) provide a thorough discussion of stakeholder roles in each phase of disaster management and suggest that these stakeholders have different objectives, which are often in conflict. Celik *et al.* (2012)

point out that not only effectiveness, but also the efficiency of post-disaster logistics activities are needed to capture performance. Strategies to improve emergency relief performance are also discussed by Synder *et al.* (2012) and Ivanov *et al.* (2014). Synder *et al.* (2012) motivate the need to understand how disruption propagates from upstream to downstream in multi-echelon systems. Ivanov *et al*. (2014) similarly highlight the *ripple effect* in supply chains to understand how changes to some variables influence performance in the rest of the chain. Christopher and Tatham (2011) also discuss the need for developing appropriate performance metrics for humanitarian operations that capture aid recipients' viewpoints; one such metric is fairness or equity.

The concept of equity and its measurement receives attention from several researchers in the literature (e.g., Ogryczak 2000, Kostreva *et al.* 2003, Singh 2007, Zhu *et al.* 2010, and Ransikarbum and Mason 2014). Minimax, maximin, and maxisum techniques are frequently used in equity- or fairness-related research. While minimax objectives determine equitable solutions for problems wherein smaller objective function values are desirable, maximin objectives are used when larger performance function values are considered better (Luss 1999). The maximin approach has been applied in several problems (Kaplan 1973, Zhang and Melachrinoudis 1999, Salles and Barria 2008, Sayin 2013). Kaplan (1973) initially discusses the concept of a maximin objective function and shows that it can be transformed and solved by linear programming. Salles and Barria (2008) assert that this approach often requires complex optimization procedures and significant computation time to find a solution.

The humanitarian logistics literature can be categorized into the four phases of the disaster management cycle related to pre- and post-disaster operations (McLoughlin 1985). While most previous research models are related to pre-disaster issues (Jia *et al.* 2007, Balcik and Beamon 2008, and Doerner *et al.* 2009), recent research points to the need for post-disaster-related operations as well as integrated disaster management cycle phases (Celik *et al.* 2012, Galindo and Batta 2013). A similar line of research addresses the models in a resilience and reliability domain for an infrastructure network during the pre- and post- disasters (Synder *et al*. 2006, Liberatore *et al*. 2012, Akgun *et al.* 2014, and Alderson *et al.* 2014). For example, Liberatore *et al.* (2012) propose a facility protection model considering the possibility of interdependencies among the disruptions to improve the reliability of an existing network using attacker-defender models. Similarly, Alderson *et al.* (2014) illustrate how to build and solve a sequence of models to improve the resilience of an infrastructure system from disruptive events based on the attacker-defender paradigm.

Previous research using mathematical models to alleviate issues in post-disaster relief operations typically considers each problem phase individually (Matisziw *et al.* 2009, Vitoriano *et al.* 2010, Ortuño *et al.* 2011, and Vitoriano *et al*. 2011). Matisziw *et al.* (2009) focus on the recovery phase via a telecommunication network restoration problem wherein decision variables are used to restore disrupted nodes and arcs in a multi-period problem. Vitoriano *et al.* (2011) develop a goal programming model for the response phase based on loads and vehicles to support the aid distribution problem using equity, reliability, and security as goals. Recent research also proposes phase-integrating models

(Balcik *et al.* 2008, Liberatore *et al.* 2014, and Ransikarbum and Mason 2014). Balcik *et al.* (2008) develop a model that integrates pre- and post- disaster operations—an integrated preparedness and response model for a last mile distribution system in which a local distribution center stores inventories and distributes emergency relief supplies to a number of demand locations. Liberatore *et al.* (2014) develop a hierarchical compromise model "RecHADS" that considers both relief distribution and recovery for disrupted arcs alone. The authors compare sequential and coordinated optimization to highlight the importance of cooperation among agents.

One important outcome in multiple-objective mathematical research is the generation of non-dominated or Pareto-efficient solutions. For any two points in the efficient frontier, there exists the "trade-off" property: a gain in objective value from one efficient point to another can only happen given a sacrifice in at least one other objective's value (Ravindran 2007 and Deb 2011). Several researchers state that evolutionary algorithms (EAs) can be used to find "near" Pareto-optimal solutions via a population-based search procedure (Murata *et al.* 1996, Deb 2011, and Auger and Bader 2012). EA-based techniques can be used for both single- and multiple-objective problems. Deb (2011) suggests the pros and cons of an EA as compared to a mathematical algorithm. For example, while the use of a population in an EA's search mechanism causes an inherent parallel search in one single simulation run that makes it computationally attractive, it is not necessarily guaranteed to find Pareto-optimal points as would a provable mathematical algorithm. Murata *et al.* (1996) propose a multiple-objective genetic algorithm (GA) for a flowshop scheduling problem. The authors introduce variable weights in the selection procedure to obtain a spread or diversified Pareto-optimal front. Deb *et al.* (2002) develop NSGA-II and show that it has three key features: an elitist principle, an explicit diversity preserving mechanism, and a non-dominated sorting emphasis. NSGA-II has been adapted by several researchers since its publication (Cakici *et al.* 2012 and Bandyopadhyay and Bhattacharya 2013). Cakici *et al.* (2012) develop an integrated production and distribution model and apply NSGA-II-based algorithms to the distribution part of the integrated problem. The authors suggest that, in addition to crossover and mutation operators, an immigration operator should be added. Bandyopadhyay and Bhattacharya (2013) propose a modified NSGA-II based on a new crossover algorithm for a fuzzy variable in a supply chain problem. The authors point out that there is no universal crossover or mutation operator that may be applicable to all types of problems.

Performance measurement for the EA-based techniques is an important issue (Deb 2011). Zitzler *et al.* (2003) suggest that the two ideal goals of multiple-objective optimization are 1) to find multiple, non-dominated points as close to the Pareto-optimal front as possible and 2) to find solutions that are diverse enough to represent the entire range of the front. Three different sets of performance measures exist in the literature: 1) metrics evaluating convergence to the Pareto-optimal front alone (e.g., error ratio measure); 2) metrics evaluating the spread of solutions alone (e.g., chi-square deviation measure); and 3) metrics evaluating certain combinations of convergence and spread of solutions (e.g., Hypervolume coverage, and R-metrics). The authors suggest that the notion of performance includes both the quality of the outcome (e.g., the Pareto-optimal front) and the computational resource requirements (e.g., overall run-time). Auger and Bader (2012) discuss a theoretical framework for the Hypervolume indicator and discuss the influence of a reference point used in the Hypervolume indicator calculation to its quality. While *et al.* (2012) describe an algorithm for calculating the Hypervolume and suggest that the Hypervolume measures the size of the portion of objective space that is dominated by those solutions collectively. Hall and Posner (2007) suggest that in addition to performance measure, it is also important to correctly predict the relative performance difference between an optimization algorithm and a heuristic solution procedure by using the mean, the variance, and computing a confidence interval (CI).

In this chapter, we develop a metaheuristic programming model "Hybrid NSGA-II" that combines the evolutionary heuristic from NSGA-II and an optimization-based technique. We demonstrate this model by solving the MOIRR problem developed by Ransikarbum and Mason (2014) with two objectives. Our Hybrid NSGA-II uses an evolutionary heuristic for the network restoration portion of the MOIRR problem and an optimization-based technique for supply distribution decisions. The Hybrid NSGA-II is applied to the MOIRR problem in an effort to generate non-dominated solutions in a timely manner for disaster relief operations support.

4.3 Multiple-Objective Integrated Response and Recovery (MOIRR) Model

The MOIRR model with a partial restoration (Ransikarbum and Mason 2014) integrates both response-phase supply distribution options and recovery-phase network restoration decisions to reestablish services in a damaged network to pre-disruption performance levels so that relief supplies can be transported to affected areas. The model also directs decision makers to restore disrupted node(s) and/or disrupted arc(s) when necessary such that fairness, unsatisfied demand, and cost-based criteria are optimized. In the partial restoration analysis, while all or nothing restoration is required for disrupted supply points, relief warehouse nodes can be alternatively not restored, have one-half of their capabilities restored, or be fully restored. Finally, each disrupted arc in the relief network can be restored in increments of 25% of its capacity (i.e., 0%, 25%, 50%, 75%, or 100% restoration). The bi-criteria MOIRR model of Ransikarbum and Mason (2014) is now presented here for completeness.

4.3.1 MOIRR Model Notation

<u>*Sets*</u>

$G(N,A)$	Graph consisting of nodes N and arcs A
N (A)	Set of nodes (arcs)
S (D)	Set of supply port (demand) nodes $\in N$
T	Set of transhipment (relief warehouse) nodes $\in N$
S^F (S^D)	Set of functional (disrupted) supply port nodes $\in S$
T^F (T^D)	Set of functional (disrupted) transhipment (relief warehouse) nodes $\in T$
Λ	Set of arcs between supply port and relief warehouse nodes $\in A$
Π	Set of arcs between relief warehouse and demand nodes $\in A$
Λ^F (Λ^D)	Set of functional (disrupted) arcs between supply port and warehouse nodes $\in \Lambda$
Π^F (Π^D)	Set of functional (disrupted) arcs between relief warehouse and demand nodes $\in \Pi$
Γ^N	Set of disrupted nodes, where $\Gamma^N = S^D \cup T^D$
Γ^A	Set of disrupted arcs, where $\Gamma^A = \Lambda^D \cup \Pi^D$

Parameters

s_i	Supply units available at each supply port node $i \in S$
d_i	Demand units required at each demand node $i \in D$
α_i	Relief warehouse capacity for each relief warehouse node $i \in T$
$\delta_{i,j}^{ST}$	Road capacity for each arc between port and warehouse node $(i, j) \in \Lambda$
$\delta_{i,j}^{TD}$	Road capacity for each arc between warehouse and demand $(i, j) \in \Pi$
φ_i	Capacity needed for each unit flow to use relief warehouse node $i \in T$
$\psi_{i,j}^{ST}$	Capacity needed for each unit flow to use road (arc) between supply port and relief warehouse node $(i, j) \in \Lambda$
$\psi_{i,j}^{TD}$	Capacity needed for each unit flow to use road (arc) between relief warehouse and demand node $(i, j) \in \Pi$
$c_{i,j}$	Cost of transporting each unit flow per mile through each arc $(i, j) \in A$
η_i^S (η_i^T)	Cost of restoring each disrupted supply port node $i \in S^D$ (relief warehouse node $i \in T^D$)
$\lambda_{i,j}^{ST}$	Cost of restoring each disrupted arc between port and relief warehouse node $(i, j) \in \Lambda^D$
$\lambda_{i,j}^{TD}$	Cost of restoring each disrupted arc between warehouse and demand node $(i, j) \in \Pi^D$
b^N (b^A)	Budget for total disrupted node (arc) restoration
b^F	Budget for total network flow transportation
ν^S (ν^T)	Fixed charge for restoring disrupted supply port (relief warehouse) node
ω^{ST}	Fixed charge for restoring disrupted arc between supply port and relief warehouse node
ω^{TD}	Fixed charge for restoring disrupted arc between relief warehouse and demand node
θ^N (θ^A)	Maximum allowable number for disrupted node (arc) restoration
$d_{i,j}^{OD}$	Distance in miles between each origin and destination pair $(i, j) \in A$

$w_i\ (p_i)$ Importance weight setting (priority) associated with objective *i*

Partial Restoration Parameters

$f_i^{T1},\ (f_i^{T2})$ 50%, (100%) restoration for disrupted warehouse node $i \in T^D$

$f_{i,j}^{ST1}, (f_{i,j}^{ST2}), (f_{i,j}^{ST3})$ 25%, (50%), (100%) restoration for damaged arc between supply port and relief warehouse node $(i, j) \in \Lambda^D$

$f_{i,j}^{TD1}, (f_{i,j}^{TD2}), (f_{i,j}^{TD3})$ 25%, (50%), (100%) restoration for damaged arc between relief warehouse and demand node $(i, j) \in \Pi^D$

Decision Variables

$X_{i,j}$ Commodity flow variable for supplies through arc $(i, j) \in A$; integer

K_i Restore disrupted supply port node $i \in S^D$; binary

L_i Partially restore disrupted warehouse node $i \in T^D$

$M_{i,j}$ Partially restore disrupted arc between supply port and relief warehouse node $(i, j) \in \Lambda^D$

$N_{i,j}$ Partially restore disrupted arc between relief warehouse and demand node $(i, j) \in \Lambda^D$

R_i Units of unsatisfied demand for each demand node $i \in D$; integer

V Minimum percentage of satisfied demand

Y_i^S Setup cost to restore disrupted supply port $i \in S^D$; binary

Y_i^T Setup cost to restore disrupted warehouse $i \in T^D$; binary

$Y_{i,j}^{ST}$ Setup cost to restore disrupted arc between supply port and warehouse $(i, j) \in \Lambda^D$; binary

$Y_{i,j}^{TD}$ Setup cost to restore disrupted arc between relief warehouse and demand $(i, j) \in \Pi^D$; binary

Partial Restoration Decision Variables

Q_i^{T1}, (Q_i^{T2}) Restrict 50%, (100%) restoration for disrupted warehouse node $i \in T^D$; binary

$Q_{i,j}^{ST1}$, $(Q_{i,j}^{ST2})$, $(Q_{i,j}^{ST3})$ Restrict 25%, (50%), (100%) restoration for disrupted arc between supply port and relief warehouse node $(i, j) \in \Lambda^D$; binary

$Q_{i,j}^{TD1}$, $(Q_{i,j}^{TD2})$, $(Q_{i,j}^{TD3})$ Restrict 25%, (50%), (100%) restoration for disrupted arc between relief warehouse and demand node $(i, j) \in \Pi^D$; binary

4.3.2 MOIRR Model Formulation

The MOIRR model with two objective functions are shown below: maximizing equity (fairness) and minimizing total network costs.

$$\text{Maximize } Z_1 = V \tag{4.1}$$

$$\text{Minimize } Z_2 = \left[\begin{aligned} &\left(\sum_{i \in S^D} \eta_i^S K_i\right) + \left(\sum_{i \in T^D} \eta_i^T L_i\right) + \left(\sum_{i \in S^D} \nu^S Y_i^S\right) + \left(\sum_{i \in T^D} \nu^T Y_i^T\right) + \cdots \\ &\left(\sum_{(i,j) \in \Lambda^D} \lambda_{i,j}^{ST} M_{i,j}\right) + \left(\sum_{(i,j) \in \Pi^D} \lambda_{i,j}^{TD} N_{i,j}\right) + \left(\sum_{(i,j) \in \Lambda^D} \omega^{ST} Y_{i,j}^{ST}\right) + \ldots \\ &\left(\sum_{(i,j) \in \Pi^D} \omega^{TD} Y_{i,j}^{TD}\right) + \left(\sum_{(i,j) \in A} c_{i,j} d_{i,j}^{OD} X_{i,j}\right) \end{aligned}\right] \tag{4.2}$$

Objective function (4.1), when coupled with constraint set (4.2), maximizes equity (fairness) via a maximin approach.

$$V \le \left(\sum_{i \in T} \frac{X_{i,j}}{d_j}\right) 100 \qquad ; \forall \ j \in D \tag{4.3}$$

Objective function (4.2) minimizes total network costs which are calculated as the total funds spent to restore disrupted nodes, restore disrupted arcs, and transport supply units between origin-destination pairs.

The model's constraint sets ensure that any required restrictions or limits are followed by any of the model's recommended solutions. Constraint set (4.4) ensures that total transportation costs do not exceed the available transportation budget. Similarly, constraint sets (4.5) and (4.6) ensure that total restoration costs do not exceed available restoration funds.

$$\left(\sum_{(i,j)\in A} c_{i,j} d_{i,j}^{OD} X_{i,j} \right) \leq b^F \tag{4.4}$$

$$\left(\sum_{i\in S^D} \eta_i^S K_i \right) + \left(\sum_{i\in T^D} \eta_i^T L_i \right) + \left(\sum_{i\in S^D} \nu^S Y_i^S \right) + \left(\sum_{i\in T^D} \nu^T Y_i^T \right) \leq b^N \tag{4.5}$$

$$\left(\sum_{(i,j)\in \Lambda^D} \lambda_{i,j}^{ST} M_{i,j} \right) + \left(\sum_{(i,j)\in \Pi^D} \lambda_{i,j}^{TD} N_{i,j} \right) + \left(\sum_{(i,j)\in \Lambda^D} \omega^{ST} Y_{i,j}^{ST} \right) + \left(\sum_{(i,j)\in \Pi^D} \omega^{TD} Y_{i,j}^{TD} \right) \leq b^A \tag{4.6}$$

As it is possible that all demands may not be satisfied, constraint set (4.7) accounts for demand uncertainty (i.e., demand is higher or lower than available supply units).

$$\sum_{i\in T} X_{i,j} + R_j = d_j \qquad ;\forall\ j\in D \tag{4.7}$$

Constraint sets (4.8) and (4.9) ensure that total flow out of the supply nodes does not exceed the available supply. While supply items are available from functional supply nodes, supply items for disrupted supply nodes are available if and only if the disrupted node is restored.

$$\sum_{j\in T} X_{i,j} \leq s_i \qquad ;\forall\ i\in S^F \tag{4.8}$$

$$\sum_{j\in T} X_{i,j} \leq s_i K_i \qquad ;\forall\ i\in S^D \tag{4.9}$$

Constraint set (4.10) ensures flow conservation such that unit flows out of and into each relief warehouse are equal.

$$\sum_{i \in S} X_{i,j} - \sum_{k \in D} X_{j,k} = 0 \qquad ; \forall \; j \in T \tag{4.10}$$

Relief warehouse capacities are restricted by constraint sets (4.11) and (4.12), as relief warehouse nodes only provide capacity when the node is functional.

$$\sum_{i \in S} \varphi_j X_{i,j} \le \alpha_j \qquad ; \forall \; j \in T^F \tag{4.11}$$

$$\sum_{i \in S} \varphi_j X_{i,j} \le \alpha_j L_j \qquad ; \forall \; j \in T^D \tag{4.12}$$

Constraint sets (4.13) and (4.14) restrict road capacities between supply nodes and relief warehouse nodes by ensuring that road capacities are available only if the corresponding roads are functional. Similarly, constraint sets (4.15) and (4.16) restrict road capacity utilization between relief warehouses and demand nodes.

$$\psi_{i,j}^{ST} X_{i,j} \le \delta_{i,j}^{ST} \qquad ; \forall \; (i, j) \in \varLambda^F \tag{4.13}$$

$$\psi_{i,j}^{ST} X_{i,j} \le \delta_{i,j}^{ST} M_{i,j} \qquad ; \forall \; (i, j) \in \varLambda^D \tag{4.14}$$

$$\psi_{i,j}^{TD} X_{i,j} \le \delta_{i,j}^{TD} \qquad ; \forall \; (i, j) \in \varPi^F \tag{4.15}$$

$$\psi_{i,j}^{TD} X_{i,j} \le \delta_{i,j}^{TD} N_{i,j} \qquad ; \forall \; (i, j) \in \varPi^D \tag{4.16}$$

Constraint sets (4.17) through (4.20) enforce setup cost realization when restoration decisions for disrupted supply points (4.17), disrupted warehouses (4.18), disrupted arcs between a supply point and a warehouse (4.19), and disrupted arcs between a warehouse and demand nodes (4.20) are prescribed by the model.

$$K_j \le Y_j^S \qquad ; \forall \; j \in S^D \tag{4.17}$$

$$L_j \le Y_j^T \qquad ; \forall \; j \in T^D \tag{4.18}$$

$$M_{i,j} \le Y_{i,j}^{ST} \qquad ; \forall \; (i, j) \in \Lambda^D \tag{4.19}$$

$$N_{i,j} \leq Y_{i,j}^{TD} \qquad ;\forall\,(i,j)\in \Pi^{D} \tag{4.20}$$

Next, constraint sets (4.21) and (4.22) restrict the number of disrupted nodes and disrupted arcs that can be restored based on available resources.

$$\sum_{j\in S^{D}} K_{j} + \sum_{j\in T^{D}} L_{j} \leq \theta^{N} \tag{4.21}$$

$$\sum_{(i,j)\in \Lambda^{D}} M_{i,j} + \sum_{(i,j)\in \Pi^{D}} N_{i,j} \leq \theta^{A} \tag{4.22}$$

In terms of the partial restoration decisions, constraint sets (4.23) and (4.24) combine to restrict the model's decision variables to partially restore disrupted relief warehouse nodes at only two levels: 50% or 100%.

$$L_{i} = f_{i}^{T1}Q_{i}^{T1} + f_{i}^{T2}Q_{i}^{T2} \qquad ;\forall\, i\in T^{D} \tag{4.23}$$

$$L_{i} \leq f_{i}^{T2} \qquad ;\forall\, i\in T^{D} \tag{4.24}$$

Similarly, constraint sets (4.25) and (4.26) allow partially disrupted arcs between supply points and relief warehouses to be restored at four levels: 25%, 50%, 75%, or 100%, while constraint sets (4.27) and (4.28) restrict the partial restoration of disrupted arcs between relief warehouses and demand nodes.

$$M_{i,j} = f_{i,j}^{ST1}Q_{i,j}^{ST1} + f_{i,j}^{ST2}Q_{i,j}^{ST2} + f_{i,j}^{ST3}Q_{i,j}^{ST3} \qquad ;\forall\,(i,j)\in \Lambda^{D} \tag{4.25}$$

$$M_{i,j} \leq f_{i,j}^{ST3} \qquad ;\forall\,(i,j)\in \Lambda^{D} \tag{4.26}$$

$$N_{i,j} = f_{i,j}^{TD1}Q_{i,j}^{TD1} + f_{i,j}^{TD2}Q_{i,j}^{TD2} + f_{i,j}^{TD3}Q_{i,j}^{TD3} \qquad ;\forall\,(i,j)\in \Pi^{D} \tag{4.27}$$

$$N_{i,j} \leq f_{i,j}^{TD3} \qquad ;\forall\,(i,j)\in \Pi^{D} \tag{4.28}$$

Finally, constraint sets (4.29) through (4.39) are variable-type constraints for the MOIRR model and constraint sets (4.40) through (4.47) are binary variables required for the partial restoration.

$$X_{i,j} = \{0,1,2,\ldots,n\} \quad ;\forall\ (i,j) \in A \qquad (4.29), \qquad K_i = \{0,1\} \quad ;\forall i \in S^D \qquad (4.30)$$

$$L_i \geq 0 \quad ;\forall i \in T^D \qquad (4.31), \qquad M_{i,j} \geq 0 \quad ;\forall\ (i,j) \in \Lambda^D \qquad (4.32)$$

$$N_{i,j} \geq 0 \quad ;\forall\ (i,j) \in \Pi^D \qquad (4.33), \qquad R_i \geq 0 \quad ;\forall\ i \in D \qquad (4.34)$$

$$V \geq 0 \qquad (4.35), \qquad Y_i^S = \{0,1\} \quad ;\forall i \in S^D \qquad (4.36)$$

$$Y_i^T = \{0,1\} \quad ;\forall i \in T^D \qquad (4.37), \qquad Y_{i,j}^{ST} = \{0,1\} \quad ;\forall\ (i,j) \in \Lambda^D \qquad (4.38)$$

$$Y_{i,j}^{ST} = \{0,1\} \quad ;\forall\ (i,j) \in \Lambda^D \qquad (4.39), \qquad Q_i^{T1} = \{0,1\} \quad ;\forall\ i \in T^D \qquad (4.40)$$

$$Q_i^{T2} = \{0,1\} \quad ;\forall\ i \in T^D \qquad (4.41), \qquad Q_{i,j}^{ST1} = \{0,1\} \quad ;\forall\ (i,j) \in \Lambda^D \qquad (4.42)$$

$$Q_{i,j}^{ST2} = \{0,1\} \quad ;\forall\ (i,j) \in \Lambda^D \qquad (4.43), \qquad Q_{i,j}^{ST3} = \{0,1\} \quad ;\forall\ (i,j) \in \Lambda^D \qquad (4.44)$$

$$Q_{i,j}^{TD1} = \{0,1\} \quad ;\forall\ (i,j) \in \Pi^D \qquad (4.45), \qquad Q_{i,j}^{TD2} = \{0,1\} \quad ;\forall\ (i,j) \in \Pi^D \qquad (4.46)$$

$$Q_{i,j}^{TD3} = \{0,1\} \quad ;\forall\ (i,j) \in \Pi^D \qquad (4.47)$$

4.3.3 Seeking the Efficient Frontier

4.3.3.1 Hazus Case Study

FEMA's GIS-based natural hazard loss estimation software Hazus is used in Ransikarbum and Mason (2014) to obtain predicted loss data from an earthquake scenario in South Carolina (SC). The parameter data and assumptions associated with the Hazus case study are given in Table 4.1. Six major SC airports are chosen as relief supply points: Charleston, Columbia, Florence, Greenville, Hilton Head, and Myrtle Beach. Hazus' inventory collection module reports that there are 47 emergency operations centers (EOCs) in the state, which are modeled as relief warehouses. A 9.0 magnitude earthquake is simulated to occur in the Columbia, SC metropolitan area. Hazus-based "before and after" disaster instance maps are shown in Figure 4.1. Figure 4.1(a) presents the position of the earthquake and overviews the existing infrastructure in SC. Next, Figure 4.1(b) shows loss data output from Hazus: one disrupted relief supply point, 16 disrupted relief warehouses, and 143 demand census tracks affected by the earthquake.

Table 4.1: Hazus-related parameter and data assumption list

Activities	Symbol	Category	Descriptive detail
Supply relief port node			
Number of supply port nodes	S	Hazus	
Number of disrupted supply port nodes	S^D	Hazus	
Cost for restoring each disrupted supply port node	η_i^S	Hazus	
Supply units available at each supply port node	s_i	Extrapolation	From port size and demand units
Fixed charge for restoring disrupted supply port node	ν^S	Extrapolation	From port node's restoration cost
Relief warehouse node			
Number of transhipment (relief warehouse) nodes	T	Hazus	
Number of disrupted transhipment (relief warehouse) nodes	T^D	Hazus	
Cost for restoring each disrupted relief warehouse node	η_i^T	Hazus	
Fixed charge for restoring disrupted relief warehouse node	ν^T	Extrapolation	From warehouse node's restoration cost
Capacity for each transhipment (relief warehouse) node	α_i	Extrapolation	From warehouse size (Hazus's inventory)
Capacity needed for each unit flow to use relief warehouse node	φ_i	Not available	1 unit assumption
Demand node			
Number of demand/ beneficiary nodes	D	Hazus	
Demand units required at each demand/ beneficiary node	d_i	Hazus	
Arc between supply port and relief warehouse nodes			
Cost for restoring each disrupted arc between supply port and warehouse node	$\lambda_{i,j}^{ST}$	Hazus	
Distance in miles between each origin and destination pair based on latitude/longitude	$d_{i,j}^{OD}$	Hazus	
Fixed charge for restoring disrupted arc between supply port and warehouse node	ω^{ST}	Extrapolation	From arc's restoration cost
Number of disrupted arcs between supply port and relief warehouse nodes	Λ^D	Not available	Randomly distributed; 30% disruption
Road capacity for each arc between port and relief warehouse node	$\delta_{i,j}^{ST}$	Not available	5000 unit assumption
Capacity needed to use road (arc) between supply port and relief warehouse node	$\psi_{i,j}^{ST}$	Not available	1 unit assumption
Cost for transporting each unit flow per mile through each arc	$c_{i,j}$	Not abailable	$15 per unit per mile assumption
Arc between relief warehouse and demand nodes			
Cost for restoring each disrupted arc between warehouse and demand node	$\lambda_{i,j}^{TD}$	Hazus	
Distance in miles between each origin and destination pair based on latitude/longitude	$d_{i,j}^{OD}$	Hazus	
Fixed charge for restoring disrupted arc between warehouse and demand node	ω^{TD}	Extrapolation	From arc's restoration cost
Number of disrupted arcs between relief warehouse and demand nodes	Π^D	Not available	Randomly distributed; 30% disruption
Road capacity for each arc between warehouse and demand node	$\delta_{i,j}^{TD}$	Not available	2500 unit assumption
Capacity needed to use road (arc) between warehouse and demand node	$\psi_{i,j}^{TD}$	Not available	1 unit assumption
Cost for transporting each unit flow per mile through each arc	$c_{i,j}$	Not available	$8 per unit per mile assumption
Others			
Budget for total disrupted node restoration	b^N	Extrapolation	Based on total node restoration cost
Budget for total disrupted arc restoration	b^A	Extrapolation	Based on total arc restoration cost
Budget for total network flow transportation	b^F	Extrapolation	Based on total transportation cost
Maximum allowable number for disrupted node restoration	θ^N	Not available	At most 8 node assumption
Maximum allowable number for disrupted arc restoration	θ^A	Not available	At most 300 arc assumption

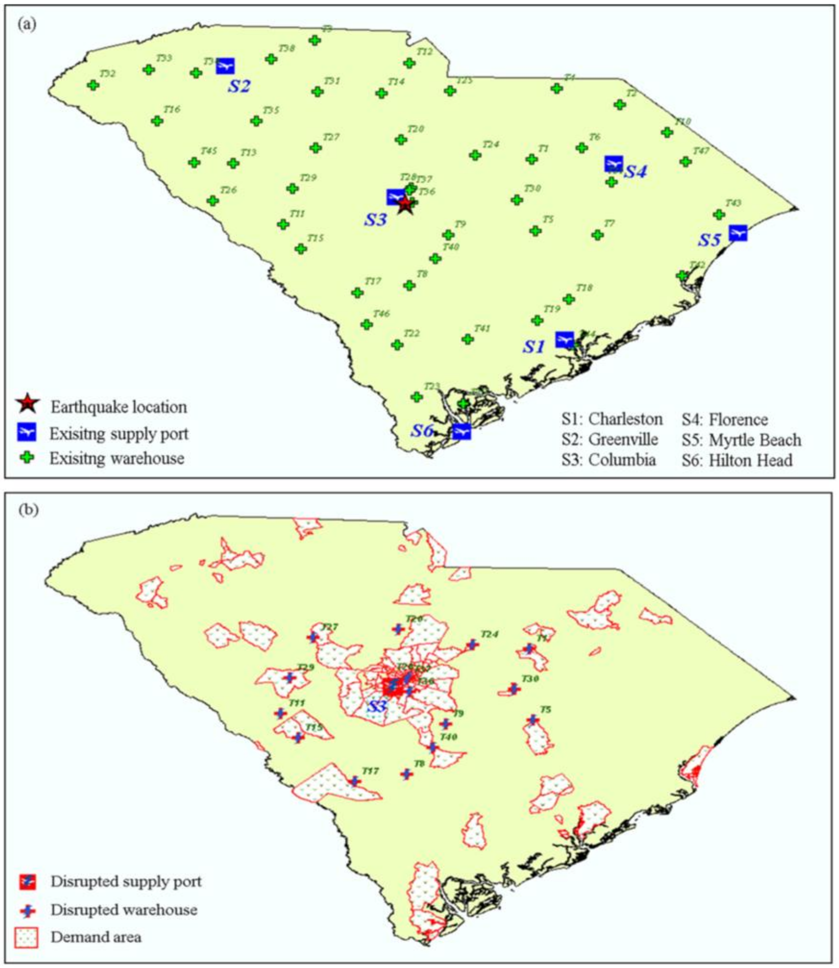

Figure 4.1: Hazus-based SC map illustration: (a) infrastructure before a disaster, (b) loss data after a disaster.

4.3.3.2 Pareto-Optimal Front from the Mathematical Model

A Pareto-optimal solution is a feasible solution that is not dominated by any other feasible solution and has the property that an improvement in any one objective is possible only at the expense of at least one other objective (Ravindran 2007). The set of all Pareto-optimal solutions, the "Pareto front," is commonly used to visually evaluate trade-offs among decision criteria in objective space.

Using the SC case study, the Pareto front for the fairness vs. cost study in Ransikarbum and Mason (2014) is adapted to compare previous solutions generated by the mathematical model with the EA-based technique proposed in this paper. By using the non-preemptive (weighted) method, the fairness and cost objective functions in (4.1) and (4.2) are normalized using a linear normalization technique to allow inter-criterion comparison:

$$\text{Maximize} \quad w_1\left(\frac{Z_1 - L_1^*}{H_1^* - L_1^*}\right) + w_2\left(\frac{L_2^* - Z_2}{L_2^* - H_2^*}\right), \text{ where} \sum_{i=1}^{2} w_i = 1 \tag{4.48}$$

This technique converts a criterion to value between 0 and 1 along the allowed range of the measure based on ideal (H_j^*) and anti-ideal (L_j^*) solutions which we obtain from solving each objective alone. The terms $\frac{C_j(x) - L_j^*}{H_j^* - L_j^*}$ and $\frac{L_j^* - C_j(x)}{L_j^* - H_j^*}$ are normalized terms for benefit and cost criteria, respectively, where $C_j(x)$ is the criterion value before normalization.

The MOIRR is modeled in AMPL (Fourer *et al.* 2002) and analyzed using CPLEX on a PC with an Intel® Core™ i7- 2600 CPU running @3.40 GHz with 16 GB of RAM. The Pareto front is generated by varying weight w_i for objective i discretely from 0.1 to 0.9 at increments of 0.1; this yields a total of nine points (Figure 4.2). The front illustrates objective function trade-offs and informs decision makers on how improving one objective can deteriorate the second objective. For example, when more weight is given to the fairness objective (e.g., w_1=0.7, w_2=0.3), the objective values for fairness and total cost are 72% demand satisfaction and $1.245 billion, respectively.

However, when more weight is given to the cost objective (e.g., w_1 =0.3 and w_2 =0.7), the corresponding objective values are 28% percent demand satisfaction and $0.239 billion for total cost, respectively.

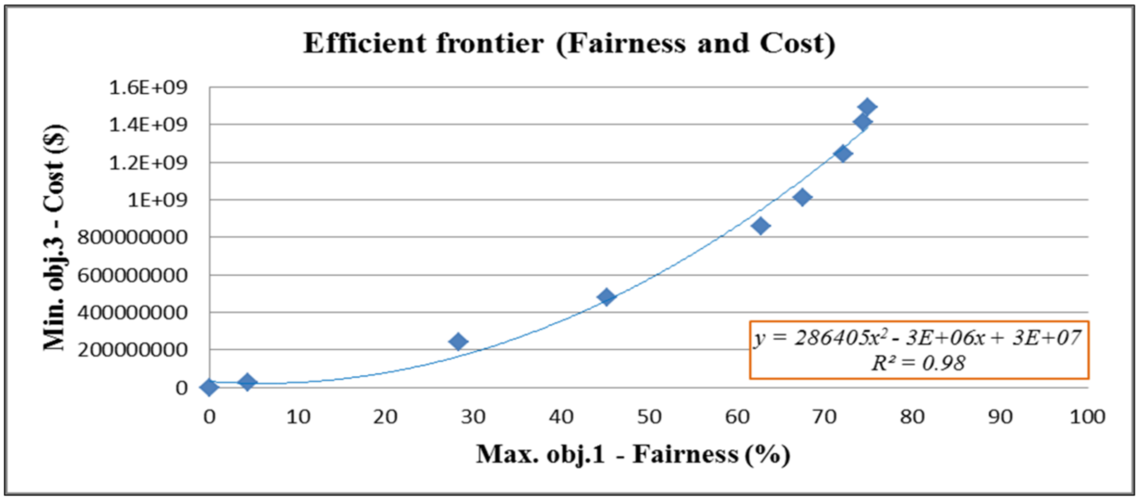

Figure 4.2: Pareto-optimal front for the objectives fairness and cost

4.4 A Proposed Hybrid NSGA-II Algorithm

4.4.1 Hybrid NSGA- II Algorithm

We develop our Hybrid NSGA-II algorithm using the evolutionary algorithm NSGA-II (Deb *et al.* 2002) and an optimization technique. After decomposing the MOIRR model, NSGA-II is applied to the network restoration problem, while the optimization technique is employed in the supply distribution problem. NSGA-II uses a population-based approach to simultaneously find multiple, non-dominated solutions portraying the trade-off among objectives in a single simulation run (Deb 2011). Three properties that make the NSGA-II algorithm efficient are 1) an elitist principle, 2) an explicit diversity-preserving mechanism, and 3) a non-dominated sorting emphasis (Deb *et al.* 2002). Figure 4.3 shows the outline of the Hybrid NSGA-II procedure. The key differences between the Hybrid NSGA-II and the NSGA-II algorithms are also highlighted in the Figure (Steps 1.3-1.4 and 2.1-2.4).

4.4.1.1 Step 1 Initialize Parent Population

Step 1.1 *Create a Representation for Each Chromosome*

Deb *et al.* (2002) illustrate the NSGA-II with both real number and binary representations and suggest that a real number-coded NSGA-II can find better solution spreads. In our analysis, a real-number representation is obtained using the uniform distribution (0,1). By concatenating all variables involved in the restoration process, we are able to obtain the chromosome representation. Figure 4.4(a) illustrates a real number-coded chromosome representation concatenated from restoration decision variables for disrupted supplied ports, disrupted warehouses, disrupted arcs between ports and warehouses, and disrupted arcs between warehouses and demand points.

Step 1: Initialize a parent population P_k, where k = 0 with size N

Step 1.1: Create a representation for each chromosome from Uniform (0,1)
Step 1.2: Return restoration variables from generated chromosomes
Step 1.3 : Check the feasibility related to restoration variables
Step 1.4: Call the mathematical model to obtain supply flow variables

Step 2: Generate an offspring population Q_k with size N from a parent population P_k

Step 2.1: Use a binary selection operator based on the sorting procedure
Step 2.2 : Use a crossover operator based on a crossover probability (Cp)
Step 2.3: Use a mutation operator based on a mutation probability (Mp)
Step 2.4: Use an immigration operator based on an immigration probability (Ip)
Step 2.5: Check the feasibility (similar to Step 1.3)

Step 3: Mate parent and offspring populations to create $R_k = P_k \cup Q_k$ with size 2N

Step 4: Sort R_k to form non-dominated fronts

Step 4.1: Start with h = 1 (first front). For each chromosome i, identify the number of solutions that dominate i (ni), and create the set of solutions that i dominates (Si)
Step 4.2: Place each unplaced solution i with ni = 0 in the h^{th} front (F_h)
Step 4.3: For each solution i in F_h, find each chromosome j in Si and reduce nj by one
Step 4.4: If all solutions are placed in a front, stop. Otherwise, update $h \leftarrow h+1$ and go to Step 4.2

Step 5: Calculate a crowding distance

Step 5.1: For each objective m, sort all solutions in a particular front h (F_h) in a non-increasing order of the m^{th} objective function value
Step 5.2: Calculate the crowding distance of each chromosome i with respect to objective m (CD_{im})
Step 5.3: Compute the total crowding disatnce of each chromosome i

Step 6: Update a next parent population by selecting N best solutions from 2N solutions in R_k to form $P_{(k+1)}$ based on sorted fronts and crowding distance for the last front

Step 7: Update a new iteration ($k \leftarrow k+1$) and go to Step 2. When the stoping criteria is reached (k_{max}), stop the algorithm

Figure 4.3: Outline of the Hybrid NSGA-II procedure for the MOIRR model

Step 1.2 Return Restoration Variables from Chromosome Representation

After obtaining the chromosome representation, each genotype is transformed to a restoration variable with the aid of a probability restriction (Figure 4.4(b)). In terms of the percent restoration, we allow disrupted supply ports to be fully restored or not (0 or 1), disrupted relief warehouses to be partially restored (0, 0.5, or 1), and disrupted highways to be partially restored (0, 0.25, 0.50, 0.75, or 1).

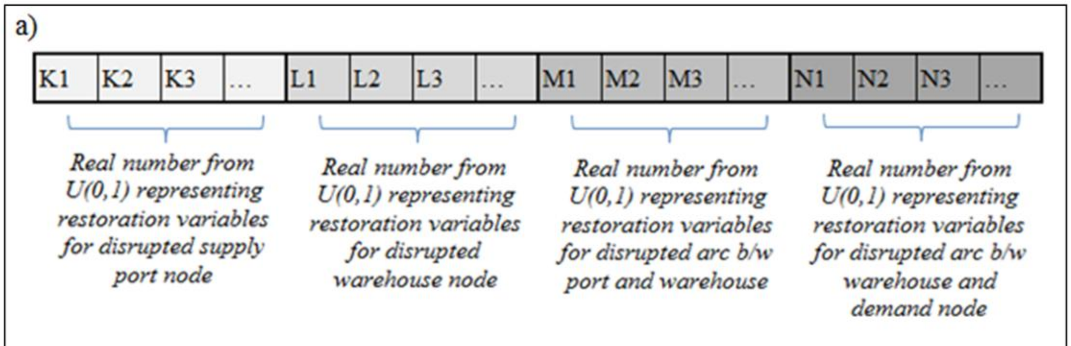

b)

```
For each Ki generated from Uniform (0,1)
        If Ki ϵ [0,0.5]                      Ki ← 0
        Else                                 Ki ← 1
End For
For each Li generated from Uniform (0,1)
        If Li ϵ [0,0.33]                     Li ← 0
        Else If  Li ϵ (0.33,0.66]            Li ← 0.5
        Else                                 Li ← 1
End For
For each Mi generated from Uniform (0,1)
        If Mi ϵ [0,0.2]                      Mi ← 0
        Else If  Mi ϵ (0.2,0.4],             Mi ← 0.25
        Else If  Mi ϵ (0.4,0.6],             Mi ← 0.5
        Else If  Mi ϵ (0.6,0.8],             Mi ← 0.75
        Else                                 Mi ← 1
End For
For each Ni generated from Uniform (0,1)
        If Ni ϵ [0,0.2]                      Ni ← 0
        Else If  Ni ϵ (0.2,0.4],             Ni ← 0.25
        Else If  Ni ϵ (0.4,0.6],             Ni ← 0.5
        Else If  Ni ϵ (0.6,0.8],             Ni ← 0.75
        Else                                 Ni ← 1
End For
```

Figure 4.4: A chromosome (a) representation for the restoration variables, (b) logic to return restoration variables

<u>Step 1.3</u> Check Restoration Variable Feasibility

After obtaining the restoration variables, it is possible that the limits in constraint sets (4.6), (4.7), (4.22), and/or (4.23) are violated. While constraint sets (4.6) and (4.7) relate to budgetary limits for disrupted nodes and disrupted arcs, respectively, constraint sets (4.22) and (4.23) correspond to the maximum allowable numbers of disrupted nodes and disrupted arcs, respectively. Thus, restoration variables are checked for feasibility. If infeasibility is found either in budgetary or maximum allowable restoration aspects, a non-zero genotype in a chromosome is randomly reduced by 1.0, 0.5, or 0.25 if it represents a disrupted supply port, a disrupted relief warehouse, or a disrupted arc, respectively. A reduction loop continues until feasibility is obtained. Then, an updated restoration variable is reverse-transformed to a real number-coded genotype using the probability restriction in Figure 4.5 for subsequent processing.

<u>Step 1.4</u> Obtain Supply Flow Variables

After obtaining feasible restoration variables, they are used as inputs in the MOIRR model. The model is solved to find optimal solutions for supply flow variables. Murata *et al.* (1996) suggest variable weights in the selection procedure of their heuristic algorithm to obtain a spread for the Pareto front. Similarly, by varying weights in 0.1 increments for different objectives, the algorithm randomly chooses a weight pair in the updated mathematical model so that a spread of Pareto-optimal front is ensured. The mathematical model then returns objective values associated with objectives (4.1) and (4.2). We note that when all restoration variables are treated as parameters and all supply flow variables are assumed to be continuous, the problem becomes linear program (LP) which can easily be solved.

a)

P1	K1	K2	K3	L1	L2	L3	M1	M2	M3	N1	N2	N3
P2	K1	K2	K3	L1	L2	L3	M1	M2	M3	N1	N2	N3

(Parent 1 and Parent 2 representations)

P1	0.796	0.721	0.163	0.898	0.543	0.257	0.364	0.166	0.282	0.172	0.757	0.397
P2	0.058	0.978	0.972	0.465	0.690	0.733	0.471	0.929	0.217	0.230	0.932	0.185

(Alpha vector is randomly generated to obtain a string of real number)

Alpha	0.696	0.562	0.675	0.618	0.840	0.436	0.281	0.185	0.515	0.938	0.069	0.748

*(Alpha.*P1 + (1-Alpha).*P2)*

C1	0.571	0.834	0.426	0.732	0.566	0.526	0.441	0.788	0.250	0.176	0.920	0.344

*(Alpha.*P2 + (1-Alpha).*P1)*

C2	0.282	0.866	0.709	0.630	0.667	0.465	0.394	0.307	0.248	0.226	0.769	0.239

b)

P1	K1	K2	K3	L1	L2	L3	M1	M2	M3	N1	N2	N3

(Parent 1 representation)

P1	0.796	0.721	0.163	0.898	0.543	0.257	0.364	0.166	0.282	0.172	0.757	0.397

(Two positions from P1 are randomly chosen)

I	3
J	11

(Mutation Case 1: Swap the chromosome)

M1	0.796	0.721	0.757	0.898	0.543	0.257	0.364	0.166	0.282	0.172	0.163	0.397

(Mutation Case 2: Slide the chromosome)

M2	0.796	0.721	0.898	0.543	0.257	0.364	0.166	0.282	0.172	0.163	0.757	0.397

(Mutation Case 3: Flip the chromosome)

M2	0.796	0.721	0.757	0.172	0.282	0.166	0.364	0.257	0.543	0.898	0.163	0.397

Figure 4.5: Variation operator (a) crossover operation, (b) mutation operation

4.4.1.2 Step 2 Generate Offspring Population

<u>Step 2.1</u> Use a Binary Selection Operator for Crossover/Mutation Operations

Prior to performing any crossover or mutation operation, a binary selection operator is used such that two chromosomes are randomly picked from the population and the better of the two based on rank and crowding distance (i.e., Steps 4 and 5) is selected. This operation ensures that better solutions are chosen to be in the mating pool.

Step 2.2 Perform Crossover Operations

Both the crossover and mutation operators are 'variation' operators used to generate a modified population (Deb 2011). Crossover picks two chromosomes (parents) from the pool and creates two child chromosomes by exchanging information among the parent chromosomes. In this analysis, a string of real numbers is randomly generated ("alpha vector"). Then, child chromosomes from two parent chromosomes (P1 and P2) are generated according to equations (49) and (50). Crossover probability C_p is used to limit the number of chromosomes in the parent pool that participate in crossover operations.

$$(Child1):(alpha * P1 + (1 - alpha) * P2) \tag{4.49}$$

$$(Child2):(alpha * P2 + (1 - alpha) * P1) \tag{4.50}$$

For example, given two parent chromosomes and the alpha vector in Figure 5(a), the first genotype of both child 1 and child 2 chromosomes is calculated based on information from the first genotype of both parents 1 and 2 and the alpha vector. That is, 0.571 = (0.696*0.796) + (1-0.696)*0.058 for child 1 and 0.282 = (0.696*0.058) + (1-0.696)*0.796 for child 2. Other genotypes are calculated in a similar manner.

Step 2.3 Perform Mutation Operations

For mutation operations, a parent operator is chosen via binary selection and then perturbed in its neighborhood to create a mutant. We randomly choose two locations (genotypes) I and J from the parent chromosome to perform the mutation. In our analysis, the mutation operator is randomly selected as one of three types: swap, slide, and flip. In the swap operation, genotypes in locations I and J are swapped, while in a slide operation, the genotype in location I is replaced with the genotype in location I+1, and so on until the genotype in location J is reached; it is replaced by the genotype in location I. Finally, in a flip operation, the genotypes in locations I and J replace each other, the genotypes in locations $I+1$ and $J-1$ replace each other, and so on (Figure 4.5(b)). A mutation probability M_p is used to limit the number of chromosomes in the parent pool that participate in mutation operations.

Step 2.4 Perform Immigration Operations

An immigration operation is a simple move of a chromosome in one generation to the next generation without making any perturbation (Cakici *et al.* 2012). Cakici *et al.* (2012) evaluate NSGA-II with 10% immigration probability and find that it is competitive with NSGA-II without any immigration. We use immigration probability I_p to indicate the proportion of population members to immigrate to the next generation.

4.4.1.3 Step 3 Mate Parent and Offspring Populations

After the parent population of size N and the offspring population (also of size N) are obtained, they are combined to create a mating pool of size $2N$. Because it contains both the old and the newly created population members, elitism ensures that algorithm's performance is monotonically non-degrading.

4.4.1.4 Step 4 Sort Non-Dominated Front

Steps 4.1 – 4.4 illustrate the non-dominated sorting procedure used to obtain different non-dominated fronts. Figure 6 (adapted from Deb *et al.* (2002)) gives a schematic for this algorithm when the combined population is classified/sorted into different non-dominated fronts. While all solutions in the same front are not dominated by each other, they dominate other solutions in different fronts, such that the points in the first front dominate the points in the second front, and so on. Then, after all fronts are obtained, the new population is filled by starting with points in the first non-dominated front and continuing with the second non-dominated front, and so on. Given *2N* solutions in the mating pool, it is clear that not all fronts can be accommodated within the *N* slots available for the new population. Thus, all fronts that cannot be accommodated are deleted. For the last allowed front (e.g., the 3rd front in Figure 4.6), the most diverse points are chosen using crowding distance as in Step 5.

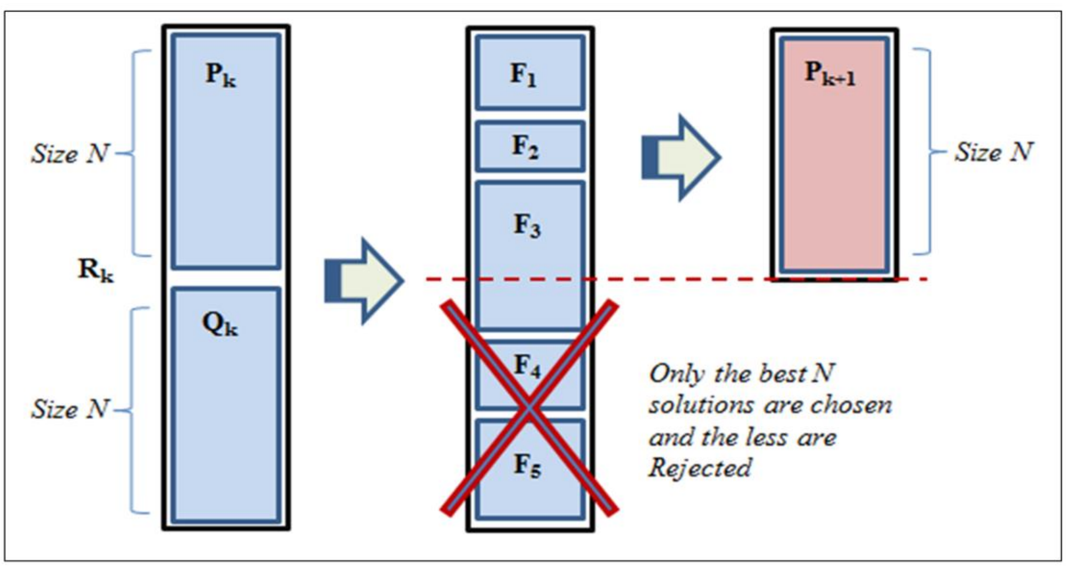

Figure 4.6: Non-dominated sorting procedure (adapted from Deb et al. 2002)

4.4.1.5 Step 5 Calculate Crowding Distance

Crowding distance values are calculated in descending order to preserve diversity for all points in the last allowed front, where points from the top of the ordered list are chosen first (i.e., greater crowding distance value means more diversity). Steps 5.1-5.3 detail how crowding distance is calculated. For example, by setting the crowding distance values of the first (*i*=1) and last (*i*=n) points in the front to infinity, the crowding distance of solution *i* for objective *m*, CD_{im}, is calculated (4.51). Then, a total crowding distance scalar of each solution *i*, CD_i, can be calculated across all the objectives as in (4.52).

$$CD_{im} = \begin{bmatrix} \infty & ; \quad i=1, \\ \left(\dfrac{f_m(i+1) - f_m(i-1)}{f_m \max - f_m \min} \right) & ; \quad i = 2, \ldots, n-1, \\ \infty & ; \quad i = n \end{bmatrix} \tag{4.51}$$

$$CD_i = \left[\sum_{m=1}^{2} CD_{im} \right] \tag{4.52}$$

4.4.1.6 Step 6 Choose Next Parent Population

Based on the non-dominated sorting and crowding distance procedures in Steps 4 and 5, the next parent population containing the *N* best solutions is selected from the mating pool.

4.4.1.7 Step 7 Update Next Iteration

The algorithm continues until the stopping criterion is met. Deb (2011) suggests that a predetermined number of iterations are commonly used as a termination criterion in an EA. Other stopping criteria include computation time limits or tolerance gap limits. We use a maximum number of iterations to limit the searching procedure in our approach.

4.4.2 Experimental Design

We test the performance of our Hybrid NSGA-II algorithm using the experimental design in Table 2. Four levels of population size (N_{pop} = 10, 20, 50, and 100) and four levels of stopping criterion (IT_{max} = 10, 20, 50, and 100) are considered. Further, two levels of variation operators based on different proportions of C_p, M_p, and I_p are examined: 1) (C_p, M_p, I_p) = (0.6, 0.3, 0.1) and 2) (C_p, M_p, I_p) = (0.3, 0.6, 0.1). Finally, two different supply flow variable types are explored: integer (resulting in an MILP) and continuous (resulting in an LP). Our experimental design yields 64 test combinations. Hall and Posner (2007) suggest that mean and variance measures are used to predict the relative performance of any developed algorithm. Thus, for each test combination for examining the SC Hazus case study, 10 replications are performed and mean and standard deviation values are collected to form a 95% confidence interval.

Table 4.2: An experimental design for the Hybrid NSGA-II algorithm

Factors	**Levels**	**Level Description**
Population Number (Npop)	4	10, 20, 50, 100
Iteration Number (ITmax)	4	10, 20, 50, 100
Variation Operator	2	Cp (0.6), Mp (0.3), Ip (0.1)
- *Crossover probability (Cp)*		Cp (0.3), Mp (0.6), Ip (0.1)
- *Mutation (Mp)*		
- *Immigration (Ip)*		
Flow Decision Model	2	MILP, LP Relaxation

4.5 Performance Assessment

In multiple-objective research, a typical desired outcome is the non-dominated or Pareto-optimal frontier (Deb 2011 and Auger and Bader 2012). The goals of multiple-objective optimization are 1) to find multiple non-dominated solutions as close to the Pareto-optimal front as possible and 2) to find solutions that are diverse to represent the entire range of the Pareto-optimal front. We use the Hypervolume indicator in our analysis as it evaluates convergence to the Pareto-optimal front (While *et al*. 2012). Further, there are trade-offs between using mathematical- and EA-based algorithms. Although a mathematical algorithm may guarantee optimal solutions on the Pareto front, it can require several runs and consume computational resources (Deb 2011). Thus, the percentage of non-dominated solutions in the first frontier is used as a second performance criterion in our analysis. Finally, as computational resource requirements (e.g., overall run-time) are also essential to assess the performance of an algorithm (Zitzler *et al.* 2003), we use overall computation time (in seconds) as our third performance criterion.

4.5.1 Comparing the Non-Dominated Fronts

Each of the non-dominated fronts from our Hybrid NSGA-II is compared with the Pareto-optimal front generated by the mathematical approach in Section 4.3.2. Figures 4.7(a) and 4.7(b) illustrate such comparison with 50 populations at 10 and 100 iterations, respectively. Then, to depict elitism progress over time, we graphically illustrate the fronts for our Hybrid NSGA-II with four levels of population size and four levels of total iterations for the (C_p, M_p, I_p) = (0.6, 0.3, 0.1) and MILP case in Figure 4.8. Figures 4.8(a)-

4.8(d) show the non-dominated front results for population size 10 with 10, 20, 50, and 100 iterations, respectively. Similarly, Figures 4.8(e)-4.8(h), 4.8(i)-4.8(l), and 4.8(m)-4.8(p) show the non-dominated front results for a population size of 20, 50, and 100 for the same numbers of total iterations.

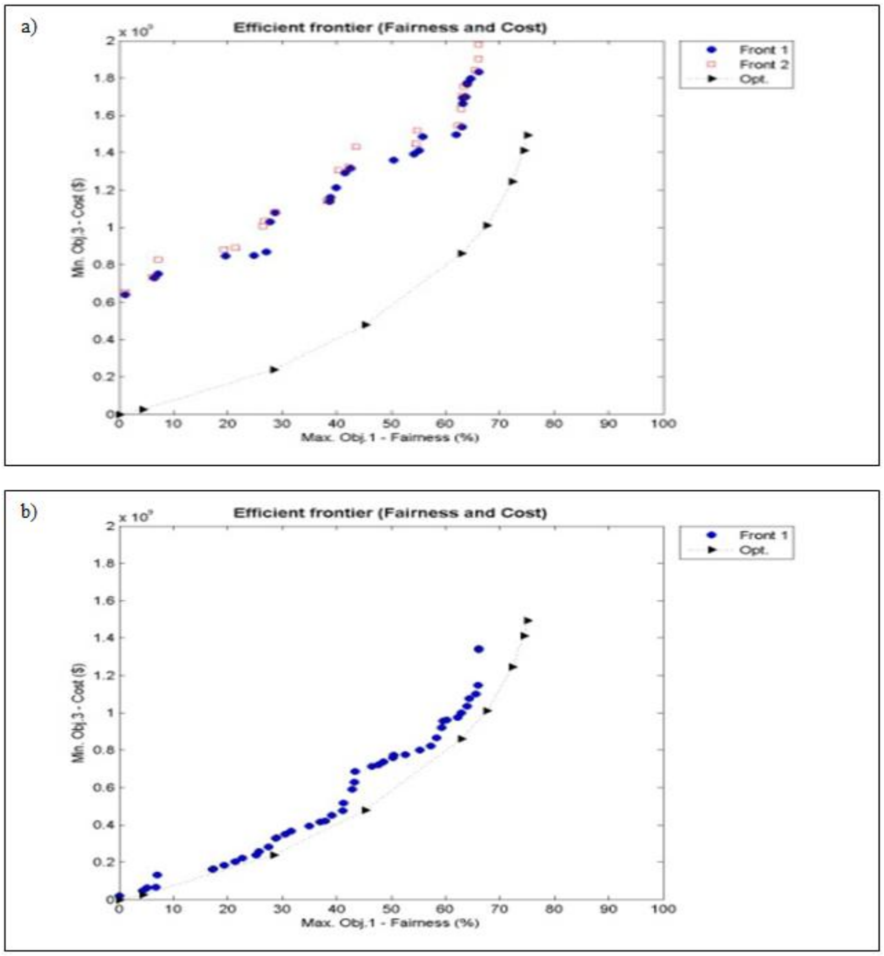

Figure 4.7: Non-dominated frontier examples with 50 populations (a) 10 iterations, and (b) 100 iterations

It is clear that as elitism progresses, an increased number of total iterations causes the non-dominated front to converge to the Pareto-optimal front. Further, with a relatively small population size of 10 and 20, only the first sorted front is found at a different iteration levels (Figures 4.8(a)-4.8(h)). However, different sorted fronts result as population size increases (Figures 4.8(i)-4.8(p)). As solutions in the first front dominate solutions in the second front and so on, the non-dominated solutions in the first front are more desirable. Clearly, trade-offs exist in population size and total number of iterations (which combine to dictate computation time) and solution quality.

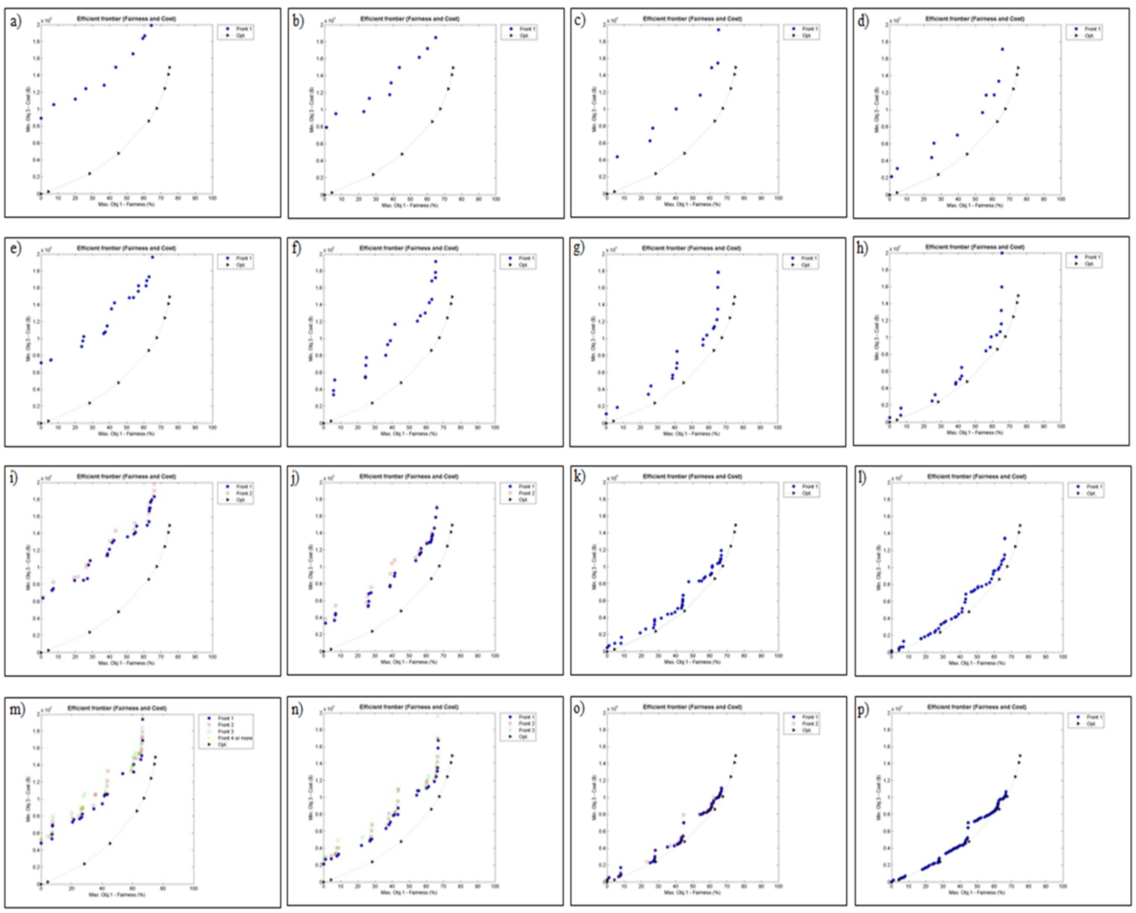

Figure 4.8: Non-dominated frontier from the Hybrid-NSGA II with varied population and iteration levels (a-d) population size 10, (e-h) population size 20, (i-l) population size 50, and (m-p) population size 100

4.5.2 Hypervolume Indicator Result and Discussion

To assess both our algorithm's convergence to the Pareto-optimal front and the diversity of our solutions, we employ a hypervolume indicator. The Hypervolume of a set of solutions measures the size of the portion of objective space dominated by those solutions collectively (While *et al.* 2012). It is usually measured relative to a reference point, often the anti-optimal or "worst" possible point in space. If a set of solutions *S'* has a greater Hypervolume than a set of solutions *S''*, *S'* is considered to be a better set of solutions than *S''*. Figure 4.9 illustrates the Hypervolume area (*Hyp-1*) of a set of solutions generated using a population size of 10, given the reference point (0, $2*10^9$). In our analysis, we define the Hypervolume based performance ratio (PR_H) as the ratio between the Hypervolume of a set of solutions generated from our Hybrid NSGA-II and the one from the mathematical modelling-based algorithm:

$$PR_H = \frac{Hyp\,(Hybrid-NSGA\ II)}{Hyp\,(Pareto\ Optimization)} \tag{4.53}$$

The PR_H results from our designed experiment are shown in Table 4.3. The average, standard deviation, lower bound (LB), and upper bound (UB) of the 95% CI are reported. It is clear that higher PR_H values result when larger populations and/or number of iterations are used; however, this comes at the expense of higher computation times. We highlight a combination of levels that yields $PR_H \geq 0.8$ in bold italics. Further, bolded, italicized, and underlined values represent recommended or desired performance combinations with regard to PR_H value, the percentage of solutions in the first front, and computation time.

When comparing different population levels or numbers of total iterations, the non-overlapping LB and UB regions confirm that PR_H is significantly different. For example, in the MILP case with 0.6-0.3-0.1 variation operator type and 10 iterations, there is a significant difference between population sizes of 10 populations ([LB, UB] = [0.38, 0.43]) and size 20 ([0.48, 0.51]). When we compare variation operator types, the overall mean of the PR_H value for the 0.6-0.3-0.1 case is found to be higher than the 0.3-0.6-0.1 case for both the MILP and LP relaxation cases. Further, the overall mean of PR_H across all cases is found to be at 0.73.

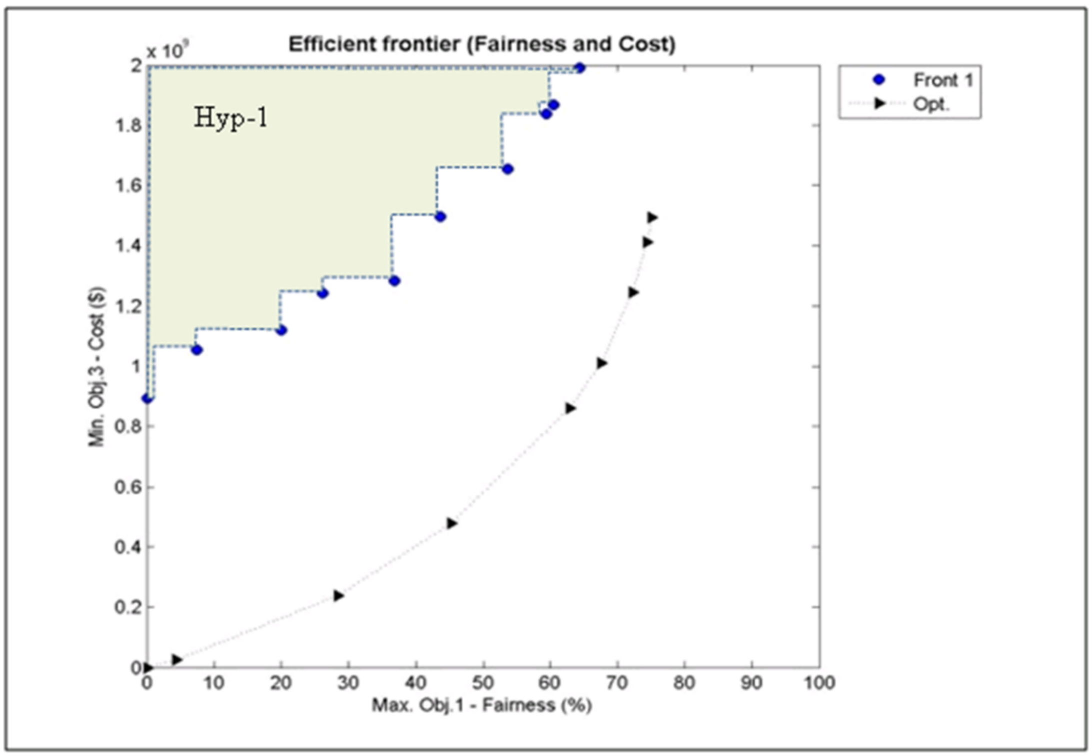

Figure 4.9: The example of Hypervolume (Hyp-1) area calculation

Table 4.3: Hypervolume based performance ratio (PR_H) results

Population \ Iteration		Variation operator : 0.6-0.3-01				Variation operator : 0.3-0.6-0.1				Overall Mean
		10 ite.	20 ite.	50 ite.	100 ite.	10 ite.	20 ite.	50 ite.	100 ite.	
MILP Case										
10 pop.	Mean	0.39	0.44	0.60	0.75	0.38	0.43	0.61	0.78	0.55
	Std. Dev.	0.01	0.03	0.06	0.04	0.02	0.05	0.05	0.05	
	LB	0.38	0.43	0.57	0.73	0.37	0.40	0.58	0.76	
	UB	0.40	0.46	0.64	0.78	0.39	0.46	0.65	0.81	
20 pop.	Mean	0.50	0.62	***0.82***	***0.91***	0.43	0.54	0.77	***0.91***	0.69
	Std. Dev.	0.02	0.03	0.05	0.02	0.03	0.05	0.06	0.03	
	LB	0.48	0.60	0.79	0.90	0.41	0.51	0.73	0.89	
	UB	0.51	0.64	0.85	0.93	0.45	0.57	0.80	0.92	
50 pop.	Mean	0.61	0.79	***0.93***	***0.96***	0.51	0.72	***0.93***	***0.97***	0.80
	Std. Dev.	0.03	0.03	0.02	0.02	0.03	0.03	0.02	0.01	
	LB	0.59	0.77	0.92	0.95	0.49	0.70	0.92	0.97	
	UB	0.63	0.81	0.94	0.97	0.54	0.74	0.94	0.98	
100 pop.	Mean	0.70	***0.89***	***0.97***	***0.99***	0.59	***0.82***	***0.95***	***0.98***	0.86
	Std. Dev.	0.03	0.03	0.01	0.01	0.03	0.02	0.02	0.01	
	LB	0.68	0.87	0.96	0.98	0.57	0.81	0.94	0.98	
	UB	0.72	0.90	0.98	0.99	0.60	0.83	0.97	0.99	
	Overall Mean	0.55	0.68	0.83	0.90	0.48	0.63	0.82	0.91	0.73
LP Relaxation Case										
10 pop.	Mean	0.39	0.44	0.56	0.74	0.39	0.42	0.64	***0.81***	0.55
	Std. Dev.	0.02	0.05	0.04	0.05	0.02	0.05	0.08	0.06	
	LB	0.38	0.41	0.54	0.71	0.38	0.39	0.58	0.78	
	UB	0.40	0.47	0.59	0.77	0.40	0.45	0.69	0.85	
20 pop.	Mean	0.50	0.62	***0.82***	***0.91***	0.44	0.56	***0.81***	***0.91***	0.70
	Std. Dev.	0.03	0.05	0.05	0.02	0.03	0.08	0.06	0.02	
	LB	0.48	0.59	0.79	0.90	0.42	0.51	0.77	0.90	
	UB	0.52	0.65	0.85	0.93	0.46	0.61	0.84	0.92	
50 pop.	Mean	0.62	0.79	***0.94***	***0.97***	0.53	0.75	***0.94***	***0.97***	0.81
	Std. Dev.	0.03	0.04	0.02	0.01	0.04	0.03	0.02	0.01	
	LB	0.61	0.77	0.93	0.96	0.51	0.73	0.93	0.96	
	UB	0.64	0.82	0.95	0.98	0.56	0.76	0.95	0.98	
100 pop.	Mean	0.70	***0.89***	***0.97***	***0.99***	0.58	***0.82***	***0.96***	***0.99***	0.86
	Std. Dev.	0.03	0.02	0.01	0.01	0.02	0.03	0.01	0.01	
	LB	0.68	0.88	0.96	0.98	0.57	0.80	0.95	0.98	
	UB	0.71	0.90	0.98	1.00	0.60	0.84	0.97	1.00	
	Overall Mean	0.55	0.69	0.82	0.90	0.49	0.64	0.84	0.92	0.73

Note: Lower bound (LB) and upper bound (UB) are at 95% confidence level with 10 replications
Bold, Italic ***number*** *denotes the hypervolume ratio at greater than or equal to 0.80*
Bold, Italic Underline ***number*** *denotes hypervolume ratio >= 0.80, percent number in the first frontier at 100%, and computation time <= 3600 seconds*

4.5.3 Percentage of Solutions in the First Front

Having a high number of solutions in the first non-dominated front is important for a decision maker to make an informed decision. In mathematical optimization, multiple runs are required to obtain more solutions to represent a Pareto-optimal front (Deb 2011). As discussed in Section 4.3.3, generating nine Pareto-optimal solutions using the non-preemptive method, one at a time, imposes a burden on computational resources. The percentage of solutions in the first front is calculated in Table 4.4. Bold, italicized values illustrate an experimental design combination that caused all solutions to be present in the first front (i.e., 100% achievement when all 20 solutions in the population are non-dominated). Further, bold, italicized, and underlined values suggest a desirable combination of 100% non-dominated solutions in the first frontier, a less than one hour run time, and $PR_H \geq 0.8$.

At the smaller population levels like a population size of 10, 100% is achieved with a small number of iterations. However, as population size increases, more iterations are required to achieve 100%. Comparing the variation operators, the 0.3-0.6-0.1 setting produces more combinations that achieve 100% than does its competitor. Finally, the overall mean of both the MILP and the LP relaxation cases is approximately 85%.

Table 4.4: Percentage of non-dominated solutions in the first frontier results

Population \ Iteration		Variation operator : 0.6-0.3-01				Variation operator : 0.3-0.6-0.1				Overall Mean
		10 ite.	20 ite.	50 ite.	100 ite.	10 ite.	20 ite.	50 ite.	100 ite.	
MILP Case										
10 pop.	Mean	***100%***	***100%***	***100%***	***100%***	***100%***	***100%***	***100%***	***100%***	100%
	Std. Dev.	0%	0%	0%	0%	0%	0%	0%	0%	
	LB	100%	100%	100%	100%	100%	100%	100%	100%	
	UB	100%	100%	100%	100%	100%	100%	100%	100%	
20 pop.	Mean	99%	97%	***100%***	***100%***	98%	***100%***	***100%***	***100%***	99%
	Std. Dev.	2%	5%	0%	0%	4%	0%	0%	0%	
	LB	98%	94%	100%	100%	95%	100%	100%	100%	
	UB	100%	100%	100%	100%	101%	100%	100%	100%	
50 pop.	Mean	51%	58%	95%	***100%***	57%	60%	97%	***100%***	77%
	Std. Dev.	5%	11%	7%	1%	10%	14%	6%	0%	
	LB	48%	51%	90%	99%	50%	52%	93%	100%	
	UB	54%	65%	99%	100%	63%	68%	100%	100%	
100 pop.	Mean	26%	38%	94%	***100%***	31%	36%	94%	***100%***	65%
	Std. Dev.	4%	6%	8%	0%	5%	9%	10%	0%	
	LB	24%	34%	89%	100%	28%	30%	88%	100%	
	UB	28%	42%	99%	100%	34%	41%	100%	100%	
	Overall Mean	69%	73%	97%	100%	71%	74%	98%	100%	85%
LP Relaxation Case										
10 pop.	Mean	***100%***	***100%***	***100%***	***100%***	***100%***	***100%***	***100%***	***100%***	100%
	Std. Dev.	0%	0%	0%	0%	0%	0%	0%	0%	
	LB	100%	100%	100%	100%	100%	100%	100%	100%	
	UB	100%	100%	100%	100%	100%	100%	100%	100%	
20 pop.	Mean	95%	95%	***100%***	***100%***	95%	***100%***	***100%***	***100%***	98%
	Std. Dev.	12%	8%	0%	0%	11%	6%	0%	0%	
	LB	85%	90%	100%	100%	90%	95%	100%	100%	
	UB	100%	100%	100%	100%	100%	100%	100%	100%	
50 pop.	Mean	52%	62%	96%	***100%***	56%	54%	***100%***	***100%***	78%
	Std. Dev.	9%	9%	8%	0%	11%	14%	0%	0%	
	LB	45%	57%	92%	100%	48%	45%	100%	100%	
	UB	56%	68%	100%	100%	62%	63%	100%	100%	
100 pop.	Mean	29%	38%	93%	***100%***	32%	37%	96%	***100%***	66%
	Std. Dev.	4%	5%	13%	0%	8%	10%	9%	0%	
	LB	27%	35%	86%	100%	27%	31%	90%	100%	
	UB	32%	41%	100%	100%	36%	43%	100%	100%	
	Overall Mean	69%	74%	97%	100%	71%	73%	99%	100%	85%

Note: *Lower bound (LB) and upper bound (UB) are at 95% confidence level with 10 replications*

Bold, Italic ***number*** *denotes the percent number in the first frontier at 100*

Bold, Italic Underline ***number*** *denotes hypervolume ratio >= 0.80, percent number in the first frontier at 100%, and computation time <= 3600 seconds*

4.5.4 Computation Time Results

Both the quality of the outcome and the computation resource requirements are important to evaluate the performance of an algorithm (Zitzler *et al.* 2003). In mathematical optimization, the runtime limit for each Pareto-optimal solution is set to 3,600 seconds. It follows that the upper bound on the amount of time required to generate nine Pareto-optimal solutions representing the approximate Pareto-optimal front is 9(3600) = 32,400 seconds. However, the highest computation time reported for population size = 100 with 100 iterations (which can be considered as a similar upper bound for our Hybrid NSGA-II method) is 24,973 seconds. Not only is this faster than the mathematical optimization, but it is a more attractive option as additional non-dominated solutions are obtained (Table 4.5). Similarly, we highlight test combinations that use less than 3,600 seconds in bold italics. Again, desirable performance settings are depicted in bold, italics, underlined values.

4.6 Managerial Insights

The MOIRR model of Ransikarbum and Mason (2014) provides humanitarian relief operations decision makers with a set of restoration plans for disrupted nodes and arcs in a network such that relief items can be equitably supplied to those in need. Considering the conflicting objectives of the model, non-dominated solutions comprising the Pareto-front is a desirable output due to the trade-offs it bring to light. The use of an optimization algorithm to obtain such a front requires heavy computational efforts, thereby making it impractical in urgent, real-world scenarios. Further, the number of non-dominated solutions present in the front generated by an optimization-based algorithm is at most equal to the number of runs performed. In contrast, our Hybrid NSGA-II approach can efficiently find multiple, diverse non-dominated solutions that are close to Pareto-optimal solutions in one single run that requires significantly less computational time.

Table 4.5: Computational time results

Population \ Iteration		Variation operator : 0.6-0.3-01				Variation operator : 0.3-0.6-0.1				Overall Mean
		10 ite.	20 ite.	50 ite.	100 ite.	10 ite.	20 ite.	50 ite.	100 ite.	
MILP Case										
10 pop.	Mean	***292***	***535***	***1262***	***2472***	***316***	***587***	***1414***	***2794***	1209
	Std. Dev.	3	7	16	27	4	17	105	267	
	LB	291	531	1252	2455	314	577	1349	2629	
	UB	294	540	1272	2488	319	598	1479	2959	
20 pop.	Mean	***566***	***1050***	***2499***	4921	***570***	***1054***	***2507***	4944	2264
	Std. Dev.	7	12	26	43	10	13	24	47	
	LB	562	1043	2483	4895	564	1046	2492	4915	
	UB	571	1058	2515	4948	576	1062	2521	4973	
50 pop.	Mean	***1386***	***2597***	6221	12300	***1431***	***2661***	6466	12870	5742
	Std. Dev.	15	44	75	174	62	85	260	790	
	LB	1376	2569	6175	12192	1393	2609	6305	12381	
	UB	1395	2624	6268	12408	1470	2714	6627	13360	
100 pop.	Mean	***2738***	5144	12380	24521	***2884***	5319	12689	24973	11331
	Std. Dev.	33	54	110	218	303	343	648	909	
	LB	2718	5111	12312	24386	2696	5107	12288	24409	
	UB	2759	5178	12448	24657	3072	5532	13091	25536	
	Overall Mean	1246	2332	5591	11054	1300	2405	5769	11395	5136
LP Relaxation Case										
10 pop.	Mean	***294***	***543***	***1266***	***2473***	***314***	***577***	***1371***	***2693***	1191
	Std. Dev.	5	22	24	27	5	8	23	51	
	LB	290	529	1251	2457	311	572	1357	2662	
	UB	297	557	1282	2490	317	582	1385	2725	
20 pop.	Mean	***565***	***1047***	***2499***	4921	***562***	***1044***	***2486***	4878	2250
	Std. Dev.	7	14	26	43	14	26	61	121	
	LB	560	1038	2483	4895	553	1028	2447	4803	
	UB	569	1056	2515	4948	571	1059	2524	4953	
50 pop.	Mean	***1384***	***2612***	6246	12424	***1418***	***2641***	6301	12407	5679
	Std. Dev.	22	49	142	402	40	74	191	370	
	LB	1370	2582	6158	12175	1393	2595	6183	12178	
	UB	1397	2642	6334	12673	1443	2687	6420	12636	
100 pop.	Mean	***2727***	5132	12360	24634	***2708***	5091	12250	24350	11157
	Std. Dev.	32	54	107	533	69	130	269	503	
	LB	2707	5099	12293	24304	2665	5010	12084	24039	
	UB	2747	5165	12426	24964	2751	5171	12417	24662	
	Overall Mean	1242	2334	5593	11113	1250	2338	5602	11082	5069

***Note**: Lower bound (LB) and upper bound (UB) are at 95% confidence level with 10 replications*

*Bold, Italic **number** denotes the computation time within 3600 seconds*

*Bold, Italic Underline **number** denotes hypervolume ratio >= 0.80, percent number in the first frontier at 100%, and computation time <= 3600 seconds*

4.7 Conclusions and Future Research

Existing models for post-disaster disruption management are scarce and can lack an integrated system view. Previously, a multiple-objective model that provides equity- (fairness-) based solutions for the integrated supply distribution problem encountered during disaster response and the restoration problem that arises during recovery operations is developed. However, as it is important to find solutions quickly for real-world scenarios, we reconstitute the previous MOIRR model by developing a Hybrid NSGA-II heuristic to obtain multiple, diverse, non-dominated solutions quickly for this NP-hard problem. By decomposing the problem, the algorithm utilizes both evolutionary algorithm- and optimization-based techniques to simultaneously obtain multiple solutions in a timely manner.

Through a designed experiment, several factors are analyzed to assess the performance of the algorithm: population size, number of total iterations, variation operator associated with crossover, mutation, and immigration probabilities, and supply flow variable type restrictions. We assess the performance of the algorithm in terms of quality (e.g., convergence to the Pareto-optimal front, diversity of the solutions in the front, and number of non-dominated solutions) and computational requirements (e.g., computation time). There exist clear trade-offs among these performance assessment metrics and obtaining desired Hypervolume-based performance ratio (PR_H) values. While higher population sizes with higher number of total iterations achieve better PR_H values, smaller population sizes with higher number of iterations can attain the best percentage of non-dominated solutions in the first front. However, the fastest computation times result when small population sizes are used in concert with lower total iterations. Although the variation operator with 0.6 crossover, 0.3 mutation, and 0.1 immigration probabilities is superior to its competitor to attain the best PR_H values, it produces slightly fewer solutions in the first front. Given individual preferences for PR_H, the percentage of solutions in the first front, and/or computation time, a decision maker can choose the test settings that best suit their interest.

This chapter provides a novel multiple-objective methodology for decision makers who desire to solve large-scale disrupted network problems to obtain effective, near-optimal solutions quickly in real-world disaster scenarios. Our Hybrid NSGA-II algorithm is an effective method for obtaining multiple, non-dominated solutions quickly so that a decision maker can make a final, informed decision. Further, our method's convergence to known Pareto-optimal solutions and its ability to generate a diverse range of non-dominated solutions is demonstrated. In the future, as parameter uncertainty is an important characteristic in emergency relief logistics, stochastic programming-based methods, such as two-stage stochastic programming, could be further investigated and applied to this problem in an effort to account for data uncertainty at the time when the decision is made. Further, as different risk measures can lead to different decisions, another direction to investigate would be both risk-neutral and risk-averse decision making using a bi-level programming approach, such as leader/follower models or the well-known Stackelberg game (e.g., see Alderson *et al.* 2014).

CHAPTER FIVE

CONCLUSIONS AND FUTURE RESEARCH

5.1 Summary

We have presented three different multiple-objective programming approaches that deal with the integrated supply distribution problem encountered during disaster response and network restoration problem that arises during recovery operations of the post-disaster management cycle. Under different circumstances, a multiple-objective programming model, a goal programming model, and a metaheuristic optimization programming model are used in the analyses to provide an equity- or fairness-based solution for constrained capacity, budget, and resource problems in post-disaster logistics management.

In Chapter 2, we proposed the multiple-objective model with three objectives that integrates the supply distribution problem encountered during disaster response with the restoration problem that arises during recovery operations, the MOIRR model. The first objective function in the model is to maximize equity or fairness modelled using maximin approach. The second objective is to minimize total unsatisfied demand across all demand/beneficiary nodes. The third objective is to minimize the total network cost calculated as the funds spent to restore disrupted nodes, restore disrupted arcs, and transport supply units based on origin-destination (O-D) pair information. The MOIRR model was applied to a South Carolina-based case study using loss data estimated from FEMA's GIS-based loss estimation software, Hazus. We employed a designed experiment to investigate several important aspects of the proposed model, such as partial vs. full restoration and pooled vs. separate budgeting, with both small- and large-sized networks to gain managerial insights from the model. An approximate efficient frontier was developed based on a selected set of efficient solutions to study solution trade-offs for two different pairs of objectives: Pair 1 (fairness vs. cost) and Pair 2 (unsatisfied demand vs. cost). It is clear that these two approximated Pareto fronts (trade-off curves) can provide benefits to a decision maker in visualizing the solution space. The fronts also provide an objective trade-off in that they inform a decision maker on how improving one objective can deteriorate the second objective's performance along the curve.

Next, we extended our previously developed multiple-objective model that provides the equity- or fairness-based solution in the integrated supply distribution and the restoration problem with a goal programming approach called the GP-based MOIRR model in Chapter 3. The extended model under goal constraints provides a decision maker with compromise solutions, under desired goals. The GP analogue of the MOIRR model is guided by three different objective functions: maximizing equity (fairness), minimizing unsatisfied relief demand, and minimizing total network costs. Further, it minimizes three undesired deviational variables associated with each goal. Through a designed experiment, a number of model scenarios were developed based on three factors: multiple-objective solution method (preemptive and non-preemptive); objective function's optimality directive (optimal, non-optimal, and mixed optimal/non-optimal); and constraint set's compromise solution tolerance (compromise and non-compromise). Two levels of goal seeking (conservative and aggressive) were also illustrated in the study. It is evident that a GP-based model provides a compromise solution when no solution exists that satisfies a strict or hard constraint. Further, through a combination of these factors, trade-offs between solution quality and computation time were elaborated so that a decision maker can choose a model configuration of interest. Given hypothetical earthquake scenarios with loss data estimated from FEMA's Hazus system, the GP-based MOIRR model was validated with two different population densities: South Carolina (SC) and California (CA). Efficient frontiers and sensitivity analysis were then provided to understand trade-offs between different objectives of interest. Road capacity related strategic planning was found to increase percent fairness given an expected high disruption.

Finally, as it is important to find solutions urgently for real-world scenarios, we extended our previously developed MOIRR model by analyzing the heuristic algorithm Hybrid NSGA-II to obtain multiple, diverse, non-dominated solutions quickly for this NP-hard problem in Chapter 4. By decomposing the problem, the algorithm utilizes both evolutionary algorithm and optimization techniques to simultaneously obtain multiple solutions in a timely manner. Through a designed experiment, several factors with different levels associated with the Hybrid NSGA-II were analyzed to test the performance of the algorithm: population size; iterations; variation operator associated with crossover, mutation, and immigration probabilities; and sub-model for the supply flow variables. We assessed the performance of the algorithm for both quality (e.g., convergence to the Pareto-optimal front, diversity of the solutions in the front, and ample non-dominated solutions) and computational (e.g., computation time) aspects using the

Hypervolume-based performance ratio (PR_H), percentage of non-dominated solutions in the first front, and computation time in the analyses. There are clear trade-offs among these performance assessment metrics to obtain better PR_H and better percentage of non-dominated solutions at the expense of the computation time. That is, higher population sizes with higher iterations were found to achieve better PR_H, lower population sizes with higher iterations attained better percentage of non-dominated solutions in the first front, and lower population sizes with lower iterations resulted in faster computation times. The variation operator with 0.6 crossover, 0.3 mutation, and 0.1 immigration probabilities was found to attain the better PR_H; while the variation operator with 0.3 crossover, 0.6 mutation, and 0.1 immigration probabilities was found to obtain a higher percentage of solutions in the first front. Finally, the LP relaxation case shows to obtain better computation times than the MILP case. Given a preference in terms of either the PR_H, the percentage of solutions in the first front, and/or computation time, a decision maker can choose a test combination that suits their interest.

5.2 Concluding Remarks

Existing models in post-disaster disruption management are scarce and often lack an integrated perspective. Further, stakeholders' roles in each phase of disaster management often have different objectives, which are often in conflict. It is thus our objective to develop a multiple-objective model that integrates the supply distribution problem encountered during disaster response with the restoration problem that arises during recovery operations. Further, as performance measures of interest in relief operations are not only cost-based, we also consider an equity- or fairness-based solution approach in our multi-criteria analysis to reflect the aid recipient's viewpoint.

Through our analysis, partial restoration decisions under a pooled budgeting approach provides flexibility for organizations when budgets are limited in a highly disrupted network. Hazus is also found to be a valuable tool that can and should be employed by other researchers interested in post-disaster studies. By analyzing Pareto fronts, it is clear that Pareto fronts (trade-off curves) can provide benefits to a decision maker in visualizing the solution space, such that the preferred point on a particular Pareto front can be identified and optimal decisions can be obtained.

Although one way to treat multiple criteria is to select one criterion as primary used in the objective function and the others as secondary assigned acceptable values in constraints, if careful consideration is not given while selecting the acceptable levels by a managerial team or decision makers, a feasible solution that satisfies all the constraints may not exist. Thus, the GP-based model overcomes this issue.

By investigating a multiple-objective solution method, an optimality directive, and compromise tolerance, a trade-off clearly exists between solution quality and computation time such that a decision maker can choose a combination of model scenarios that satisfies his or her interest. That is, the non-preemptive method provides a lesser computation time than the preemptive method, but at the expense of difficulty to choose appropriate weights. If a near- or non-optimal solution is acceptable, computation time will also be less than when optimality is desired. The goal (soft) constraints also benefit decision makers with compromise solutions. The efficient frontier sensitivity analysis also suggests that capacity-related strategic planning can be implemented for a high disruption event.

Considering the conflicting objectives of the model, a non-dominated or Pareto-optimal front is an interesting outcome due to its 'trade-off' property. This property makes the non-dominated front attractive for decision makers to find a wide variety of solutions before making a final, informative decision. Although an optimization algorithm can be used to obtain such a front, it requires a heavy computational load and multiple runs, making it not practical for urgent, real-world scenarios. The number of non-dominated solutions in the front from an optimization algorithm is also limited by the number of runs. In contrast, the evolutionary algorithm-based Hybrid NSGA-II is found to efficiently find multiple, diverse non-dominated solutions closed to Pareto-optimal solutions in a single run with much less computational resources.

5.3 Future Work

As parameter uncertainties (e.g., demand and supply uncertainties) are one important characteristic of emergency relief logistics, stochastic programming, such as two-stage stochastic programming, can be further investigated and applied to this problem in an effort to account for data uncertainty at the time the decision is made during real disaster scenarios. To extend the work developed from previous chapters using a two-stage stochastic programming model, a timeframe hypothesis could be such that once a disaster occurs, information on the number of disrupted nodes and arcs are known with certainty (or high probability), while relief demands are uncertain information. Thus, a decision maker will make a first-stage restoration decision. Then, once the actual demands are realized (e.g., different scenarios with high, average, and low disruption), a recourse or second-stage distribution supply decision could be made.

In another direction, as different risk measures can lead to different decisions, an investigation on both risk-neutral and risk-averse decisions could be made. For example, a risk-neutral-based model could be developed, such that expected values of the objective functions are optimized. On the other hand, a risk-averse-based model could be developed using the bi-level programming approach following the leader/follower model, the attacker/defender model, or the well-known Stackelberg competition game. That is, the worst-case event or the event that disrupts system function the most could be chosen as the attacker model. Then, the decision to optimize the network after a worst-case attack occurs could be modeled with the defender model.

Finally, as decisions in humanitarian logistics operations are dynamic, a study using system dynamics simulation to find how one decision from a stakeholder affects other stakeholders in humanitarian operations could be studied. This would be an interesting area as it is well-observed that although several papers using simulation are proposed in the commercial SCM literature, papers related to simulation of humanitarian operations are very scarce. Further, a focus on technique combination (e.g., hybrid models between system dynamics and agent-based simulations could also be explored.

REFERENCES

Akgun, I., Gumusbuga, F., and Tansel, B. (2014) Risk based facility location by using fault tree analysis in disaster management. Omega, doi. 10.1016/j.omega.2014.04.003i.

Alderson, D. L., Brown, G. G., and Carlyle, W. M. (2014) Assessing and Improving Operational Resilience of Critical Infrastructures and Other Systems, Tutorials in Operations Research. *Institute for Annual Operations Research and the Management Sciences (INFORMS) conference*, 8-12 November, San Francisco, California, USA.

Altay, N. and Green, W.G. (2006) OR/MS research in disaster operations management. *European Journals of Operational Research*, 175, 475-493.

Arthur, J., and Ravindran, A. (1980) A Partitioning Algorithm for (Linear) Goal Programming Problems. *ACM Transactions on Mathematical Software*, 6, 378-386.

Auger, A., Bader, J. (2012) Hypervolume-based multiobjective optimization: Theoretical foundations and practical implications. *Theoretical Computer Science*, 425, 75-103.

Balcik B., and Beamon B. M. (2008) Facility location in humanitarian relief. *International Journal of Logistics Research and Applications: A Leading Journal of Supply Chain Management*, 11, 101-121.

Balcik, B., Beamon B.M., and Smilowitz K. (2008) Last Mile Distribution in Humanitarian Relief. *Journal of Intelligent Transportation Systems*, 12, 51-63.

Balcik B., Beamon B. M., Krejci C. C., Muramatsu K. M., and Ramirez M. (2009) Coordination in humanitarian relief chains: Practice, challenges and opportunities, *International Journal of Production Economics*, 126, 22-34.

Bandyopadhyay, S. and Bhattacharya, R. (2013) Applying modified NSGA-II for bi-objective supply chain problem, *Journal of Intelligent Manufacturing*, 24, 707-716.

Banipal, K. (2006) Strategic approach to disaster management: lessons learned from Hurricane Katrina, *Disaster Prevention and Management*, 15, 484-494.

Beamon B. M. and Balcik B. (2008) Performance measurement in humanitarian relief chains. *International Journal of Public Sector Management*, 21, 4-25.

Cakici, E., Mason, S. J., and Kurz, M. E. (2012) Multi-objective analysis of an integrated supply chain scheduling problem, *International Journal of Production Research*, 50, 2624-2638.

Caunhye, A. M., Nie X., and Pokharel S. (2012) Optimization models in emergency logistics: A literature review. *Socio-Economic Planning Sciences*, 46, 4-13.

Celik, M., Ergun, O., Johnson, B., Keskinocak, P., Lorca, A., Pekgun, P., and Swann, J. (2012) Humanitarian Logistics, Tutorials in Operations Research. *Institute for Annual Operations Research and the Management Sciences (INFORMS) conference*, 14-17 October, Phoenix, Arizona, USA.

Chan, F. T. S. (2003) Performance Measurement in a Supply Chain. The International Journal of Advanced Manufacturing Technology, 21, 534-548.

Chandraprakaikul, W. (2010) Humanitarian supply chain management: Literature review and future research. *The 2nd International Conference on Logistics and Transport*, Queenstown, New Zealand.

Christopher, M. and Tatham, P. (2011) Humanitarian Logistics: Meeting the Challenge of Preparing for and Responding to Disasters, London. Kogan Page.

Coles J. B., Zhuang, J., and Yates, J. (2010) Case study in disaster relief: A descriptive analysis of agency partnerships in the aftermath of the January 12th, 2010 Haitian earthquake, *Socio-Economic Planning Sciences*, 46, 67-77.

Cui, L., Kumara, S., and Lee, D. (2011) Scenario Analysis of Web Service Composition based on Multi-Criteria Mathematical Programming. *Service Science*, 3, 280- 303.

Day, J. M. (2014) Fostering emergent resilience: the complex adaptive supply network of disaster relief. *International journal of production research*, 52, 1970-1988.

Deb, K. (2011) Multi-objective optimization using evolutionary algorithms: an introduction, *Multi-objective evolutionary optimization for product design and manufacturing*, 3-34.

Deb, K., Pratap, A. Agarwal, S., and Meyarivan, T. (2002) A fast and elitist multiobjective genetic algorithm: NSGA-II, *IEEE Transactions on Evolutionary Computation*, 6, 182-197.

Doerner, K. F., Gutjahr, W. J., and Nolz, P. C. (2009) Multi-criteria location planning for public facilities in tsunami-prone coastal areas, *OR Spectrum*, 3, 651-678.

EIU (2005), Disaster Response Management: Going the Last Mile- Thailand and Indonesia, Economist Intelligence Unit briefing paper, DHL, Asia-Pacific, London. [Online] URL: http://www.fritzinstitute.org/ [Accessed 10/18/2012].

Even, S., Itai, A., and Shamir, A. (1976) On the Complexity of Timetable and Multicommodity Flow Problems. *SIAM Journal on Computing*, 5, 691-703.

Federal Emergency Management Agency (2011) National Disaster Recovery Framework: Strengthening Disaster Recovery for the Nation. [Online] URL: http://www.fema.gov/ [Accessed 1/13/2013].

Federal Emergency Management Agency (2014) Hazus [Online] URL: http://www.fema.gov/hazus/ [Accessed 1/10/2014].

Fourer, R., Gay, D., and Kernighan, B. (2002) AMPL: A Modeling Language for Mathematical Programming (2nd edition). Monterey, CA: Duxbury Press, Brooks/Cole Publishing.

Fuse, A., and Yokota, H. (2012) Lessons Learned from the Japan Earthquake and Tsunami, Journal of Nippon Medical School, 79, 312-315.

Galindo, G. and Batta, R. (2013) Review of recent developments in OR/MS research in disaster operations management. *European Journal of Operational Research*, 230, 201-211.

Haddow, G. D., Bullock, J. A., Coppola, D. P. (2011) Introduction to Emergency Management (4th edition). Elsevier.

Hall, N. G. and Posner M. E. (2007) Performance prediction and preselection for optimization and heuristic solution procedures, *Operations Research*, 55, 703-716.

Hildreth, W. B. A. (2009) The Financial Logistics of Disaster: The Case of Hurricane Katrina, *Public Performance and Management Review*, 32, 400-436.

Ignizio, J. and Cavalier, T. (1993) Linear Programming (1st edition). Englewood Cliffs, NJ: Prentice Hall.

Ivanov, D., Sokolov, B., and Pavlov, A. (2013) Dual Problem Formulation and Its Application to Optimal Redesign of an Integrated Production–Distribution Network with Structure Dynamics and Ripple Effect Considerations. *International Journal of Production Research*, 51, 5386-5403.

Ivanov, D., Sokolov, B., and Dolgui, A. (2014) The Ripple effect in supply chains: trade-off 'efficiency-flexibility-resilience' in disruption management. *International Journal of Production Research*, 52, 2154-2172.

International Federation of Red Cross and Red Crescent Societies (2012) World Disaster Reports. [Online] URL: http://www.ifrc.org/publications-and-reports/ [Accessed 8/25/2013].

Jia, H., Ordonez, F., and Dessouky, M. (2007) A modeling framework for facility location of medical services for large-scale emergencies. *IIE Transactions*, 39, 41-55.

Kaplan, S. (1973) Application of programs with maximin objective functions to problems of optimal resource allocations. *Operations Research*, 22, 802- 807.

Karakostas, G. (2008) Faster Approximation Schemes for Fractional Multicommodity Flow Problems. *ACM Transactions on Algorithms*, 4, 1-17.

Karp, R. M. (1972) Reducibility Among Combinatorial Problems. *Complexity of Computer Computations*, 85-103.

Karp, R. M. (1975) On the complexity of combinatorial problems. *Networks*, 5, 45- 68.

Kostreva, M., Ogryczak, W., and Wierzbicki, A. (2003) Equitable aggregations and multiple criteria analysis. *European Journal of Operations Research*, 158, 362-377.

Liberatore, F., Ortuño, M.T., Tirado, G., Vitoriano, B., and Scaparra, M.P. (2014) A hierarchical compromise model for the joint optimization of recovery operations and distribution of emergency goods in Humanitarian Logistics. *Computers & Operations Research*, 42, 3-13.

Liberatore, F., Scaparra, M. P., and Daskin, M. S. (2012) Hedging against disruptions with ripple effects in location analysis. Omega, 40, 21-30.

Luss, H. (1999) On Equitable Resource Allocation Problems: A Lexicographic Minimax Approach. *Operations Research*, 47, 361-378.

Ogryczak, W. (2000) Inequality measures and equitable approaches to location problems. *European Journal of Operational Research*, 122, 374-391.

Marsh, M., and David, A. (1994) Equity measurement in facility location analysis: A review and framework. *European Journal of Operational Research*, 74, 1-17.

Matisziw, T. C., Murray, A. T., and Grubesic, T. H. (2009) Strategic Network Restoration. *Network & Spatial Economics*, 10, 345- 361.

McLoughlin, D. (1985) A framework for integrated emergency management. *Public Administration Review*, 45, 165-172.

Mimura, N., Yasuhara, K., Kawagoe, S., Yokoki, H., and Kazama, S. (2011) Damage from the Great East Japan Earthquake and Tsunami, *Mitigation and Adaption Strategies for Global Change*, 16, 803-818.

Murata, T., Ishibuchi, H., and Tanaka, H. (1996) Multi-objective genetic algorithm and its applications to flowshop scheduling, *Computers and Industrial Engineering*, 30, 957-968.

National Hazards Center (2006) Holistic Disaster Recovery: Ideas for Building Local Sustainability After a Natural Disaster. [Online] URL: http://www.colorado.edu/hazards/publications/holistic/ [Accessed 1/13//2013].

Ogryczak, W. (2000) Inequality measures and equitable approaches to location problems. *European Journal of Operational Research*, 122, 374-391.

Ortuño, M.T., Tirado, G., and Vitoriano, B. (2011) A lexicographical goal programming based decision support system for logistics of Humanitarian Aid, *TOP*, 19, 464-479.

Pettit, S., Beresford, A., Whiting, M., and Banomyong, R. (2011) The 2004 Thailand tsunami reviewed: lessons learned, Humanitarian Logistics: Meeting the challenge of preparing for and responding to disasters, Kogan page, [Online] URL: http://www.lib.myilibrary.com/ [Accessed 10/22/2012].

Ravindran, A. R. (2007) Operations Research and Management Science Handbook, 4, Boca Raton, FL: CRC Press.

Ransikarbum, K. and Mason, S. J. (2014) Multiple-Objective Analysis of Integrated Relief Supply and Network Restoration in Humanitarian Logistics Operations. *International Journal of Production Research, In Press.*

Ransikarbum, K. and Mason, S. J. (2015a). Goal programming model for an integrated relief supply and network restoration during post-disaster decisions- Hazus based case studies, *Working Paper*.

Ransikarbum, K. and Mason, S. J. (2015b) A Bi-Criteria Metaheuristic for Integrated Post-Disaster Relief Supply and Network Restoration Decisions. *Working Paper.*

Salles, R. M. and Barria J. A. (2008) Lexicographic Maximin Optimisation for Fair Bandwidth Allocation in Computer Networks. *European Journal of Operational Research*, 185, 778- 794.

Sayin S. (2013) A Mixed integer programming formulation for the l-maximin problem. *Journal of the operational research society*, 51, 371-375.

Sheu, J. B. (2007) Challenges of emergency logistics management. *Transportation Research Part E: Logistics and Transportation Review*, 43, 655-659.

Singh, V. K. (2007) Equitable efficiency in multiple criteria optimization. *PhD dissertation*, Department of Mathematical Sciences, Clemson University.

Synder, L. V., Atan, Z., Peng, P., Rong, Y., Schmitti, A., and Sinsovsal, B. (2012) OR/MS models for supply chain disruptions: a review. Available from http://ssrn.com/abstract= 1689882.

Synder, L. V., Scaparra, M. P., Daskin, M. S., and Church, R. L. (2006) Planning for disruptions in supply chain networks, Tutorials in Operations Research INFORMS, 234-257.

Tang, C. S. (1987) A Max-min allocation problem: Its solutions and applications. *Operations Research*, 36, 359-367.

Tatham, P. H. and Pettit, S. J. (2010) Transforming humanitarian logistics: the journey to supply network management. *International Journal of Physical Distribution and Logistics Management*, 40, 609-622.

Vitoriano, B., Ortuño, T., and Tirado, G. (2010) HADS, a Goal Programming-Based Humanitarian Aid Distribution System. *Journal of Multi-Criteria Decision Analysis*, 16, 55-64.

Vitoriano B., Ortuño, M. T., Tirado, G., and Montero, J. (2011) A multi-criteria optimization model for humanitarian aid distribution. *Journal of Global Optimization*, 51, 189-208.

Wassenhove, L. N. V. (2005) Blackett Memorial Lecture- Humanitarian aid logistics: supply chain management in high gear. *Journal of the Operational Research Society*, 57, 475-489.

While, L., Bradstreet, L., and Barone, L. (2012) A fast way of calculating exact hypervolumes, *IEEE Transactions on Evolutionary Computation*, 16, 86-95.

Yan, C., Banerjee, A., and Yang, L. (2011) An integrated production-distribution model for a deteriorating inventory item. *International Journal of Production Economics,* 133, 228-232.

Zhang, F. G. and Melachrinoudis E. (1999) The maximin-maxisum network location problem. *Computational Optimization and Applications*, 19, 209- 234.

Zhu, J., Huang, J., and Liu, D. (2010) Equitable resource allocation problem with multiple depots in emergency management. *IEEE International Conference on Emergency Management and Management Sciences*, Beijing, China, 37-40.

Zitzler, E., Thiele, L., Laumanns, M., Fonseca, C. M., and Da Fonseca, V. G. (2003) Performance assessment of multiobjective optimizers: an analysis and review, *IEEE Transactions on Evolutionary Computation*, 7, 117-132.